

AD-774 471

RESEARCH AND DEVELOPMENT OF RARE EARTH-  
TRANSITION METAL ALLOYS AS PERMANENT-  
MAGNET MATERIALS

Alden E. Ray, et al

Dayton University

Prepared for:

Air Force Materials Laboratory

October 1973

DISTRIBUTED BY:

**NTIS**

National Technical Information Service  
U. S. DEPARTMENT OF COMMERCE  
5285 Port Royal Road, Springfield Va. 22151

NOTICE

When Government drawings, specifications, or other data are used for any purpose other than in connection with a definitely related Government procurement operation, the United States Government thereby incurs no responsibility nor any obligation whatsoever; and the fact that the Government may have formulated, furnished, or in any way supplied the said drawings, specifications, or other data, is not to be regarded by implication or otherwise as in any manner licensing the holder or any other person or corporation, or conveying any rights or permission to manufacture, use, or sell any patented invention that may in any way be related thereto.

ACCESSION for	
NTIS	Army Section <input checked="" type="checkbox"/>
DTIC	Naval Section <input type="checkbox"/>
UNANNOUNCED	<input type="checkbox"/>
JUSTIFICATION	
BY	
DISTRIBUTION/AVAILABILITY CODES	
Dist.	AVAIL. CODE OR SP. CTRL.
A	

Copies of this report should not be returned unless return is required by security considerations, contractual obligations, or notice on a specific document.

## DOCUMENT CONTROL DATA - R&amp;D

(Security classification of title, body of abstract and indexing annotation must be entered when the overall report is classified)

1. ORIGINATING ACTIVITY (Corporate author) University of Dayton Research Institute Dayton, Ohio 45469		2. REPORT SECURITY CLASSIFICATION Unclassified	
		2b. GROUP	
3. REPORT TITLE RESEARCH AND DEVELOPMENT OF RARE EARTH-TRANSITION METAL ALLOYS AS PERMANENT-MAGNET MATERIALS			
4. DESCRIPTIVE NOTES (Type of report and inclusive dates) Technical Report, 1 January 1973 - 30 June 1973			
5. AUTHOR(S) (Last name, first name, initial) Ray, Alden E. and Strnat, Karl J.			
6. REPORT DATE October 1973		7a. TOTAL NO. OF PAGES 118	7b. NO. OF REFS 23
8a. CONTRACT OR GRANT NO. F33615-70-C-1625		9a. ORIGINATOR'S REPORT NUMBER(S) UDRI-TR-73-50	
b. PROJECT NO. 7371			
c. Task No. 73103		9b. OTHER REPORT NO(S) (Any other numbers that may be assigned this report) AFML-TR-73-276	
d.			
10. AVAILABILITY/LIMITATION NOTICES Approved for public release; distribution unlimited.			
11. SUPPLEMENTARY NOTES Reproduced by NATIONAL TECHNICAL INFORMATION SERVICE U S Department of Commerce Springfield VA 22151		12. SPONSORING MILITARY ACTIVITY Air Force Materials Laboratory Wright-Patterson AFB, Ohio 45433	
13. ABSTRACT The significant accomplishments of investigations conducted over the past three years are summarized. Topics covered include: the metallurgy and magnetic properties of the rare earth-cobalt-iron alloys $R_2(\text{Co}_{1-x}\text{Fe}_x)_{17}$ with $R = \text{Y, Ce, Pr, Nd, Sm}$ and MM (Ce-rich mischmetal); the rare earth cobalt binary phase diagrams Ce-Co, Pr-Co and Nd-Co; the sintering and magnetic properties of the mixed rare earth-cobalt alloys $R_{1-x}\text{Pr}_x\text{Co}_5$ , $R = \text{Sm, Didymium}$ and $R_{1-x}\text{Nd}_x\text{Co}_5$ , $R = \text{Pr, Sm, Didymium}$ . The results of both room temperature and liquid nitrogen temperature saturation magnetization and anisotropy measurements made using an oscillating specimen magnetometer are reported for single crystals of the compositions $\text{Pr}_2(\text{Co}_{1-x}\text{Fe}_x)_{17}$ , $x = 0.2, 0.3, 0.4$ and $\text{Y}_2(\text{Co}_{1-x}\text{Fe}_x)_{17}$ , $x = 0.1, 0.2, 0.4, 0.5$ . All compositions exhibit easy-axis anisotropy at both temperatures except $\text{Pr}_2(\text{Co}_{0.8}\text{Fe}_{0.2})_{17}$ which on cooling transforms to easy-plane anisotropy at approximately 140°K. Values for the anisotropy constants, $K_1$ and $K_2$ , and the calculated anisotropy field, $H_A$ , are also given. First quadrant magnetization curves obtained with powder specimens and with the aid of an oscillating specimen magnetization are presented for the $R_2(\text{Co}_{1-x}\text{Fe}_x)_{17}$ alloys, $R = \text{Y, Ce, Pr, Sm}$ . The qualitative and quantitative aspects of the magnetocrystalline anisotropy of these alloys is discussed in detail. As in the $\text{RCO}_5$ alloys, $\text{Sm}_2(\text{Co}_{1-x}\text{Fe}_x)_{17}$ alloys exhibit the greatest anisotropy. A review of the published binary rare earth-cobalt alloy systems is presented. Systems discussed include Y-Co, La-Co, Ce-Co, Pr-Co, Nd-Co and Sm-Co.			

14 KEY WORDS  Magnetic Materials Magnetic Properties Permanent Magnets Rare Earth Alloys Intermetallic Compounds	LINK A		LINK B		LINK C	
	ROLE	WT	ROLE	WT	ROLE	WT

**INSTRUCTIONS**

1. **ORIGINATING ACTIVITY:** Enter the name and address of the contractor, subcontractor, grantee, Department of Defense activity or other organization (*corporate author*) issuing the report.
- 2a. **REPORT SECURITY CLASSIFICATION:** Enter the overall security classification of the report. Indicate whether "Restricted Data" is included. Marking is to be in accordance with appropriate security regulations.
- 2b. **GROUP:** Automatic downgrading is specified in DoD Directive 5200.10 and Armed Forces Industrial Manual. Enter the group number. Also, when applicable, show that optional markings have been used for Group 3 and Group 4 as authorized.
3. **REPORT TITLE:** Enter the complete report title in all capital letters. Titles in all cases should be unclassified. If a meaningful title cannot be selected without classification, show title classification in all capitals in parenthesis immediately following the title.
4. **DESCRIPTIVE NOTES:** If appropriate, enter the type of report, e.g., interim, progress, summary, annual, or final. Give the inclusive dates when a specific reporting period is covered.
5. **AUTHOR(S):** Enter the name(s) of author(s) as shown on or in the report. Enter last name, first name, middle initial. If military, show rank and branch of service. The name of the principal author is an absolute minimum requirement.
6. **REPORT DATE:** Enter the date of the report as day, month, year; or month, year. If more than one date appears on the report, use date of publication.
- 7a. **TOTAL NUMBER OF PAGES:** The total page count should follow normal pagination procedures, i.e., enter the number of pages containing information.
- 7b. **NUMBER OF REFERENCES:** Enter the total number of references cited in the report.
- 8a. **CONTRACT OR GRANT NUMBER:** If appropriate, enter the applicable number of the contract or grant under which the report was written.
- 8b, 8c, & 8d. **PROJECT NUMBER:** Enter the appropriate military department identification, such as project number, subproject number, system numbers, task number, etc.
- 9a. **ORIGINATOR'S REPORT NUMBER(S):** Enter the official report number by which the document will be identified and controlled by the originating activity. This number must be unique to this report.
- 9b. **OTHER REPORT NUMBER(S):** If the report has been assigned any other report numbers (*either by the originator or by the sponsor*), also enter this number(s).
10. **AVAILABILITY/LIMITATION NOTICES:** Enter any limitations on further dissemination of the report, other than those

- imposed by security classification, using standard statements such as:
- (1) "Qualified requesters may obtain copies of this report from DDC."
  - (2) "Foreign announcement and dissemination of this report by DDC is not authorized."
  - (3) "U. S. Government agencies may obtain copies of this report directly from DDC. Other qualified DDC users shall request through \_\_\_\_\_."
  - (4) "U. S. military agencies may obtain copies of this report directly from DDC. Other qualified users shall request through \_\_\_\_\_."
  - (5) "All distribution of this report is controlled. Qualified DDC users shall request through \_\_\_\_\_."

If the report has been furnished to the Office of Technical Services, Department of Commerce, for sale to the public, indicate this fact and enter the price, if known.

11. **SUPPLEMENTARY NOTES:** Use for additional explanatory notes.
12. **SPONSORING MILITARY ACTIVITY:** Enter the name of the departmental project office or laboratory sponsoring (*paying for*) the research and development. Include address.
13. **ABSTRACT:** Enter an abstract giving a brief and factual summary of the document indicative of the report, even though it may also appear elsewhere in the body of the technical report. If additional space is required, a continuation sheet shall be attached.

It is highly desirable that the abstract of classified reports be unclassified. Each paragraph of the abstract shall end with an indication of the military security classification of the information in the paragraph, represented as (TS), (S), (C), or (U).

There is no limitation on the length of the abstract. However, the suggested length is from 150 to 225 words.

14. **KEY WORDS:** Key words are technically meaningful terms or short phrases that characterize a report and may be used as index entries for cataloging the report. Key words must be selected so that no security classification is required. Identifiers, such as equipment model designation, trade name, military project code name, geographic location, may be used as key words but will be followed by an indication of technical context. The assignment of links, rules, and weights is optional.

RESEARCH AND DEVELOPMENT OF RARE EARTH-TRANSITION  
METAL ALLOYS AS PERMANENT-MAGNET MATERIALS

By:

Dr. Alden E. Ray and Dr. Karl J. Strnat, Principal Investigators  
University of Dayton, Research Institute and Electrical Engineering Dept.  
300 College Park Ave., Dayton, Ohio 45469  
Tel. Numbers (513) 229-3527 and (513) 229-3535

Sponsored by:

Advanced Research Projects Agency  
ARPA Order No. 1617

Program Code No. OD10  
Contract effective date: 30 June 1970  
Expiration date: 30 June 1973  
Amount of contract: \$525,012

Submitted to:

Air Force Materials Laboratory, AFSC, USAF  
Project Scientist: Mr. Donald J. Evans, LPE Tel. (513) 255-4474

Approved for public release;  
distribution unlimited.

ib

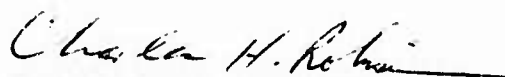
## FOREWORD

The research described in this report is part of the contractual research program of the Electromagnetic Materials Division, Air Force Materials Laboratory. It was performed by the authors at the University of Dayton, Dayton, Ohio 45469, and was sponsored by the Advanced Research Projects Agency, ARPA Order No. 1617, Program Code No. OD10. The contract is administered under Project No. 7371, Task No. 737103, by the Air Force Materials Laboratory, Air Force Systems Command, Wright-Patterson Air Force Base, Ohio. The work was performed under contract F33615-70-C-1625, project scientist, Mr. Donald Evans (AFML/LPE/513-255-4474).

The participants in this research were Adolf Biermann, Stephen Cowdery, Richard Harmer, Michael Hartings, Andrew Kraus, Robert Leasure, Herbert Mildrum, Alden Ray, Charles Shanley, Karl Strnat and Joseph Tront.

This report covers research conducted between 1 January 1973 and 30 June 1973. The report was submitted by the authors in October 1973.

Publication of this report does not constitute Air Force approval of the report's findings and conclusions. It is published only for the exchange and stimulation of ideas.

  
CHARLES H. ROBISON, Major, USAF  
Chief, Solid State Materials Branch  
Electromagnetic Materials Division  
Air Force Materials Laboratory

## ABSTRACT

The significant accomplishments of investigations conducted over the past three years are summarized. Topics covered include: the metallurgy and magnetic properties of the rare earth-cobalt-iron alloys  $R_2(\text{Co}_{1-x}\text{Fe}_x)_{17}$  with  $R = \text{Y, Ce, Pr, Nd, Sm}$  and MM (Ce-rich mischmetal); the rare earth-cobalt binary phase diagrams Ce-Co, Pr-Co and Nd-Co; the sintering and magnetic properties of the mixed rare earth-cobalt alloys  $R_{1-x}\text{Pr}_x\text{Co}_5$ ,  $R = \text{Sm, Didymium}$  and  $R_{1-x}\text{Nd}_x\text{Co}_5$ ,  $R = \text{Pr, Sm, Didymium}$ .

The results of both room temperature and liquid nitrogen temperature saturation magnetization and anisotropy measurements made using an oscillating specimen magnetometer are reported for single crystals of the compositions  $\text{Pr}_2(\text{Co}_{1-x}\text{Fe}_x)_{17}$ ,  $x = 0.2, 0.3, 0.4$  and  $\text{Y}_2(\text{Co}_{1-x}\text{Fe}_x)_{17}$ ,  $x = 0.1, 0.2, 0.4, 0.5$ . All compositions exhibit easy-axis anisotropy at both temperatures except  $\text{Pr}_2(\text{Co}_{0.8}\text{Fe}_{0.2})_{17}$  which on cooling transforms to easy-plane anisotropy at approximately  $140^\circ\text{K}$ . Values for the anisotropy constants,  $K_1$  and  $K_2$ , and the calculated anisotropy field,  $H_A$ , are also given.

First quadrant magnetization curves obtained with powder specimens and with the aid of an oscillating-specimen magnetometer are presented for the  $R_2(\text{Co}_{1-x}\text{Fe}_x)_{17}$  alloys,  $R = \text{Y, Ce, Pr, Sm}$ . The qualitative and quantitative aspects of the magnetocrystalline anisotropy of these alloys is discussed in detail. As in the  $\text{RCo}_5$  alloys,  $\text{Sm}_2(\text{Co}_{1-x}\text{Fe}_x)_{17}$  alloys exhibit the greatest anisotropy.

A review of the published binary rare earth-cobalt alloy systems is presented. Systems discussed include Y-Co, La-Co, Ce-Co, Pr-Co, Nd-Co and Sm-Co.

## TABLE OF CONTENTS

Section	Page	
I	SUMMARY OF WORK DONE DURING ENTIRE CONTRACT PERIOD . . . . .	1
A.	REVIEW OF THE PROGRAM OBJECTIVES . . . . .	1
B.	$R_2(\text{Co}, \text{Fe})_{17}$ PHASES . . . . .	3
C.	BINARY RARE EARTH-COBALT PHASE DIAGRAMS . . . . .	10
D.	$\text{RCo}_5$ PHASES . . . . .	13
II	RESULTS OF FINAL SIX MONTHS OF CONTRACT . . . . .	18
A.	MAGNETIC MEASUREMENTS ON SINGLE CRYSTALS IN THE $\text{Y}_2(\text{Co}_{1-x}\text{Fe}_x)_{17}$ AND $\text{Pr}_2(\text{Co}_{1-x}\text{Fe}_x)_{17}$ SYSTEMS . . . . .	18
B.	THE CRYSTAL ANISOTROPY OF $R_2(\text{Co}, \text{Fe})_{17}$ PHASES . . . . .	20
C.	REVIEW OF THE BINARY RARE EARTH-COBALT PHASE DIAGRAMS . . . . .	30
D.	LIST OF PUBLICATIONS AND PRESENTATIONS . . . . .	31
	REFERENCES . . . . .	34
	APPENDIX I: Thesis by Charles W. Shanley, "Magnetic Measurements on Single Crystals in the $\text{Y}_2(\text{Co}_{1-x}\text{Fe}_x)_{17}$ and $\text{Pr}_2(\text{Co}_{1-x}\text{Fe}_x)_{17}$ Systems" . . . . .	36
	APPENDIX II: Manuscript by A. E. Ray, et al., "Revised Phase Diagrams for the Binary Systems Cerium-Cobalt, Praseodymium-Cobalt, and Neodymium-Cobalt" . . . . .	37
	APPENDIX III: Manuscript by A. E. Ray, "A Review of the Binary Rare Earth-Cobalt Alloy Systems" . . . . .	38

## LIST OF ILLUSTRATIONS

Figure		Page
1	Illustration of the Procedure Used in Correcting for the Estimated Demagnetizing Field. For all easy-axis curves (1, 2, 3), the estimated internal field strength $H_i$ is measured from the tangent (a) to the steepest curve (1) of the set. For all hard-axis curves (1', 2', 3'), the tangent (b) to the steepest curve of this set is used as the reference line $H_i' = 0$ . . . . .	23
2	Pairs of Magnetization Curves Measured on Oriented Powder Samples of $Ce_2(Co_{1-x}Fe_x)_{17}$ Alloys . . . . .	25
3	Pairs of Magnetization Curves Measured on Oriented Powder Samples of $Pr_2(Co_{1-x}Fe_x)_{17}$ Alloys . . . . .	26
4	Pairs of Magnetization Curves Measured on Oriented Powder Samples of $Sm_2(Co_{1-x}Fe_x)_{17}$ Alloys . . . . .	27
5	Pairs of Magnetization Curves Measured on Oriented Powder Samples of $Y_2(Co_{1-x}Fe_x)_{17}$ Alloys . . . . .	28

SECTION I  
SUMMARY OF WORK DONE  
DURING ENTIRE CONTRACT PERIOD

A. REVIEW OF THE PROGRAM OBJECTIVES

The overall objective of this program, conducted under ARPA sponsorship over a period of three years, was to generate information on the properties of selected rare earth-transition metal phases and thereby support and complement concurrent efforts by other contractors to develop technologically useful permanent magnets. During this period, commercial magnet development, stimulated by earlier work done at the Air Force Materials Laboratory and the University of Dayton by the principal investigators, concentrated on compounds of the composition  $\text{RCo}_5$ , where R is one of the "light" rare earth elements, notably samarium.

We suggested at the start of this program that some of the compounds  $\text{R}_2\text{Co}_{17}$  of the same light rare earths, Ce, Pr, Nd, Sm, and Y, or the mixed intermetallic phases  $\text{R}_2(\text{Co}_{1-x}\text{Fe}_x)_{17}$ , should have a combination of basic properties which could make them superior even to  $\text{SmCo}_5$  for use in permanent magnets. One main task was therefore to prepare a large number of such 2:17 alloys and to study those metallurgical, magnetic and crystallographic properties which have a bearing on their potential utility as hard-magnetic materials.

While  $\text{SmCo}_5$ -based magnets were well on their way toward commercial production when this research program began, and while copper-substituted  $\text{SmCo}_5$  and  $\text{CeCo}_5$  had been shown to possess desirable hard-magnetic properties, the technological development of magnets based on other  $\text{RCo}_5$  compounds had run into considerable practical difficulties. We selected two problem areas related to the use of rare earth metals other than samarium in  $\text{RCo}_5$  magnet alloys for study under this contract.

The rare earth neodymium is considerably more abundant and potentially less expensive than samarium.  $\text{NdCo}_5$  has the highest saturation magnetization in the  $\text{RCo}_5$  series and its Curie point is favorably high, but the magnetic crystal anisotropy is low and the temperature dependence of its coercivity unfavorable, thus pure  $\text{NdCo}_5$  is unsuitable for magnet fabrication. These practical questions then arose: 1) Can minor metallurgical modifications of  $\text{NdCo}_5$  make it useful for magnets? 2) In what quantity may Nd be present along with other rare earths in a  $\text{Nd}_{1-x}\text{R}_x\text{Co}_5$  alloy before its undesirable traits interfere too severely? 3) Can the presence of small quantities of Nd bring advantages in addition to the cost reduction? With these ultimate objectives in mind, we studied metallurgical, crystal and magnetic properties of several quasi-binary systems  $\text{Nd}_{1-x}\text{R}_x\text{Co}_5$ . We also conducted liquid-phase sintering experiments with  $\text{NdCo}_5$  and (Didymium)  $\text{Co}_5$  to test promising consequences of a hypothesis about the origin of coercivity in sintered magnets.

All work on the properties of rare earth-transition metal phases presupposes a fairly detailed metallurgical knowledge, such as, the way they form from the melt, their crystal structure, the relations between phases, the extent of their solubility in each other, etc. Since such knowledge of the phase diagrams was still quite incomplete three years ago, we also undertook extensive investigations of the phase relations in several important R-Co binary alloy systems as well as the quasi-binary systems mentioned above.

The last area of concern was the stability of the  $\text{CaZn}_5$ -type structure of the  $\text{RCo}_5$  phases of proven interest for permanent magnet application. We had initially planned to study the extent to which Co may be replaced by Fe or Mn (elements which enhance the saturation but are known to make the structure unstable), and which additional alloying elements might help stabilize the substituted phases. However, we soon became aware of serious efforts with the same objective at several other

institutions, and more basic questions arose concerning the thermal stability of binary  $R\text{Co}_5$  compounds and of the  $R_2(\text{Co}, \text{Fe})_{17}$  phases. We, therefore, redirected our stability studies at these latter problems.

In the following sections of this report, I-B, C and D, we summarize the important results of the work conducted during the entire contract period, with reference to previous reports where details were presented. This is supplemented with a list of journal or conference publications which have resulted from this effort (Section I-E). The work of the last six months and some previously unreported older results are described in detail in Section II.

## B. $R_2(\text{Co}, \text{Fe})_{17}$ PHASES

### 1. Alloy Preparation, Metallurgical and Crystallographic Studies

Six quasi-binary alloy systems,  $R_2(\text{Co}_{1-x}\text{Fe}_x)_{17}$  were investigated. The rare earth metals used were  $R = \text{Ce}, \text{Pr}, \text{Nd}, \text{Sm}$ , the rare earth-like element  $\text{Y}$ , and cerium-rich mischmetal (MM), the least expensive commercial mixed rare earth product. In each of these systems, between 10 and 30 alloys were prepared, initially covering the entire composition range from  $x = 0$  to 1 in  $R_2(\text{Co}_{1-x}\text{Fe}_x)_{17}$  in ten approximately equidistant steps, and later interpolating and duplicating as required.

Difficulties were incurred with crucible corrosion,<sup>(1)</sup> loss of rare earth by vaporization<sup>(2)</sup> and gross segregation<sup>(1,2)</sup> in some alloys. These problems were studied and in most cases overcome. Procedures for the preparation of single-phase samples were developed, and well-defined materials were made available for the various physical property measurements.

Differential thermal analysis (DTA) was performed on all alloys and yielded information on the melting behavior ( $\text{Y}$  alloys congruent, all others peritectic), values for liquidus and peritectic temperatures,

polymorphic and magnetic transformations, and in the system  $R = \text{Ce}$  evidence of a liquid miscibility gap.<sup>(2)</sup> Thermomagnetic analysis (TMA) revealed that many of the Fe-rich alloys,  $x \geq 0.5$ , were metastable at room temperature.<sup>(3)</sup> The nature of this instability was further studied by X-ray diffraction (XRD) and electron microprobe analysis using  $\text{Ce}_2(\text{Co}_{0.5}\text{Fe}_{0.5})_{17}$  as the typical alloy.<sup>(4)</sup> The 2:17 phase was observed to undergo a eutectoid decomposition resulting in a  $\text{R}_2(\text{Co, Fe})_7$  phase and (Co, Fe) phase at temperatures below about  $750^\circ\text{C}$ . This behavior, which appears to be typical of many  $\text{R}_2(\text{Co, Fe})_{17}$  alloys, results in difficulties in the preparation of single-phase ingots, and it could interfere with intended technological uses.

The room temperature crystal lattice parameters of the  $\text{R}_2(\text{Co}_{1-x}\text{Fe}_x)_{17}$  phases were measured by XRD across all alloy systems.<sup>(2)</sup> In every system, a strongly nonlinear expansion of the c-parameter with increasing Fe content was observed: the maximum occurring between  $x = 0.7$  to  $0.8$ . We interpret this as being due to the strongly antiferromagnetic exchange interaction of Fe atoms introduced in the "dumbbell" positions (6c positions) of the 2:17 structure with their transition-metal neighbors. In turn, this magnetically-caused lattice distortion appears to be the reason for the low-temperature decomposition of these compounds, whose crystal structure otherwise seems to be primarily size stabilized.

Successful attempts were made to prepare single crystals large enough for magnetic crystal anisotropy measurements with an oscillating-specimen magnetometer. A crystal weight of  $\sim 10$  mg is sufficient for this purpose. Arc melted and homogenized ingots were annealed just below their peritectic temperatures for periods of several weeks to induce grain growth. They were then crushed, the fragments inspected with the aid of microscopy and XRD, and grains identified as single crystals were mechanically spheroidized and chemically etched. Fourteen crystals of eight compositions in the systems  $\text{Y}_2(\text{Co, Fe})_{17}$ ,  $\text{Pr}_2(\text{Co, Fe})_{17}$  and  $\text{MM}_2(\text{Co, Fe})_{17}$  were initially obtained, but some of them did not survive the spheroidization process.

## 2. Magnetic Property Measurements

Magnetic studies concentrated on those basic properties which can be used as criteria in determining if a new substance may have utility as a permanent magnet material. These are the Curie temperature, the saturation magnetization, and the room temperature magnetocrystalline anisotropy.

The Curie temperatures of stable and metastable  $R_2(\text{Co}, \text{Fe})_{17}$  phases were measured by DTA<sup>(2)</sup> and TMA.<sup>(3, 4)</sup> They were found to drop monotonically from the high values of the iron-free  $R_2\text{Co}_{17}$  compounds ( $800^\circ$  to  $930^\circ\text{C}$ ) to the very low ones of the pure  $R_2\text{Fe}_{17}$  ( $-180^\circ$  to  $+130^\circ\text{C}$ ). From a practical point of view, it is very important that small additions of Fe leave the Curie point virtually unchanged and that  $T_c$  remains above  $\sim 600^\circ\text{C}$  for up to 50% substitutions of Fe for Co in all systems studied.

Magnetometric saturation magnetization measurements on oriented powders<sup>(4)</sup> revealed that in all alloy systems the room temperature saturation has a pronounced maximum in the compositional range,  $x = 0.5$  to  $0.7$ . This is analogous to the behavior of binary Co-Fe alloys.<sup>(5)</sup> The measured peak values of the intrinsic induction range from about  $4\pi M_s = 14$  kG for  $\text{Ce}_2(\text{Co}_{0.4}\text{Fe}_{0.6})_{17}$  to 16.5 kG for  $\text{Pr}_2(\text{Co}_{0.4}\text{Fe}_{0.6})_{17}$ .

The first step in evaluating the magnetocrystalline anisotropy was to determine those alloy compositions for which the crystallographic c-axis is the direction of easy magnetization; these are of greatest interest for permanent magnets. This was done by preparing powder samples consisting largely of single crystal particles, orienting them with the aid of a magnetic field, fixing their position with a binder, and then identifying by XRD the crystal axis which aligned parallel to the field. Thus we found composition regions in the Co-rich half of each system, except for  $R = \text{Nd}$ , in which easy c-axis anisotropy exists.<sup>(3)</sup>

Quantitative estimates of the anisotropy fields and uniaxial anisotropy constants were obtained for the easy-axis compositions. Magnetically oriented powder samples were prepared as above, but in a different shape and size, and magnetization curves were obtained both parallel and perpendicular to the easy direction of magnetization. The shape of the hard-axis  $M$  versus  $H$  curve and the area between curves, were used to obtain anisotropy data. Results for the Sm, Pr and MM systems were previously presented<sup>(3, 4)</sup> and additional data can be found in Section II of this report. Very high anisotropy field values,  $H_A \approx 108$  kOe, were found for the Sm alloys, while those for the other investigated alloy systems were much lower--up to 30 kOe for Pr alloys and  $< 10$  kOe for the other systems. This means in practical terms that Co-rich  $\text{Sm}_2(\text{Co}, \text{Fe})_{17}$  phases show the highest promise for permanent-magnet application; some Pr alloys may be of interest, but alloys based on the rare earth metals Ce, Nd, Y or MM do not merit consideration for magnet development efforts at this time.

Magnetometer measurements were also made recently on some of the single crystals of  $\text{Pr}_2(\text{Co}, \text{Fe})_{17}$  and  $\text{Y}_2(\text{Co}, \text{Fe})_{17}$  phases which became available. These were performed at room temperature and down to  $77^\circ\text{K}$ . Some data were reported before,<sup>(6)</sup> and more results can be found in Section II of this report. The single-crystal measurements yielded improved room-temperature values for the first- and second-order anisotropy constants and for the saturation magnetization as well as information about the temperature dependence of these properties. One of the compositions,  $\text{Pr}_2(\text{Co}_{0.8}\text{Fe}_{0.2})_{17}$ , shows a transition on cooling from easy-axis anisotropy to easy-plane behavior at  $\sim 140^\circ\text{K}$  and a step anomaly in the hard-axis magnetization curve measured below this transition temperature.

3. Potential Application of  $R_2(\text{Co, Fe})_{17}$  Phases for Permanent Magnets

Perhaps the most important, and certainly the most exciting, result of the efforts under this contract was the realization that some of the  $R_2(\text{Co, Fe})_{17}$  phases hold out the promise of being excellent permanent magnet materials.<sup>(3)</sup> Particularly, the cobalt-rich  $\text{Sm}_2(\text{Co}_{1-x}\text{Fe}_x)_{17}$  phases with  $x \leq 0.4$  meet the three necessary conditions quite well. They have high saturation, high Curie temperature, and a pronounced magnetic anisotropy with a single easy-axis.

Permanent magnets based on these phases of 2:17 stoichiometry could be superior to  $\text{SmCo}_5$  in several ways. Even the iron-free  $R_2\text{Co}_{17}$  compounds have higher saturation magnetization than the corresponding 1:5 phases and this advantage is magnified when iron is substituted for a part of the cobalt.<sup>(4)</sup> This means that the useful remanent flux and the theoretically possible maximum energy product are substantially increased. The 2:17 phases contain approximately 10 weight percent less rare earth than 1:5 compounds. This means that they are less susceptible to oxidation which is a problem with magnets based on  $R\text{Co}_5$ , and that 2:17-based magnets should therefore have better long-term stability at elevated temperatures. Another favorable consequence of the lower R-content is the reduced raw material cost, particularly for the alloys using the expensive metal samarium as the sole or principal rare-earth constituent. Partial iron substitution brings an additional economic advantage, since Fe is much less expensive than Co. A corresponding advantage is not possible for  $\text{SmCo}_5$  in which iron has a very low solubility.

Assuming that the energy product is limited by the saturation magnetization only, one may consider the theoretical upper limit for the static energy product about 64 MGOe for  $\text{Sm}_2(\text{Co, Fe})_{17}$  68 MGOe for  $\text{Pr}_2(\text{Co, Fe})_{17}$  alloys. Considering, however, that a

realistic chance of obtaining a sufficiently high coercive force seems to exist only for the highest-anisotropy compositions in each of these systems, and also considering the previously discussed metallurgical stability problems of high-iron alloys, we must probably restrict our view to the Fe-content range of  $x \leq 0.3$ . The energy-product potential is then reduced to approximately 50 MGOe for  $\text{Sm}_2(\text{Co}_{0.7}\text{Fe}_{0.3})_{17}$  and 55 MGOe for  $\text{Pr}_2(\text{Co}_{0.7}\text{Fe}_{0.3})_{17}$  about double that for  $\text{SmCo}_5$  or 1-1/2 times that for  $\text{PrCo}_5$ .

#### 4. Recommendations for Future Work

The work done to date with the  $\text{R}_2(\text{Co, Fe})_{17}$  phases has defined promising candidate materials for the development of improved rare earth permanent magnets. It has also revealed a number of obstacles which must be overcome before such magnets can be made and has identified several research problems which must be solved both in support of magnet development work and in leading to important insights into the magnetic behavior of materials.

Working toward the practical goal of making improved magnets possible, the main objective now must be to develop a sufficiently high coercive force, 6-10 kOe, in bodies which are made predominantly of  $\text{Sm}_2(\text{Co, Fe})_{17}$ , or  $\text{Pr}_2(\text{Co, Fe})_{17}$ , or perhaps a modification thereof containing a mixture of rare earths. With  $\text{RCo}_5$  alloys, high coercivity can be achieved in three principal ways: 1) By finely subdividing the alloy, e. g., by mechanical grinding or precipitation in a nonmagnetic matrix; 2) by sintering powder compacts with an addition of a rare earth-rich phase (especially with a samarium excess); and 3) by alloying it with a third element, typically copper, which is capable of producing a fine-grained, nonmagnetic precipitate in the  $\text{RCo}_5$  matrix.

Attempts should be made to apply all three of these techniques to the 2:17 phases. Grinding alone has so far resulted in powders with coercive forces too low for permanent magnets. This is similar to

the early experiences with  $RCo_5$  alloys other than  $SmCo_5$ . For these  $RCo_5$  phases, chemical and metallurgical surface treatments of the particles have been found which raise the coercivity to useful levels. These surface-etching, polishing and coating techniques should be systematically tried on, and adapted to, the 2:17 phases.

Liquid-phase sintering with the addition of a Sm-rich Sm-Co phase is the preferred commercial manufacturing process for  $RCo_5$ -based magnets. It also may well be the most promising approach to the preparation of 2:17 magnets, but early attempts by us and by others have not been encouraging. Since the physical origin of coercivity in sintered R-Co magnets is not yet understood and at present the subject of considerable controversy, a systematic study of the magnetization reversal process in such sintered bodies and its relationship to the microstructure appears to be an urgent need.

A first successful attempt to obtain high coercive force through the addition of copper and subsequent appropriate precipitation heat treatment has been reported by other scientists.<sup>(7)</sup> They achieved  $M_c H_c = 6.1$  kOe and  $(BH)_{max} = 18.3$  MGOe with an alloy of the composition  $Sm_{0.7}Ce_{0.3}(Co_{0.8}Fe_{0.05}Cu_{0.15})_7$  which lies in the range of total rare earth-to-total transition metal ratio between the 1:5 and 2:17. This is a very encouraging result, and similar approaches to the bulk hardening of  $R_2(Co, Fe)_{17}$  alloys should be systematically explored.

More basic tasks which relate to the practical objective of making outstanding magnets can be formulated in the physics of magnetism and the physical metallurgy areas.

The magnetocrystalline anisotropy remains the key basic property, but its origin and the factors controlling it are still only very poorly understood. Therefore, much theoretical work remains to be done in this field, and as a prerequisite for it, reliable systematic experimental studies of the crystal anisotropy and its temperature and

composition dependence must be done. In addition to the ternary  $R_2(\text{Co, Fe})_{17}$  phases, it will be necessary to study modifications containing a second rare earth or another transition element, both magnetic and non-magnetic, to shed light on the roles which the individual ions and their positions in the crystal lattice play in the magnetic exchange interactions and the crystal anisotropy. A step closer to the practical magnet problems is the need to better understand the various physical causes of coercivity and to correlate them to anisotropy and other physical properties. While we emphasize here the importance of such studies for the  $R_2(\text{Co, Fe})_{17}$  alloys, they must indeed encompass all magnetic rare earth-transition metal compositions which may be present in sintered or cast permanent magnets.

Important physical metallurgy problems to be studied include the eutectoid decomposition of the  $R_2(\text{Co}_{1-x}\text{Fe}_x)_{17}$  phases observed for certain ranges of  $x$ , the factors causing this instability, and possible measures of suppressing it. The extent of the homogeneity regions of these phases with respect to the rare earth-to-transition metal ratio is of great practical importance especially with respect to the effects which deviations from the 2:17 stoichiometric ratio have on the magnetic properties of these materials.

## C. BINARY RARE EARTH-COBALT PHASE DIAGRAMS

### 1. Introduction

Early investigations of the magnetic properties of  $\text{PrCo}_5$  magnets sintered with Pr-rich Pr-Co alloys showed the coercivities and energy products to be very sensitive to the sintering temperature.<sup>(8)</sup> In addition, critical sintering temperatures were observed to correlate closely with thermal events observed in the Pr-Co phase diagram. In view of the importance of reliable phase diagrams, not only for determining methods for alloy preparation and heat treatment, but also as guides to understanding and controlling the magnetic behavior of the rare earth-cobalt

alloys, the partial phase diagrams Ce-Co, Pr-Co, and Nd-Co reported earlier by Ray and Hoffer<sup>(9)</sup> were revised and completed. In light of these investigations, the La-Co phase diagram was also revised from existing data.

## 2. Summary of Results

Studies of the four phase diagrams listed above resulted in the identification of previously unreported phases, more complete characterization of some of the less well understood phases and a more accurate definition of the phase boundaries in the systems.

The most significant discovery was the identification of the rare earth-cobalt compounds of compositions  $R_5Co_{19}$ , located at 79.2 at. % Co. This phase was definitely established in the Pr, Nd and Ce systems and data strongly suggests its presence in the La system. These compounds exhibit both rhombohedral and hexagonal polymorphs with the rhombohedral modification,  $R\bar{3}m$ , strongly dominant.

The identification of the  $R_5Co_{19}$  compounds, their composition lying immediately to the rare earth-rich side of the  $RCo_5$  phase field, indicates that these intermetallic phases may play a significant role in the achievement of high coercive forces in  $RCo_5$ -based permanent magnets. This may be especially true in the magnet fabrication methods involving liquid phase sintering processes with overall magnet compositions rare earth-rich with respect to  $RCo_5$  stoichiometry.

Earlier data for the Nd-Co system<sup>(9)</sup> indicated a  $Nd_xCo_y$  phase located at approximately 30 at. % Co. An isostructural phase in the Pr-Co system,  $Pr_xCo_y$ , was also identified. Both compounds were found to melt incongruently and from X-ray diffraction data were found not to be isostructural with  $Sm_9Co_4$  as would be suspected from their compositions. Quantitative electron microprobe analysis showed the  $Pr_xCo_y$  alloys to contain  $29.09 \pm 0.31$  at. % Co and the  $Nd_xCo_y$  alloy to contain  $28.96 \pm 0.22$  at. % Co.

A new phase containing 45.9 at. % Co was identified in the Nd-Co, Pr-Co, and La-Co systems. The crystal structure for these compounds,  $R_2Co_{1.7}$ , was determined to be hexagonal. Lattice parameters were measured<sup>(10)</sup> but no refinement of atomic positions was attempted. All three compounds were observed to melt incongruently.

In the Nd-Co system, the intermetallic compound  $Nd_2Co_3$  was identified and X-ray diffraction showed this compound to be isostructural with  $La_2Co_3$ .

### 3. Recommendations for Future Work

Results of our current investigations into rare earth-cobalt phase stability suggest two specific areas for future investigations. One area to be studied is a review of the phase stability of the two technologically significant rare earth-cobalt alloy systems, Sm-Co and Y-Co. The second area for future study is the technological importance of the recently reported  $R_5Co_{19}$  phases with special attention to be given to the role these phases play in obtaining high coercive force permanent magnets.

Several factors indicate the necessity of a review of the phase equilibrium in the Sm-Co system and in the Y-Co system. In the course of our investigations of the  $R_2Co_{17}$  intermetallics, we have observed  $Sm_2Co_{17}$  to melt peritectically at  $1310^\circ C$  rather than congruently at  $1335^\circ C$  or  $1375^\circ C$  as reported by others.<sup>(11, 12)</sup> Additionally, we have observed the peritectic isotherms for the more Sm-rich compounds to differ significantly with those reported earlier. An examination of XRD and DTA data for certain Sm-Co compositions strongly suggests the existence of a  $Sm_5Co_{19}$  phase isostructural with the previously reported  $Pr_5Co_{19}$ . Finally, recent reports<sup>(13)</sup> have suggested that  $SmCo_5$  and indeed all  $RCo_5$  phases are unstable at low temperatures, decomposing by eutectoidal reaction. Although our results do not support this view, the magnitude of the technological impact of such a reaction requires a definitive investigation of the report.

Past investigations of the Y-Co phase diagrams have differed greatly. (14, 15, 16) In the course of our studies, we have had the opportunity to work with both "high purity yttrium" (2000 ppm oxygen) and very pure yttrium (< 250 ppm oxygen). Results of heat treating of identical alloy compositions,  $\text{YCo}_2$ , made from these different purity level yttrium lots indicates 2000 ppm yttrium to be much too impure to be considered for use in phase diagram study. From these studies we also have concluded that the currently reported diagrams most likely represent various cuts through the Y-Co-O ternary system. A thorough understanding of both methods for the prevention of oxygen contamination of Y-Co alloys and the true Y-Co phase equilibrium will be required for successful production of high energy permanent  $\text{YCo}_5$  magnets.

Past experience has shown that successful manufacture of  $\text{RCo}_5$ -based permanent magnets always requires an overall magnet composition which is rare earth-rich relative to  $\text{RCo}_5$  stoichiometry. Although it is recognized that excess rare earth is required to compensate for the oxygen content of the alloy, calculations show that it is common to add more rare earth than that required to compensate the oxide content. The recent identification of the  $\text{R}_5\text{Co}_{19}$  phases in the Pr, Nd, and Ce systems and the strong indication of its existence in the Sm-Co systems indicates that these new phases may play an important role in attaining high coercive forces in  $\text{RCo}_5$ -based permanent magnets. A thorough characterization of the magnetic properties of these phases is thus an important area for future investigation.

#### D. $\text{RCo}_5$ PHASES

##### 1. $\frac{(\text{Nd}_{1-x}\text{R}_x)\text{Co}_5}{x}$ Alloys

Of the light rare earth-cobalt intermetallic compounds of the type  $\text{RCo}_5$ , only  $\text{SmCo}_5$  has enjoyed substantial success as a permanent magnet material.  $\text{NdCo}_5$ , although attractive due to its high saturation and Curie temperature and the relative abundance of neodymium, has been found unacceptable as a permanent magnet material due to its very low intrinsic coercive force.

Earlier studies of  $\text{PrCo}_5$  alloys at the University of Dayton.<sup>(17)</sup> showed that through liquid phase sintering, utilizing a magnetically hard sintering aid, Sm-Co, a significant increase in intrinsic coercivity could be attained. It was also thought that a similar increase might be possible in  $\text{NdCo}_5$ -based magnets using either Pr-Co or Sm-Co sintering aids.

Preliminary investigations<sup>(2, 4)</sup> were made using a Pr-Co alloy sintering aid, 70 w/o Pr-30 w/o Co, in sintering studies of both  $\text{NdCo}_5$  and  $\text{DiCo}_5$  (Didymium metal: 70-75% Nd, 17-19% Pr, 0.3-0.5% Ce, 8-12% other rare earths). Magnets were prepared by blending powders of the base alloys with the sintering aids using 20, 30, 40 and 50 w/o sintering aid. The mixed powders were pressed into bricks and sintered 30 minutes at  $1140^\circ\text{C}$ .

Magnetic measurements made on the sintered magnets revealed a substantial increase in the intrinsic coercivity of both the  $\text{NdCo}_5$ -based and  $\text{DiCo}_5$ -based magnet compositions. In the unsintered states,  $M^H_c$  for all samples was less than 200 Oe and in the sintered state,  $M^H_c$  was as high as 4000 Oe in the case of the 40 w/o sintering aid additions. These values were similar in both the  $\text{NdCo}_5$  and  $\text{DiCo}_5$  compositions.

The effect of sintering temperature on the intrinsic coercivity was also investigated using a 80 w/o  $\text{DiCo}_5$  20 w/o sintering aid composition. Results were similar to those reported for  $\text{PrCo}_5$  and  $\text{SmCo}_5$  by Westendorp,<sup>(18)</sup> that is, a decrease in  $M^H_c$  up to  $\approx 1120^\circ\text{C}$  ( $M^H_c \approx 400$  Oe) followed by a sharp rise to the maximum  $M^H_c$  at  $1150^\circ\text{C}$  ( $M^H_c \approx 4000$  Oe). Sintering times during this phase of the study were 30 minutes.

A second series of compositions using a 60 w/o Sm - 40 w/o Co sintering aid with a  $\text{DiCo}_5$ -base alloy were also investigated. Additions of 10 w/o to 40 w/o sintering aid were studied sintering at  $1160^\circ\text{C}$  for 30 minutes. Again, the coercive force was observed to increase from  $M^H_c \approx 200$  Oe in the unsintered state to  $M^H_c = 5140$  Oe in the case of the

the 25 w/o sintering aid composition. The effect of sintering temperature, investigated using a 22.5 w/o sintering aid composition, showed the highest coercive force was developed at 1040°C ( $H_c = 7700$  Oe). Other maxima were observed in this study at 1100°C and 1140°C. The significance of these secondary maxima is not currently understood.

The effect of sintering time on the coercivity of  $\text{DyCo}_5$ -based magnets was investigated using the Sm-Co sintering aid with additions of 17.5 w/o and 22.5 w/o. Sintering was carried out at 1040°C. A broad maximum was observed around 60 minutes in the 22.5 w/o addition specimen ( $H_c \approx 8000$  Oe). A sharp maximum was observed at the same sintering time for the 17.5 w/o composition ( $H_c = 10,280$  Oe).

In conclusion, it has been demonstrated that a substantial increase in  $\text{NdCo}_5$ -based and  $\text{PrCo}_5$ -based alloys may be produced through liquid phase sintering procedures using a magnetically hard sintering aid. Dr. Strnat has suggested that the increase in intrinsic coercivity produced by these procedures may result from the pinning of domain walls in a magnetically hard second phase or "shell," which is contiguous with the  $\text{RCo}_5$  primary phase. Further experiments, definitive rather than empirical in nature, should be performed in order to clearly elucidate the role of the sintering aid in producing the increase in the intrinsic coercivity of the light rare earth-cobalt,  $\text{RCo}_5$  alloys.

## 2. Stability of $\text{RCo}_5$ Phases

Recent investigations have reported that the rare earth-cobalt intermetallic phases,  $\text{RCo}_5$ , with the  $\text{CaZn}_5$ -type structure are stable only over a limited temperature range.<sup>(13)</sup> For the light rare earth  $\text{RCo}_5$  phases, this stability range was reported to be from a lower limit of 600 to 700°C to an upper limit defined by the peritectic melting temperature of the particular composition. The practical implications of these reports are significant if the  $\text{RCo}_5$  materials currently being used in high energy permanent magnet production are indeed only metastable at normal ambient temperatures.

In order to gain some understanding of the reported decomposition behavior of the light rare earth  $\text{RCo}_5$  alloys, two studies were conducted using  $\text{CeCo}_5$ ,  $\text{PrCo}_5$  and  $\text{NdCo}_5$ .<sup>(6)</sup> Using single phase alloys, specimens were heat treated at  $500^\circ\text{C}$  for 80 hours in a differential thermal analyzer and following heat treatment were thermally analyzed anticipating an endothermic reaction corresponding to the reformation of the  $\text{RCo}_5$  phases from its decomposition products. According to Buschow,<sup>(13)</sup> 80 hours at  $500^\circ\text{C}$  should be sufficient to at least initiate decomposition. Results of the subsequent thermal analyses showed no indication of the anticipated reformation endotherm nor any other anomalous events in the temperature range anticipated for the reformation reactions.

A second study of the same alloys was conducted on alloys heat treated at  $500^\circ\text{C}$  for 420 hours. Following detailed metallographic examination and X-ray diffraction analyses, no discernible alteration of the initial alloys could be observed. For the heat treated  $\text{CeCo}_5$  alloy, an extensive thermomagnetic analysis (TMA) program was initiated. A series of 17 TMA examinations were conducted on a single  $\text{CeCo}_5$  specimen at temperatures from room temperature to  $-190^\circ\text{C}$  and from room temperature to temperature both above and below the reformation temperature reported by Buschow. At no time in the course of this investigation was any evidence (magnetic transition) found for the existence of the anticipated decomposition products  $\text{Ce}_5\text{Co}_{19}$  and  $\text{Ce}_2\text{Co}_{17}$ , nor for  $\text{Ce}_2\text{Co}_7$  as reported by Buschow. Observations of the Curie temperature for  $\text{CeCo}_5$  did however present a rather unexpected and curious behavior. The first observation was the rather considerable thermal hysteresis in the Curie temperature  $\mu$ -peak for  $\text{CeCo}_5$ . With one exception, the  $\mu$ -peak observed on cooling was observed to occur as much as  $63^\circ\text{C}$  and as little as  $34^\circ\text{C}$  below the  $\mu$ -peak observed on heating. The second observation was the rather wide temperature range over which the  $\mu$ -peaks were observed. On heating cycles, the mean temperature corresponding to  $T_c$  was  $370^\circ\text{C}$  with a temperature range of  $\pm 30^\circ\text{C}$ . On cooling, the mean  $T_c$  was  $334^\circ\text{C}$

with an identical temperature range,  $\pm 30^\circ$ . To date, no satisfactory explanation has been presented for the behavior of the  $\text{CeCo}_5$  Curie temperature as observed in the course of this investigation.

In conclusion, all of our findings to date appear to support room temperature stability of  $\text{CeCo}_5$ ,  $\text{NdCo}_5$  and  $\text{PrCo}_5$ . No evidence of a eutectoidal decomposition in these alloys was observed at anytime.

### 3. Recommendations for Further Work

From the results obtained in the course of our investigations of the binary alloy system  $(\text{Nd}_{1-x}\text{R}_x)\text{Co}_5$ , a distinct area of important investigation is evident. In the case of the reported increase in intrinsic coercivity in  $\text{NdCo}_5$  produced through utilization of a magnetically hard sintering aid, a definitive investigation, that is, one in which not only the magnetic properties of the sintered magnet are determined, but one in which a total characterization--magnetic, crystallographic, and microstructural--should be performed on both starting materials and sintered magnets. With such an investigation, it would be possible to both evaluate the validity of the "epitaxial shell" model for controlling coercive force and quite possibly identify methods for producing good permanent magnet materials from rare earth-cobalt alloys other than  $\text{SmCo}_5$ .

## SECTION II

### RESULTS OF FINAL SIX MONTHS OF CONTRACT

#### A. MAGNETIC MEASUREMENTS ON SINGLE CRYSTALS IN THE $Y_2(Co_{1-x}Fe_x)_{17}$ AND $Pr_2(Co_{1-x}Fe_x)_{17}$ SYSTEMS\*

Single crystals of the compositions  $Y_2(Co_{1-x}Fe_x)_{17}$ ,  $x = 0.1, 0.2, 0.4, 0.5$ , and  $Pr_2(Co_{1-x}Fe_x)_{17}$ ,  $x = 0.2, 0.3, 0.4$  were grown by long term annealing of single phase alloy specimens. Procedures for the preparation and selection of these crystals was described earlier.<sup>(5)</sup>

Room temperature measurements of saturation magnetization, anisotropy field, and the computed values for the first and second anisotropy constants have also been reported. Work during the final period centered on magnetic measurements at liquid nitrogen temperatures and studies of the effect of temperature on saturation magnetization. Results of both room temperature and liquid nitrogen temperature magnetic property measurements are shown in Table I.

The maximum values for anisotropy fields at room temperature, calculated from the relationship  $H_A = 2(K_1 + 2K_2)/M_s$ , were observed to correspond to the compositions  $Y_2(Co_{0.8}Fe_{0.2})_{17}$  and  $Pr_2(Co_{0.7}Fe_{0.3})_{17}$ . Maximum theoretical static energy products,  $4\pi^2 M_s^2$ , for these compositions were 53.6 MGOe and 66.5 MGOe, respectively.

The magnetization was observed to increase monotonically with decreasing temperature for all alloys except the composition  $Pr_2(Co_{0.8}Fe_{0.2})_{17}$ . This composition, although exhibiting easy c-axis magnetization at room temperature, was observed to change to easy

---

\* Part of a thesis submitted as partial fulfillment of the requirements for the Master of Science in Engineering by Charles W. Shanley.

TABLE I  
SUMMARY OF MAGNETIC PROPERTIES

x	T (°K)	$\sigma^*$ (Emu/g)	$4\pi M_s^*$ (Gauss)	$K_1$ ( $\times 10^7$ Erg/cm <sup>3</sup> )	$K_2$	H <sub>A</sub> (Oe)
			<u>Alloy System Y<sub>2</sub>(Co<sub>1-x</sub>Fe<sub>x</sub>)<sub>17</sub></u>			
0.1	300	134.5 ± 1	13,533 ± 100	0.23 ± 0.01	0.02 ± 0.01	5,100 ± 200
	77	138.9 ± 1	13,770 ± 100	0.27 ± 0.01	0.07 ± 0.01	7,500 ± 200
0.2	300	143.0 ± 1	14,020 ± 100	0.75 ± 0.01	0.03 ± 0.01	14,500 ± 200
	77	146.9 ± 1	14,400 ± 100	0.80 ± 0.01	0.04 ± 0.01	15,400 ± 200
0.4	300	153.1 ± 1	14,650 ± 100	0.67 ± 0.01	0.02 ± 0.01	12,200 ± 200
	77	161.5 ± 1	15,430 ± 100	1.14 ± 0.03	0.02 ± 0.02	19,200 ± 500
0.5	300	162.7 ± 1	15,370 ± 100	0.40 ± 0.01	0.01 ± 0.01	6,900 ± 200
	77	172.9 ± 1	16,320 ± 100	0.76 ± 0.03	0.04 ± 0.02	12,900 ± 500
			<u>Alloy System Pr<sub>2</sub>(Co<sub>1-x</sub>Fe<sub>x</sub>)</u>			
0.2	300	144.5 ± 1	15,030 ± 100	0.96 ± 0.2	-0.2 ± 0.05	9,400 ± 1,000
	77	140.9 ± 1	13,480 ± 300	-----	-----	-----
0.3	300	158.7 ± 1	16,310 ± 100	1.8 ± 0.2	-0.45 ± 0.05	13,900 ± 3,000
	77	178.4 ± 1	18,350 ± 100	5.5 ± 0.5	-0.07 ± 0.05	73,400 ± 3,000
0.4	300	157.5 ± 1	16,050 ± 100	1.7 ± 0.2	-0.38 ± 0.2	14,700 ± 3,000
	77	177.5 ± 1	18,080 ± 100	4.1 ± 0.5	-0.14 ± 0.2	53,100 ± 3,000

\* Measured in the c-axis direction.

basal plane magnetization at about 140°K. A discontinuous decrease in saturation magnetization was associated with this transition.

A reproduction of the thesis from which the above data were taken is presented in Appendix I.

## B. THE CRYSTAL ANISOTROPY OF $R_2(\text{Co, Fe})_{17}$ PHASES

### 1. Review of Work Done

Results of crystal anisotropy measurements have been given in three previous reports and in the preceding section of this report. These measurements included work with oriented powders,<sup>(3, 4)</sup> and single crystals.<sup>(6)</sup> The initial measurements on powders indicated the alloy system  $\text{Sm}_2(\text{Co}_{1-x}\text{Fe}_x)_{17}$  to be the most promising among those investigated for permanent magnet application. Because of this, a detailed data analysis was performed for the easy-axis portion of that system first and results have been published.<sup>(6, 19)</sup> For alloys of the type  $\text{Pr}_2(\text{Co, Fe})_{17}$  and  $\text{MM}_2(\text{Co, Fe})_{17}$ , a few selected pairs of magnetization curves for some compositions having easy c-axis magnetic symmetry were presented before, but without any data reduction except an estimate of the anisotropy field. (Only for one composition,  $\text{MM}_2(\text{Co}_{0.7}\text{Fe}_{0.3})_{17}$  were anisotropy constants calculated.)<sup>(20)</sup> As good single-phase samples became available, aligned powder samples were prepared and pairs of magnetization curves were measured on them. These were the  $R_2(\text{Co, Fe})_{17}$  systems where  $R = \text{Ce, Pr, Sm, Y}$  and  $\text{MM}$  (mischmetal). For the first four of these systems, complete sets of the curve pairs are presented, redrawn to uniform scale within each set, and systematically arranged to permit convenient comparison.

### 2. Critique of the Experimental and Analytical Methods Used

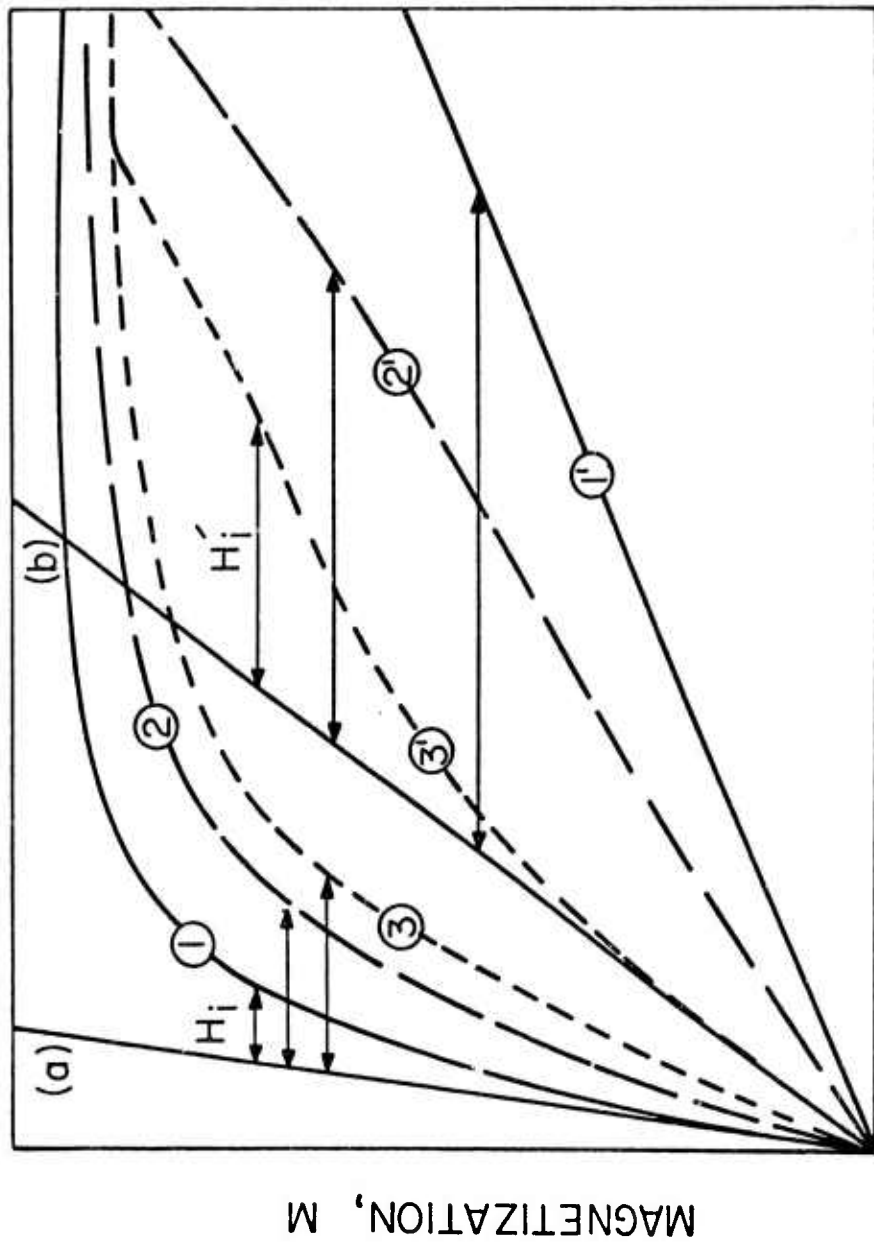
Sample preparation, the technique of measurement using an oscillating specimen magnetometer, and the methods employed in processing the measured data were discussed in a previous report.<sup>(4)</sup>

However, some additional comments concerning the interpretation of curve shapes, the accuracy of anisotropy constants deduced from them, and the general limitations of the methods of measurement and data reduction seem appropriate at this time.

The intent in making samples of fine-grained powders aligned with the aid of a magnetic field is to simulate single crystal behavior circumventing the expense and time-consuming techniques involved in the preparation of many large single crystals. Since the primary goal of our work was to identify candidate materials for fine-particle magnet development, it seemed quite adequate to employ experimental methods which allowed, first, a quick identification of those alloy compositions for which the crystallographic c-axis is the easy direction of magnetization (done by X-ray diffraction<sup>(2)</sup>), and then an estimation of the magnitude of the principal, uniaxial anisotropy energy which can be taken as an indicator whether high coercive forces may be possible. The aligned-powder-sample method is quite adequate for this latter purpose. We measure two M versus H magnetization curves with the field parallel and perpendicular to the easy direction of magnetization. In the case of alloys with easy-axis symmetry that appear to have a large enough anisotropy to be of practical interest, we determine either  $(K_1 + K_2)$  from the area between these, or  $K_1$  and  $K_2$  separately, by analyzing the shape of the "perpendicular curve" by Sucksmith and Thompson's method.<sup>(21)</sup> The results obtained by this method are quite sensitive to the crystallite alignment, and since the  $< 37 \mu\text{m}$  particles in our powder specimens are certainly not all single crystals and also have irregular external shapes that interfere with their perfect alignment, one must expect considerable inaccuracies in  $K_1$ . Although these errors are difficult to determine quantitatively, we have previously made an empirical attempt to assess the effects which the polycrystallinity of the specimen particles and poor particle alignment have on the curve shape, and to develop a correction procedure for the strong curvature of the low-field portion of the

hard-axis curve, the most obvious manifestation of poor alignment, which is attributed to wall-motion processes in the particles.<sup>(5)</sup> This graphic correction is done by extrapolating the medium-field portion of the curve ( $> 2$  kOe) to  $H = 0$ , shifting the origin of the M-scale up accordingly, and disregarding the strongly convex portion of the measured curve below about 2 kOe. It has been applied in the computation of all the anisotropy constant values reported during the course of this contract work.

Another source of error is the presence of ill defined demagnetizing fields. The precise values of the demagnetization factors to be used in shearing the measured curves before the Sucksmith-Thompson analysis are not only unknown but definitely different for the two orientations of the sample during measurement.<sup>(4)</sup> For the highly anisotropic  $\text{Sm}_2(\text{Co}_{1-x}\text{Fe}_x)_{17}$  samples in the range  $0 = x < 0.4$ , one could rightfully argue that the error made by neglecting demagnetizing fields was negligibly small. This is not the case for most of the samples on which we report here except perhaps for the "best"  $\text{Pr}_2(\text{Co,Fe})_{17}$  alloys. By neglecting the demagnetizing effects one tends to overestimate the anisotropy. We have therefore used the following correction procedure, which probably results in an overcompensation for the hard-axis demagnetizing field and, therefore, anisotropy-constant values lower than the true ones. From all the pairs of magnetization curves measured, we pick the one easy-axis and the one hard-axis curve which rise most steeply from zero field, i. e., which have the highest initial susceptibility (curves 1 and 3' in Figure 1). Assuming these to have infinite true initial susceptibility, tangents are drawn at the origin and these are considered to be the zero-internal-field lines for the respective set of curves (line (a) for all easy-axis curves and line (b) for the hard-axis curves). All curves reproduced in this report are plotted with the applied field on the H axis, measured with a Hall probe, and the demagnetizing field lines are drawn in and marked (a) and (b). Estimated internal field values,  $H_i$ , may then be determined for a given magnetization level by taking the horizontal



MAGNETIZATION, M

APPLIED FIELD,  $H_a$

Figure 1. Illustration of the Procedure Used in Correcting for the Estimated Demagnetizing Field. For all easy-axis curves (1, 2, 3), the estimated internal field strength  $H_i$  is measured from the tangent (a) to the steepest curve (1) of the set. For all hard-axis curves (1', 2', 3'), the tangent (b) to the steepest curve of this set is used as the reference line  $H_i' = 0$ .

distance between corresponding points on a magnetization curve and the appropriate demagnetizing-field line as is indicated in Figure 1.

The Sucksmith-Thompson method as applied to field aligned powders is useful only when the crystal has a unique axis of easy magnetization. For easy-plane or easy-cone symmetry, the orienting field aligns the particles with one of their several easy directions and does not impose an orientation on the c-axis. The curve shape measured with a field applied perpendicular, or at any angle, to the alignment direction is then determined by a superposition of wall-motion and spin-rotation processes; basal-plane anisotropy constants are mixed in with the uniaxial constants and the mathematical complexity of the analysis becomes prohibitive. Thus, no attempt was made to deduce anisotropy constant or field values for any samples except those which the XRD showed to have easy c-axis symmetry. It is, nevertheless, instructive to take a qualitative look at the changes in the shapes of the curves and of the area between them, which still represents a kind of anisotropy energy, through the easy-axis, easy-cone, and easy-plane regions of composition for a given  $R_2(\text{Co}_{1-x}\text{Fe}_x)_{17}$  quasi-binary system. The sets of curves shown in Figures 2 through 5 are arranged to allow such a comparison of trends. The cerium system is discussed in some detail, but the statements apply qualitatively to the other alloy systems as well.

In summary, one can say that the aligned-powder measurements are good enough for the purpose of selecting some promising materials, and rejecting others, for permanent magnet development work. Values of anisotropy constants  $K_1$  and  $K_2$  computed from powder curves can be quite accurate if, but only if, a number of favorable circumstances prevail simultaneously: the anisotropy must be single-easy-axis type and large; the powder must have a large fraction of single-crystal particles; its coercive force must be low. These conditions are, in part, conflicting and are seldom met very well. Even when they are met, no information about the anisotropy in the basal plane can be obtained from powder measurements.

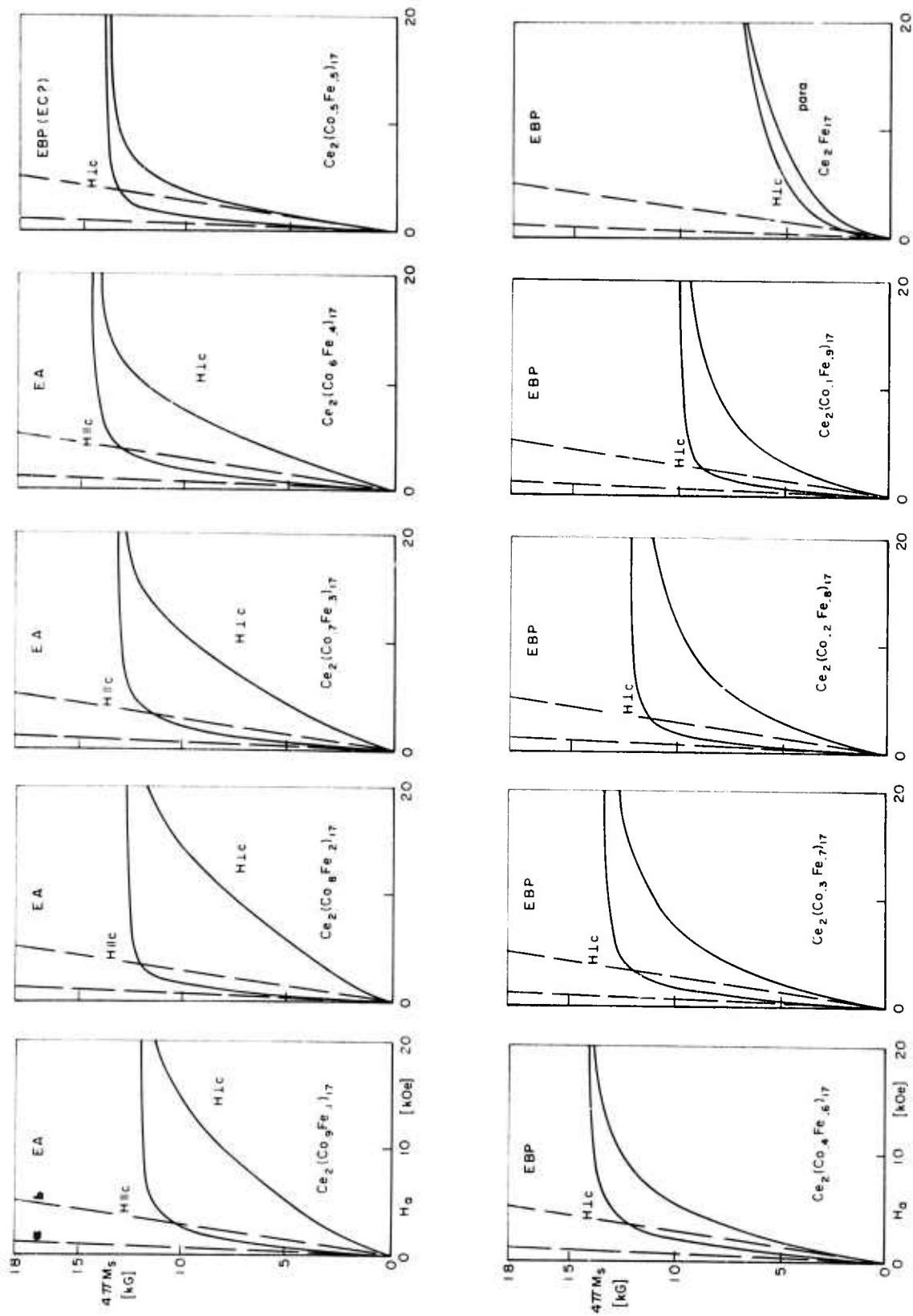


Figure 2. Pairs of Magnetization Curves Measured on Oriented Powder Samples of  $Ce_2(Co_{1-x}Fe_x)_{17}$  Alloys.

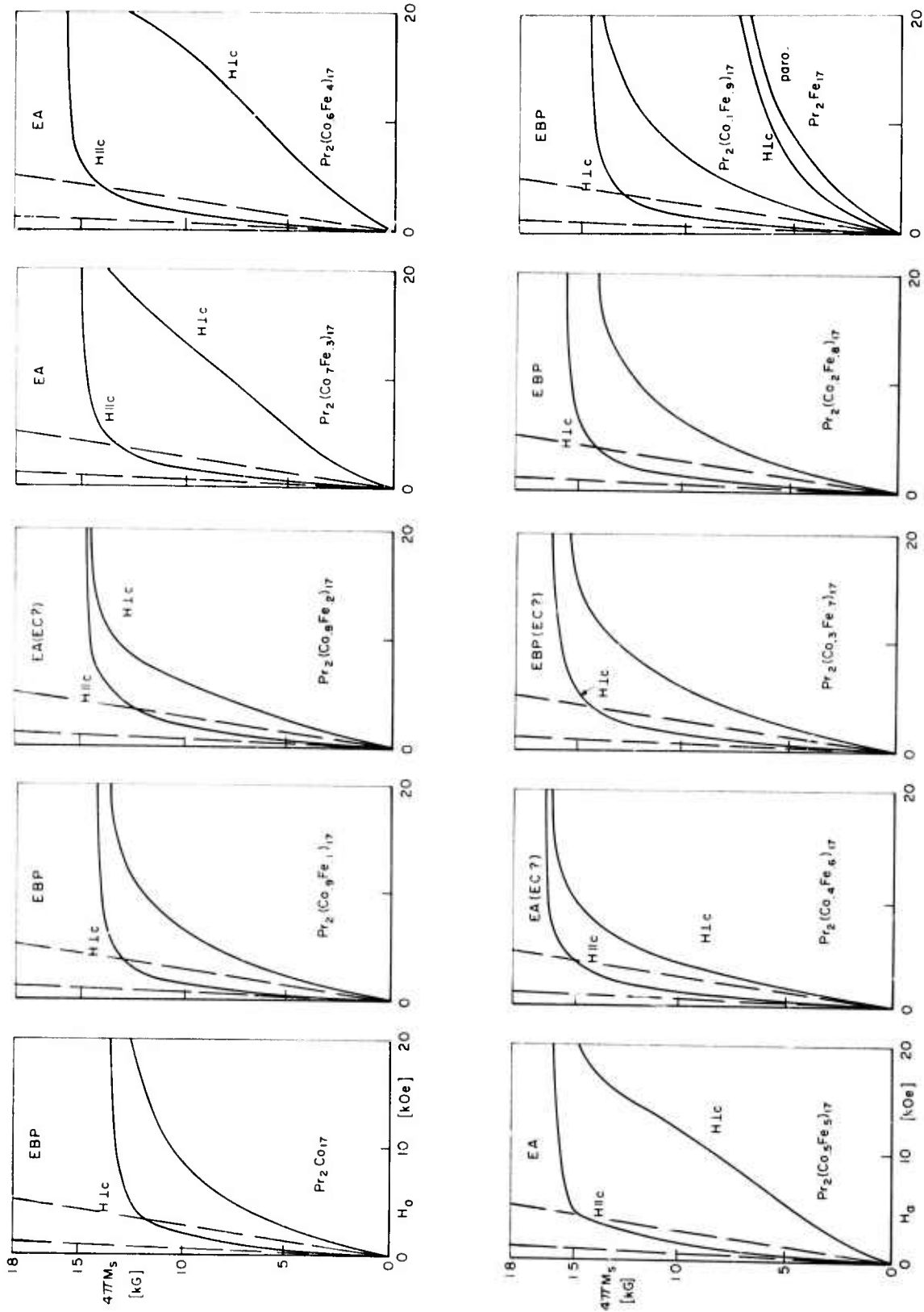


Figure 3. Pairs of Magnetization Curves Measured on Oriented Powder Samples of  $\text{Pr}_2(\text{Co}_{1-x}\text{Fe}_x)_{17}$  Alloys.

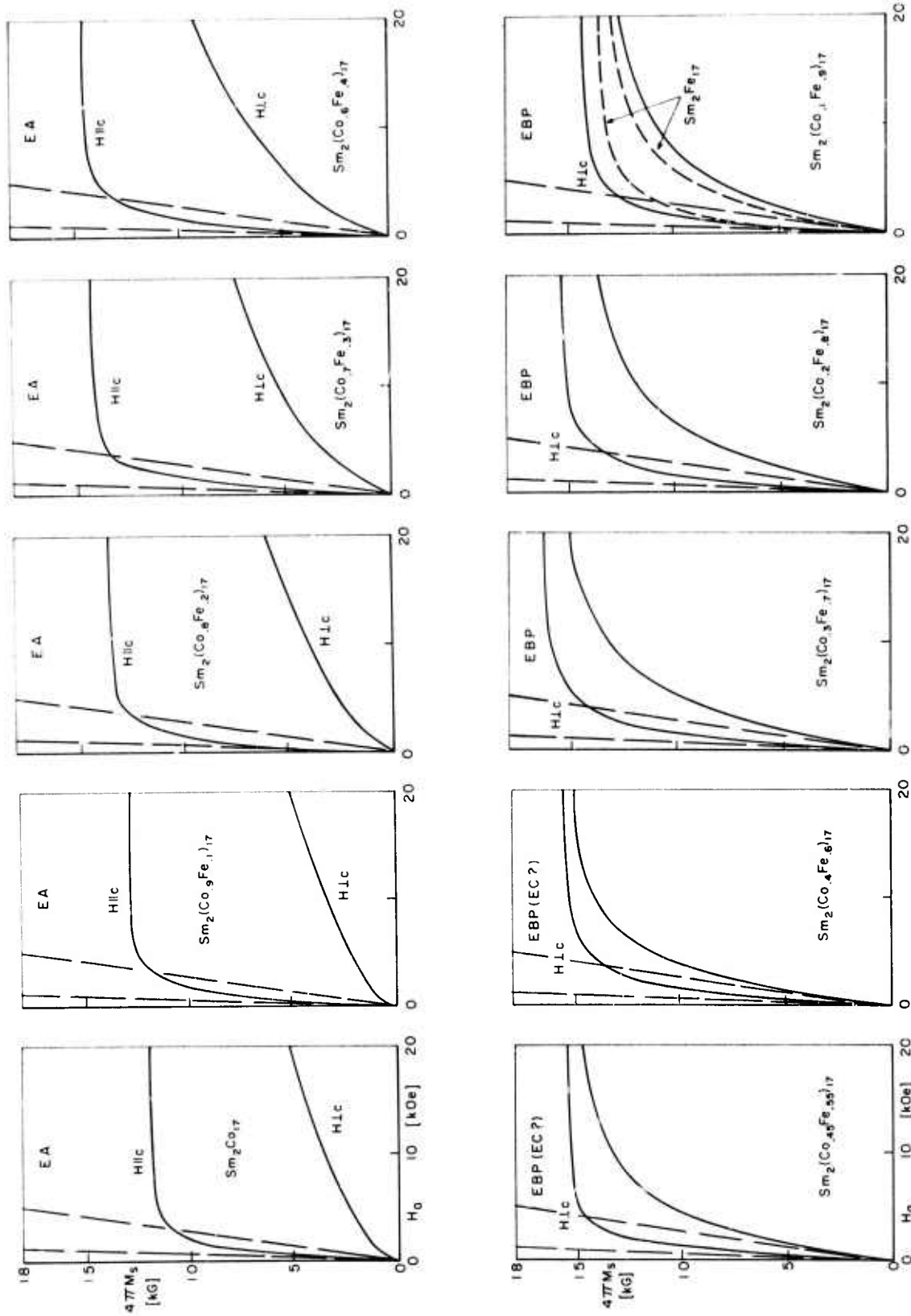


Figure 4. Pairs of Magnetization Curves Measured on Oriented Powder Samples of  $\text{Sm}_2(\text{Co}_{1-x}\text{Fe}_x)_{17}$  Alloys.

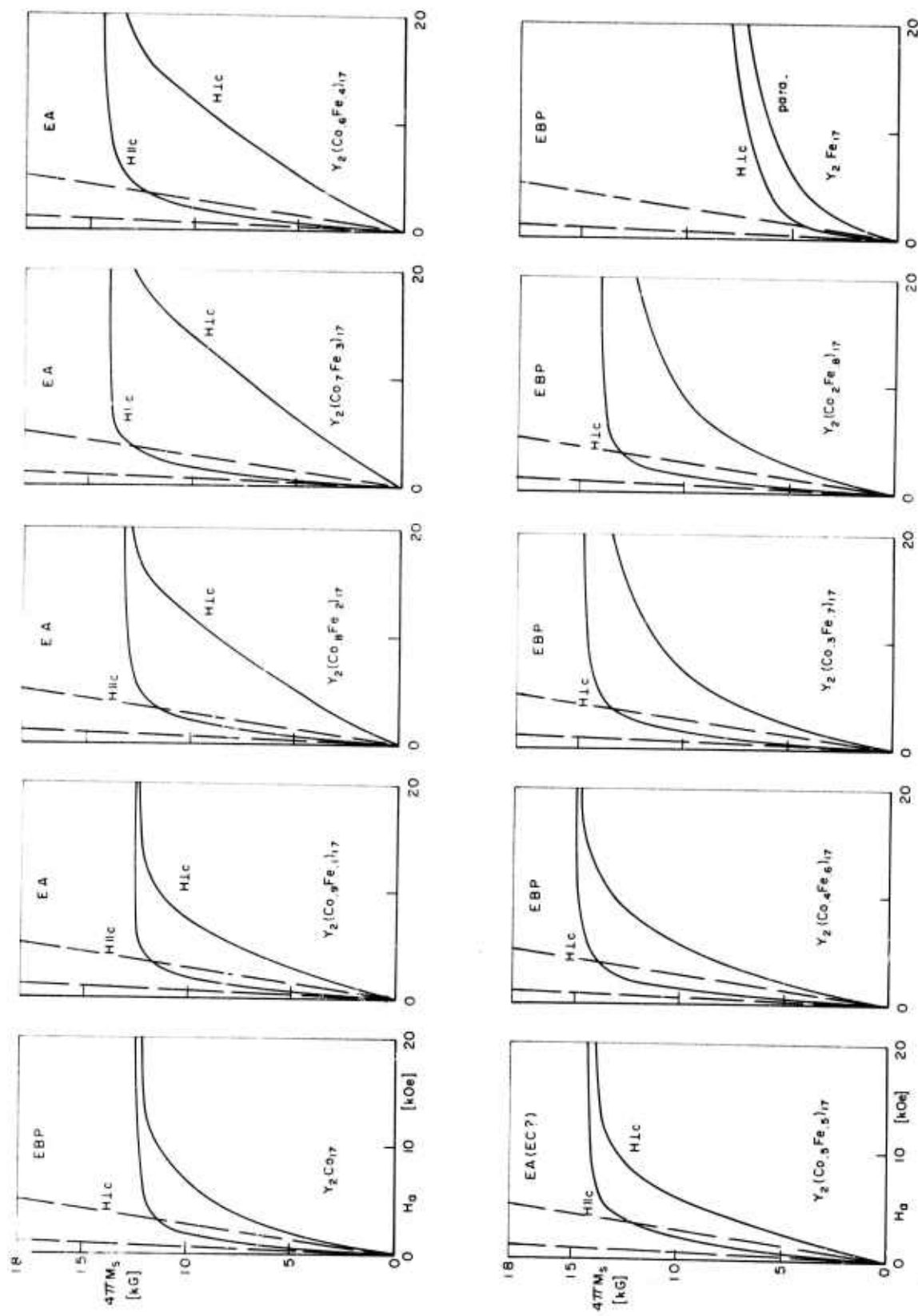


Figure 5. Pairs of Magnetization Curves Measured on Oriented Powder Samples of  $Y_2(Co_{1-x}Fe)_x_{17}$  Alloys.

Work with reasonably large single crystals (a few tenths to a few millimeters in diameters) is, therefore, absolutely indispensable for an accurate and complete description of the crystal anisotropy as it is needed for a meaningful theoretical interpretation of the data.

3. Magnetization Curve Pairs Measured on Oriented Powders

Figure 2 is a composite picture showing pairs of magnetization curves that were measured on magnetically oriented and epoxy-bonded powders of  $\text{Ce}_2(\text{Co}_{1-x}\text{Fe}_x)_{17}$  alloys. They are arranged in order of increasing iron content,  $x$ . On top of each picture is noted the magnetic symmetry as determined earlier by X-ray diffraction. (EBP = easy basal plane; EA = easy c-axis). The easy- and hard-axis curves for  $\text{Ce}_2\text{Co}_{17}$  are relatively close together; the anisotropy is small. The X-ray study indicated EBP symmetry, but the shape of the magnetization curves (low initial susceptibility for both curves) suggests that  $\text{Ce}_2\text{Co}_{17}$  may in fact have an easy cone (EC). As iron is added, EA anisotropy develops. It has its maximum near  $x = 0.2$ , with an anisotropy field of about 16 to 20 kOe, and then declines again. Near  $x = 0.5$  there is an anisotropy minimum. X-ray results indicated a flip from EA to EBP symmetry at  $x = 0.5$ , but again, there may in fact be a transition region of easy-cone symmetry in which the cone angle opens up rapidly with increasing  $x$ . This would be difficult to detect with the simple X-ray texture technique employed in the early phases of this study. In the EBP composition range, we then see again an increase in the magnitude of the anisotropy, a maximum near  $x = 0.8$ , followed by a rapid decline. The terminal compound,  $\text{Ce}_2\text{Fe}_{17}$ , which is already paramagnetic at room temperature, is almost isotropic.

The results for the other systems are qualitatively similar and the interpretation is quite analogous to that given above. The Sm-system (Figure 4) is, of course, unique among the systems investigated in that even the terminal compound  $\text{Sm}_2\text{Co}_{17}$  already has

easy-axis symmetry, and it is also distinguished by the much larger magnitude of the anisotropy. Another noteworthy fact is that  $\text{Pr}_2\text{Fe}_{17}$  and, particularly,  $\text{Y}_2\text{Fe}_{17}$  still show substantial EBP anisotropy although they are paramagnetic. These compounds are, however, much closer to their respective Curie temperature at room temperature than  $\text{Ce}_2\text{Fe}_{17}$  is. The Curie points are  $-180^\circ\text{C}$  for  $\text{Ce}_2\text{Fe}_{17}$ ,  $10^\circ\text{C}$  for  $\text{Pr}_2\text{Fe}_{17}$  and  $-29.5^\circ\text{C}$  for  $\text{Y}_2\text{Fe}_{17}$ .<sup>(22)</sup>

Finally, all four sets of curves reproduced here illustrate the composition dependence of the saturation magnetization previously reported.<sup>(23)</sup> With increasing  $x$ , the technical saturation at room temperature rises to a maximum at iron contents between  $x = 0.4$  and  $0.7$  and then decreases rapidly toward the Fe-side of the system, a consequence of the precipitous drop of the Curie point.

### C. REVIEW OF THE BINARY RARE EARTH-COBALT PHASE DIAGRAMS

A paper entitled "Revised Phase Diagrams for the Cerium-Cobalt, Praseodymium-Cobalt, and Neodymium-Cobalt Alloy Systems" was presented at the 10th Rare Earth Research Conference in Carefree, Arizona, April 30-May 3, 1973. This paper, reproduced in Appendix II, has been accepted for publication in the journal *Cobalt* and is scheduled to appear in the December 1973 issue. It is a summary of the work on these alloy systems which were discussed in detail in previous reports.<sup>(2, 4, 5)</sup>

A second paper entitled "A Review of the Binary Rare Earth-Cobalt Alloy Systems" is given in Appendix III. This paper will be presented at the 1973 Conference on Magnetism and Magnetic Materials to be held in Boston, November 13-17, 1973. The paper reviews the published phase diagrams for the Y-Co, La-Co, Ce-Co, Pr-Co, Nd-Co,

and Sm-Co alloy systems. A revised phase diagram for the La-Co system is proposed. This paper has also been submitted to the journal Cobalt and is tentatively scheduled for publication in the March 1974 issue.

#### D. LIST OF PUBLICATIONS AND PRESENTATIONS

The following is a chronological list of publications and presentations resulting from the investigations conducted during the term of ARPA support.

K. J. Strnat and J. B. Y Tsui, "Sintering of  $\text{PrCo}_5$  Permanent Magnets," Appl. Physics Letters, 18 (1971) 105.

A. E. Ray and K. J. Strnat, "Curie Temperatures and Melting Data for Some Binary and Ternary  $\text{R}_2(\text{Co}, \text{Fe})_{1.7}$  Phases," (Digest) IEEE Trans. on Magnetics, Vol. MAG-7, (1971) 656.

K. J. Strnat and J. B. Y. Tsui, "Sintering of  $\text{PrCo}_5$  Magnets with Pr-Co Alloy Addition," IEEE Trans. Magnetics, Vol. MAG-7 (1971) p. 427.

K. J. Strnat, J. Schweizer, and J. B. Y. Tsui, "Coercivity of Heat-Treated Pr-Co Powder Compacts," IEEE Trans. Magnetics, Vol. MAG-7 (1971), p. 429.

A. E. Ray and R. S. Harmer, "Lattice Constants for Mixed Intermetallic Phases of the Type  $\text{R}_2(\text{Co}_{1-x}\text{Fe}_x)_{1.7}$ ," Proceedings of the 9th Rare Earth Research Conference, Vol. 1 (1971) 368.

K. J. Strnat, J. B. Y. Tsui, and J. Schweizer, "Liquid-Phase Sintering of  $\text{PrCo}_5$  Magnets with a Sm-Co Additive," Proceedings of the 9th Rare Earth Research Conference, Blacksburg, Virginia, October 1971, Vol. I, p. 252 (P. E. Field, editor) (National Technical Information Service, US Department of Commerce, Springfield, Virginia 22151).

K. J. Strnat, J. Schweizer, and J. B. Y. Tsui, "The Crystal Structure of the Intermetallic Compounds  $\text{Pr}_2\text{Co}_{1.7}$  and  $\text{Nd}_2\text{Co}_{1.7}$ ," Proceedings of the 9th Rare Earth Research Conference, Blacksburg, Virginia, October 1971, Vol. I, p. 9 (P. E. Field, editor)(National Technical Information Service, US Department of Commerce, Springfield, Virginia 22151).

K. J. Strnat, J. B. Y. Tsui, and R. S. Harmer, "An Evaluation of the Utility of a  $(\text{Pr}, \text{Nd})\text{Co}_5$  Alloy for Permanent Magnets," J. Applied Physics 42, (1971) 1539.

- K. J. Strnat, "Current Problems and Trends in Permanent Magnet Materials" (invited) AIP Conference Proceedings Series, No. 5: Magnetism and Mag. Materials 1971, Part 2, p. 1047 (C. D. Graham and J. J. Rhyne, editors), Am. Inst. of Physics, New York, 1972.
- K. J. Strnat, J. B. Y. Tsui, D. J. Iden, and A. J. Evers, "The Effect of Intrinsic Magnetic Properties on Permanent Magnet Repulsion," IEEE Trans. Magnetics, Vol. MAG-8, (1972) p. 188.
- A. E. Ray and K. J. Strnat, "Easy Directions of Magnetization in Ternary  $R_2(\text{Co}, \text{Fe})_{17}$  Phases," IEEE Trans. on Magnetics, Vol. MAG-8 (1972) 516.
- K. J. Strnat, "Hardmagnetic Properties of Rare Earth-Transition Metal Alloys," (invited) IEEE Trans. Magnetics, Vol. MAG-8, (1972), p. 516.
- A. E. Ray and K. J. Strnat, "Metallurgical and Magnetic Properties of the Intermetallic Phases  $R_2(\text{Co}, \text{Fe})_{17}$ ," Proceedings of the 7th Rare Earth Metals Conference, September 12-17, 1972, Moscow, USSR.
- K. J. Strnat, J. B. Y. Tsui, H. Mildrum, and C. W. Shanley, "Magnetic Properties of the Intermetallic Phase  $\text{MM}_2(\text{Co}_7\text{Fe}_3)_{17}$ ," AIP Conference Proceedings No. 10, Part 1, Magnetism and Mag. Materials 1972, p. 623. Am. Inst. of Physics, New York 1973.
- K. J. Strnat, H. Mildrum, M. Hartings, and J. Tront, "Magnetic Properties of the Intermetallic Phases  $\text{Sm}_2(\text{Co}, \text{Fe})_{17}$ ," AIP Conference Proceedings, No. 10 Part 1, Magnetism and Mag. Materials 1972, p. 618. Am. Inst. of Physics, New York 1973.
- A. E. Ray, K. J. Strnat, R. S. Harmer, and M. S. Hartings, "Instability of Some  $\text{Ce}_2(\text{Co}_{1-x}\text{Fe}_x)_{17}$  Phases," AIP Conference Proceedings on Magnetism and Magnetic Materials 1972, No. 10 Part 1, p. 613.
- K. J. Strnat, H. Mildrum, J. Tront, and M. Hartings, "Saturation Magnetization of Rare Earth-Transition Metal 1 Phases of the Type  $R_2(\text{Co}, \text{Fe})_{17}$ ," Proceedings of the 10th Rare Earth Research Conference, Vol. 1, p. 476, USAEC Tech. Inf. Center, Oakridge, Tennessee, 1973.
- K. J. Strnat and A. J. Kleman, "Machinable and Solderable Composite Magnets based on Rare Earth-Cobalt," Paper 6-1, 1973 INTERMAG Conference. (To be published in 1973).
- A. E. Ray, "A Review of the Cobalt-Rare Earth Binary Alloy Systems," Invited paper for the 1973 International Magnetism Conference, April 24-27, 1973, Washington, D. C. To be published in Cobalt, March 1974.

A. E. Ray, R. S. Harmer, and A. T. Biermann, "Revised Phase Diagrams for the Ce-Co, Pr-Co, and Nd-Co Alloy Systems," Proceedings of the 10th Rare Earth Research Conference, April 30-May 3, 1973, Carefree, Arizona, Vol. II, p. 711. To be published in Cobalt, December 1973.

C. W. Shanley and R. S. Harmer, "Magnetic Measurements on Single Crystals in the  $Y_2(Co_{1-x}Fe_x)_{17}$  and  $Pr_2(Co_{1-x}Fe_x)$  Alloy Systems." To be presented at the 19th Conference on Magnetism and Magnetic Materials, November 1973.

## REFERENCES

1. A. E. Ray and K. J. Strnat, "Research and Development of Rare Earth-Transition Metal Alloys as Permanent Magnet Materials," First Progress Report, AFML-TR-71-53, March 1971, Air Force Materials, Wright-Patterson Air Force Base, Ohio.
2. Second Progress Report, AFML-TR-71-210, October 1971.
3. Third Progress Report, AFML-TR-72-99, April 1972.
4. Fourth Progress Report, AFML-TR-72-202, August 1972.
5. R. M. Bozorth, Ferromagnetism, D. Van Nostrand Co., New York (1951) pp. 194-195.
6. Fifth Progress Report, AFML-TR-73-112, May 1973.
7. Y. Tawara and H. Senno, Japan J. Appl. Physics, 7 (1968) 966.
8. J. B. Y. Tsui and K. J. Strnat, IEEE Trans. Magnetics, MAG-7 (1971) 427.
9. A. E. Ray and G. I. Hoffer, Proc. 8th Rare Earth Research Conference, Reno, Nevada, Vol. II (1970) 524.
10. J. Schweizer, "Research on Rare Earth-Cobalt Alloys and Compounds," AFML-TR-72-82, Air Force Materials Laboratory, Wright-Patterson Air Force Base, Ohio, May 1972.
11. K. H. J. Buschow and A. S. Van der Goot, J. Less-Common Metals, 14 (1968) 323.
12. F. Lihl, J. R. Ehold, H. R. Kirchmayr, and H. D. Wolf, Acta Physica Austriaca, 30 (1969) 164.
13. K. H. J. Buschow, J. Less-Common Metals, 29 (1972) 283.
14. K. J. Strnat, W. Ostertag, N. J. Adams, and J. C. Olson, Proc. 5th Rare Earth Research Conference, Iowa State University, Ames, Iowa, Book 5 (1965) 67.
15. K. H. J. Buschow, Philips. Res. Repts., 26 (1971) 49.

16. J. Pelleg and O. N. Carlson, *J. Less-Common Metals*, 9 (1965) 281.
17. J. B. Y. Tsui and K. J. Strnat, *Appl. Phys. Letters*, 18 (1971) 107.
18. F. F. Westendorp, *J. Appl. Physics*, 42 (1971) 5727.
19. H. F. Mildrum, M. S. Hartings, K. J. Strnat and J. G. Tront, "Magnetic Properties of the Intermetallic Phases  $\text{Sm}_2(\text{Co}, \text{Fe})_{17}$ ," AIP Conference Proceedings, No. 10, Magnetism and Magnetic Materials, (1972) 618-622.
20. J. B. Y. Tsui, H. F. Mildrum, K. J. Strnat and C. W. Shanley, "Magnetic Properties of the Intermetallic Phase  $\text{MM}_2(\text{Co}_{.7}\text{Fe}_{.3})_{17}$ ," AIP Conference Proceedings, No. 10, Magnetism and Magnetic Materials, (1972) 623-627.
21. W. Sucksmith and J. E. Thompson, *Proc. Royal Soc. (London)* V. 225 (1954) 362.
22. K. J. Strnat, G. I. Hoffer and A. E. Ray, *IEEE Trans. Magnetics*, MAG-2 (1966) 489.
23. H. Mildrum, J. Tront, M. Hartings and K. J. Strnat, "Saturation Magnetization of Rare Earth-Transition Metal Phases of the Type  $\text{R}_2(\text{Co}, \text{Fe})_{17}$ ," Proceedings 10th Rare Earth Research Conference, Vol. I (1973) 476.

APPENDIX I

MAGNETIC MEASUREMENTS ON SINGLE CRYSTALS IN THE  
 $Y_2(Co_{1-x}Fe_x)_{17}$  AND  $Pr_2(Co_{1-x}Fe_x)_{17}$  SYSTEMS

Submitted in Partial Fulfillment of the Requirements for the  
Degree of Master of Science in Engineering

by

Charles W. Shanley

The School of Engineering

UNIVERSITY OF DAYTON

Dayton, Ohio

April 4, 1973

## ACKNOWLEDGEMENTS

The author would like to take this opportunity to express his appreciation for the sponsorship of this work by the Advanced Research Project Agency of the Department of Defense under Contract No. F33615-70-C-1625, monitored by the Air Force Materials Laboratory, Air Force Systems Command, Wright-Patterson Air Force Base, Ohio.

I wish to express my sincerest thanks to my thesis advisor, Dr. Richard S. Harmer, for his advice, assistance, and patience; and to Dr. Karl J. Strnat and Dr. Alden E. Ray for the many technical discussions which made this work possible. Special thanks are given to Herbert Mildrum for his instruction and assistance in the use of the magnetometer.

My appreciation is also extended to all the members of the University of Dayton Magnetics Laboratory for their assistance and cooperation in this work.

## ABSTRACT

Single crystals of the compositions  $Y_2(\text{Co}_{1-x}\text{Fe}_x)_{17}$ ,  $x = 0.1, 0.2, 0.4, 0.5$ , and  $\text{Pr}_2(\text{Co}_{1-x}\text{Fe}_x)_{17}$ ,  $x = 0.2, 0.3, 0.4$ , were grown from single phase alloy buttons by long term annealing. Measurements of the room temperature and liquid nitrogen temperature saturation magnetization and anisotropy were made using an oscillating specimen magnetometer. The temperature variation of the magnetization was also investigated.

All of these alloys have the magnetically favorable c-axis magnetocrystalline anisotropy at room temperature. It was found, however, that cooling  $\text{Pr}_2(\text{Co}_{0.8}\text{Fe}_{0.2})_{17}$  below  $140^\circ\text{K}$  in a 140 kOe field caused this composition to develop an easy direction of magnetization in the basal plane of the hexagonal cell. A qualitative explanation of this phenomenon is given, based on the concept of a cone of easy directions whose opening angle is a function of temperature and applied field.

The highest saturation magnetization observed was for  $\text{Pr}_2(\text{Co}_{0.7}\text{Fe}_{0.3})_{17}$  (16,300 gauss). This alloy also had the highest room temperature anisotropy field (24 kOe).

## TABLE OF CONTENTS

I.	Introduction . . . . .	1
II.	Review of the Literature . . . . .	3
III.	Experimental Procedures . . . . .	8
	A. Alloy Preparation . . . . .	8
	B. Single Crystal Growth . . . . .	10
	C. Magnetic Measurements . . . . .	12
IV.	Results and Discussion . . . . .	16
	A. $Y_2(Co_{1-x}Fe_x)_{17}$ . . . . .	16
	B. $Pr_2(Co_{1-x}Fe_x)_{17}$ . . . . .	19
V.	Summary . . . . .	30
	References . . . . .	31
	Appendix . . . . .	33

## LIST OF TABLES

1	Analysis of Metals Used in Alloy Preparation (in PPM) .	9
2	Summary of $Y_2(Co_{1-x}Fe_x)_{17}$ Data . . . . .	17
3	Summary of $Pr_2(Co_{1-x}Fe_x)_{17}$ Data . . . . .	21

## LIST OF FIGURES

1	Demagnetization Curves for Some Magnetic Materials . . .	2
2	Curie Temperatures of the $R_2(Co_{1-x}Fe_x)_{17}$ Alloys . . . .	6
3	Magnetocrystalline Anisotropy of the $R_2(Co_{1-x}Fe_x)_{17}$ Alloys . . . . .	6
4	Magnetometer with Dewar Attached . . . . .	15
5	Magnetization Curves for $Y_2(Co_{0.6}Fe_{0.4})_{17}$ . . . . .	18
6	Temperature Dependence of Magnetization for Four $Y_2(Co, Fe)_{17}$ Alloys . . . . .	20
7	Magnetization Curves for $Pr_2(Co_{0.8}Fe_{0.2})_{17}$ . . . . .	22
8	Magnetization in the Easy Basal Plane. . . . .	24
9	Magnetization in the Hard C-Axis . . . . .	25
10	Temperature Dependence of Magnetization for Two $Pr_2(Co_{1-x}Fe_x)_{17}$ Alloys . . . . .	26
11	Temperature Dependence of Magnetization for Two $Pr_2(Co_{0.8}Fe_{0.2})_{17}$ Crystals . . . . .	28
12	Determination of the Angle $\phi$ . . . . .	35
13	Determination of Anisotropy Constants . . . . .	35

## I. INTRODUCTION

The ideal permanent magnet should exhibit high saturation magnetization and a high intrinsic coercivity. It should have a square hysteresis loop and a large energy product. In order to resist demagnetization at elevated temperatures, it should have a high Curie temperature. Finally, it should be both inexpensive and easy to make.

Both raw materials and manufacturing costs of alnico magnets are moderately expensive. They have the advantage of a very high saturation magnetization, 8-13 kG, but their energy product is severely limited by a very small coercive force, <2000 Oe. Ferrites are made from inexpensive raw materials and have a moderately high coercive force, 2-3 kOe, but they have a low saturation magnetization, 4 kG. In addition, their magnetic properties deteriorate with an increase in temperature much more quickly than those of alnicos. Platinum-cobalt magnets exhibit both high saturation and coercivity, 6.5 kG and 4.5 kOe, respectively, but a magnet of 75 wt % platinum is too expensive for virtually all commercial applications.

Rare earth-cobalt magnets combine many of the favorable properties of alnicos, ferrites, and platinum-cobalt magnets. Some rare earth-cobalt magnets, such as  $\text{SmCo}_5$ , have high Curie temperatures, high saturation magnetization and intrinsic coercivity, and an almost perfectly square hysteresis loop. Their magnetic properties exceed

those of platinum cobalt and they cost far less. Figure 1 shows the demagnetization curves for some common magnetic materials and the curve for commercially prepared  $\text{SmCo}_5$ .

Recently, some research has been done on the  $\text{R}_2\text{Co}_{17}$  inter-metallic compounds, where R is one of the rare earth metals Pr, Sm, Y, Nd, or Ce. Because of the increased cobalt content, these alloys have a somewhat higher saturation magnetization than the  $\text{RCO}_5$  phases, and also exhibit higher Curie temperatures.<sup>1, 2</sup> Substituting Fe for Co produces a ternary  $\text{R}_2(\text{Co}_{1-x}\text{Fe}_x)_{17}$  phase with still higher saturation.<sup>3</sup>

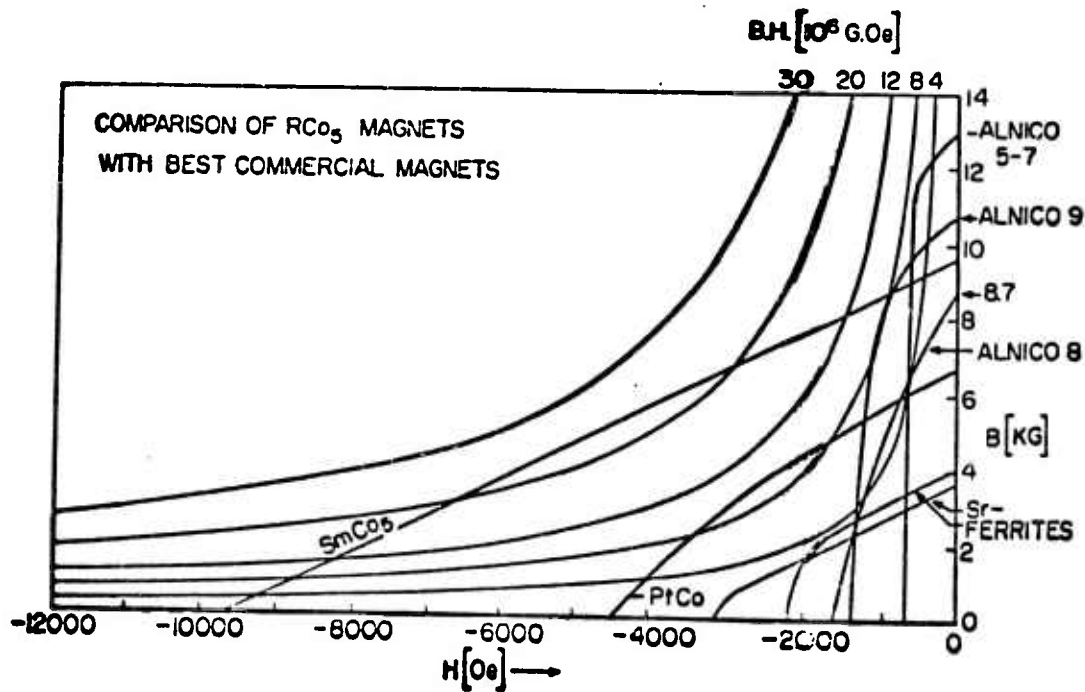


Figure 1. Demagnetization Curves for Some Magnetic Materials.

## II. REVIEW OF THE LITERATURE

The first rare earth-cobalt magnets to be developed were the intermetallic phases  $\text{RCo}_5$ , where R is one of the rare earth metals Ce, Pr, Nd, Sm, or Y. Studies by Hubbard, Adams, and Gilfrich,<sup>4</sup> Nesbit et al,<sup>5</sup> and Nassau et al,<sup>6</sup> prompted Hoffer and Strnat<sup>7</sup> to investigate the magnetocrystalline anisotropy of some of the  $\text{RCo}_5$  alloys. This stimulated extensive work in the field, including metallurgical and crystallographic studies of the rare earth-cobalt phase diagrams,<sup>8</sup> sintering techniques,<sup>9-12</sup> and magnetic measurements.<sup>13</sup> Work in these areas is continuing, but already some of the  $\text{RCo}_5$  magnets, specifically  $\text{SmCo}_5$ , have replaced the more expensive and less efficient platinum-cobalt magnets in some applications such as in traveling wave tubes.

In principle,  $\text{R}_2\text{Co}_{17}$  alloys present certain advantages over  $\text{RCo}_5$  alloys for some applications of permanent magnets requiring high fields. They are less expensive than  $\text{RCo}_5$  compounds, since cobalt is much less expensive than most rare earths, and the  $\text{R}_2\text{Co}_{17}$  phases contain approximately 10 wt % less rare earth metal than the  $\text{RCo}_5$  phases. Secondly, they have a higher saturation magnetization,<sup>2</sup> again brought about by the higher cobalt content. Thirdly, they have higher Curie temperatures, often as much as  $200^\circ\text{C}$  higher than the corresponding  $\text{RCo}_5$  phase. The only major disadvantage is that their intrinsic

coercivity, while still better than commercial magnets, is still quite inferior to the  $\text{RCO}_5$  alloys.

The intrinsic coercivity of rare earth-cobalt magnets is due primarily to magnetocrystalline anisotropy.<sup>14</sup> In the  $\text{RCO}_5$  alloys, the easy direction of magnetization is the c-axis of the hexagonal cell. To reverse the direction of magnetization of the cell, the moments must be rotated  $180^\circ$  through the hard direction (that is, through the hexagonal cross section). Schweizer<sup>15</sup> investigated the magnetocrystalline anisotropy of the  $\text{R}_2\text{Co}_{17}$  and  $\text{R}_2\text{Fe}_{17}$  alloys, and found the easy direction of magnetization in the light rare earth alloys to be the hexagonal basal plane in all cases except  $\text{Sm}_2\text{Co}_{17}$ . Since magnetization reversal in a material with an easy basal plane anisotropy may be easily accomplished by the rotation of the moments in the basal plane, it would seem that only  $\text{Sm}_2\text{Co}_{17}$  had any potential as an important magnet material.

Since  $\text{R}_2\text{Co}_{17}$  and  $\text{R}_2\text{Fe}_{17}$  alloys are isomorphous, ternary alloys of the composition  $\text{R}_2(\text{Co}_{1-x}\text{Fe}_x)_{17}$  offer interest as permanent magnet materials. Since iron is less expensive than cobalt, these alloys should be even less expensive than the  $\text{R}_2\text{Co}_{17}$  compounds. Further, iron has a higher saturation magnetization than cobalt, so it would seem reasonable that such a substitution would increase the saturation of the ternary alloys. Indeed,  $\text{Co}_{1-x}\text{Fe}_x$  with  $x = 0.5$  has the highest saturation magnetization of any substance, including both pure iron and pure cobalt. Strnat, Hoffer, and Ray<sup>16</sup> have reported the  $\text{R}_2\text{Fe}_{17}$  alloys to have low

Curie temperatures, making them unsuitable materials for permanent magnets, while those of  $R_2Co_{17}$  are very high. The  $R_2(Co_{1-x}Fe_x)_{17}$  alloys have high Curie points, normally above  $700^\circ C$ , for values of  $x$  up to 0.5.<sup>19</sup> Figure 2 shows the compositional dependence of the Curie temperature for several  $R_2(Co_{1-x}Fe_x)_{17}$  alloys.

In 1971 it was found that these substitutions of Fe for Co in  $R_2(Co_{1-x}Fe_x)_{17}$  alloys could induce the magnetically favorable c-axis magnetocrystalline anisotropy over a broad range of compositions when  $R = Ce, Pr, Sm, Y,$  and Ce-rich mischmetal (MM).<sup>17, 18</sup> Figure 3 shows these regions of c-axis anisotropy.

Saturation magnetization measurements on loose powder samples<sup>3</sup> indicated values as much as 50% greater than the  $RCo_5$  alloys. Preliminary measurements of the anisotropy were made on powder samples aligned in a magnetic field and bonded with epoxy.<sup>19</sup>

Loose packed powder measurements give a good approximation of the saturation magnetization, but are subject to oxidation problems and imperfect alignment of the grains, either of which prevent technical saturation from being attained. Anisotropy measurements on pseudo-single crystals made of epoxy bonded powders suffer from both these problems. In addition, the demagnetization correction can only be approximated. Measurements on single crystals avoid both these

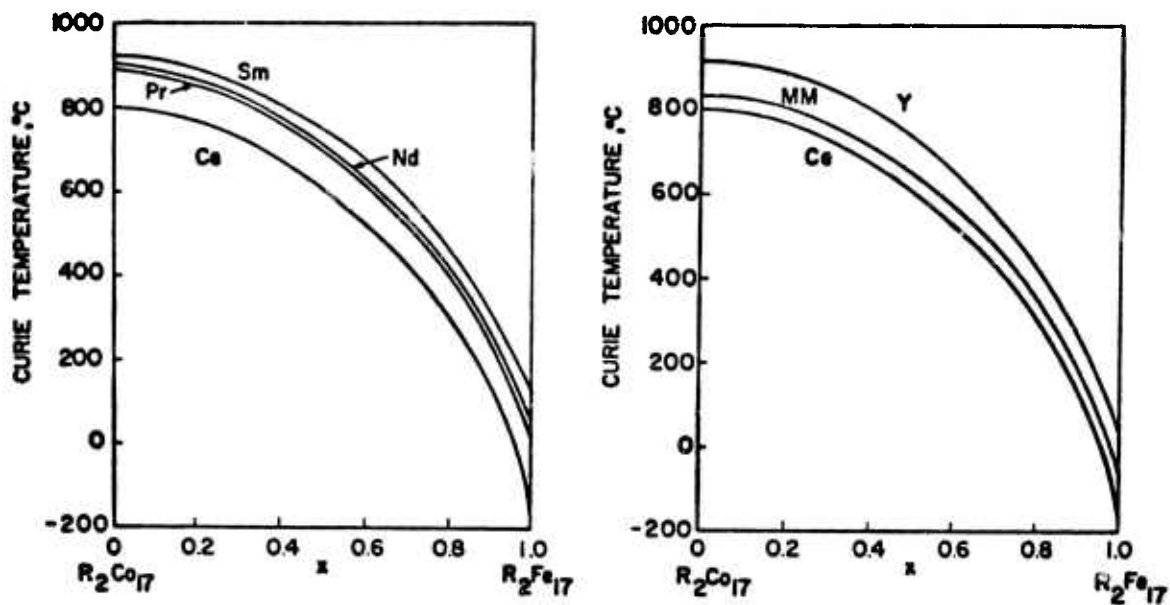


Figure 2. Curie Temperatures of the  $R_2(Co_{1-x}Fe_x)_{17}$  Alloys.

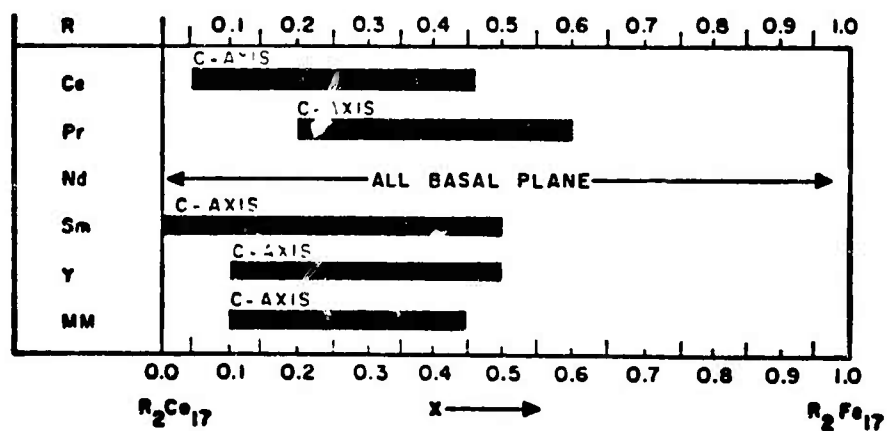


Figure 3. Magnetocrystalline Anisotropy of the  $R_2(Co_{1-x}Fe_x)_{17}$  Alloys.

problems. Oxidation effects are reduced to a minimum, and complete alignment of the dipoles is assured. The demagnetization factor may be determined from an examination of the specimen's geometry.

### III. EXPERIMENTAL PROCEDURES

#### A. ALLOY PREPARATION

Rare earth, cobalt, and iron ingots were obtained from the Lunex Company, the African Metals Corporation, and the Materials Research Corporation. Typical analyses of these materials are shown in Table 1.

The alloys were prepared in an inert gas filled arc furnace. Predetermined quantities of rare earth and transition metals in 40-gram quantities were placed in a copper hearth, and the furnace chamber evacuated to 0.1 Torr. The system was then flushed with a 75% Argon-25% Helium mixture, and the entire process repeated two more times. The final chamber pressure was 300 Torr.

The component metals were co-melted using a predetermined excess of rare earth (normally <3 wt %) to correct for non-rare earth impurities and vaporization losses. After the buttons had been melted, they were inverted and re-melted three or four times to increase homogeneity. The arc melted buttons were further homogenized by wrapping the alloys in tantalum foil and heating them for 24-196 hours in a vacuum at temperatures approximately 200° below the melting point. Standard metallographic techniques were used to check for the presence of a second phase in both the as-cast and annealed buttons.

TABLE 1

ANALYSIS OF METALS USED IN ALLOY PREPARATION (IN PPM)

Element	Pr	Co(1)	Co(2)	Fe	Element	Pr	Co(1)	Co(2)	Fe
H	*	*	*	<2	Mo	*	*	*	<50
N	12	*	*	<3	Ta	<10	*	*	<10
O	515	*	*	78	Pb	----	4	<1	<10
C	*	70	40	30	Y	*	*	*	*
F	*	*	*	*	La	<10	*	*	*
B	<50	*	*	*	Pr	*	*	*	*
Na	<5	*	*	*	Ni	<50	*	*	*
Mg	<5	----	2	<5	Sm	<5	*	*	*
Al	---	----	3	<10	Gd	----	*	*	*
Si	<50	20	<10	35	Tb	<50	*	*	*
S	*	30	<8	30	Dy	<5	*	*	*
Cl	*	*	*	*	Ho	<50	*	*	*
K	---	----	----	*	Er	<100	*	*	*
Ca	<200	----	<10	<5	Other R. E.	<5	*	*	*
Cr	<1	----	----	10					
Ti	---	*	*	*	Sm	*	*	*	<40
Mn	---	5	3	20	W	*	*	*	<10
Fe	---	30	400	*	V	*	*	*	<10
Co	<1	*	*	10					
Ni	<1	430	120	10	*	Not Reported			
Cu	<1	20	10	40	---	Not Detected			
Zn	<50	30	33	<10	Co(1)	African Metals Corporation.			
Ge	*	*	*	*	Co(2)	Materials Research Corporation			
Zn	---	*	*	<10	Fe	From Materials Research Corporation			
					Pr	From Lunex Company			
					Y	From Air Force Materials Laboratory 99.9% Pure, Source Unknown			

In addition, Debye-Scherrer X-ray diffraction patterns were taken of the annealed buttons to check for a second phase and to determine the lattice constants.

## B. SINGLE CRYSTAL GROWTH

Single phase materials were further heat treated to induce grain growth. The furnace used for this purpose was a high vacuum tube furnace; temperature was controlled to  $\pm 1^{\circ}\text{C}$ . The sample temperature was measured with a chromel-alumel thermocouple placed under the sample.

The tube was evacuated to a pressure of better than  $10^{-6}$  Torr, and the sample heated to about  $200^{\circ}\text{C}$  to outgas the tube. After baking, the tube was backfilled with helium to two psi positive pressure, and the pressure maintained throughout the heat treatment by a spring loaded safety valve. The furnace temperature was slowly increased to bring the sample up to the desired temperature, about  $20^{\circ}\text{C}$  below the melting points, where it was maintained for 7-10 days. After this treatment, the button was examined for single crystals.

The buttons were broken into a few large pieces and examined with the aid of a stereo microscope at magnifications of 10 to 45 x. The crystals were removed from the button with a dental pick and forceps. Visually, the single crystals were characterized by smooth sides and sharp edges. The crystals ranged from 0.1 to 2 mm in length and were usually elongated and irregular. Each crystal selected was

lightly etched in nitric acid to try to reveal grain boundaries which would indicate polycrystallinity. Often small crystals were discovered along the edge of a larger crystal which could be chipped off.

Each crystal was mounted on a glass fiber with a drop of mucilage and placed on a goniometer mount. Back reflection Laue patterns were taken to check for obvious flaws such as polycrystallinity or twinning. The goniometer head was rotated  $180^{\circ}$  and a second shot made of the other half of the crystal. If no polycrystallinity was indicated, an attempt to spheroidize the crystal was made using a race track spheroidizer.\*

After an attempt at spheroidizing had been made, the pseudo-spherical crystals were heavily etched in nitric acid to remove the disturbed surface layer and any metal dust which might remain on the crystal. Each crystal was then remounted on a glass fiber and a new series of Laue diffraction patterns were taken. The crystal was oriented along a major crystallographic direction, usually the c-axis, and then rotated  $180^{\circ}$  to check for an identical pattern on the other hemisphere. Normally, the crystal was smaller than the beam diameter, so that an entire hemisphere could be mapped in one exposure. When the crystal diameter exceeded the beam diameter, multiple pictures were taken. If the crystal proved to be a single crystal, free from defects such as twinning, it was cleaned in acetone in an ultrasonic cleaner and embedded in epoxy.

---

\* Nonius compressed air race track spheroidizer.

The crystals were weighed on an analytical balance and pre-magnetized in a 20 kOe field before potting in epoxy for the magnetometer measurements. The standard sample holder was designed to hold a cylindrical slug 4 mm in diameter and 4.5 mm long. Each crystal was suspended in the center of an epoxy slug of these dimensions. Originally the single crystal was simply dropped into the mold with the liquid epoxy and the mold placed between the poles of an electromagnet, but it was observed that this produced too much uncertainty in the position of the crystal in the epoxy cylinder. Instead, the epoxy was allowed to harden in the mold and a small cavity was machined out of each cylinder so that the crystal would be held at the correct height from the ends and a uniform distance from the sides of the cylinder. The mold with the crystal and some fresh epoxy was then placed in a 20 kOe field. Over a period of a few hours, the epoxy hardened and fixed the orientation of the crystal so that the crystal's easy direction of magnetization was parallel to the applied field.

### C. MAGNETIC MEASUREMENTS

Room temperature and low temperature measurements were made using an oscillating specimen magnetometer described by Mildrum.<sup>20</sup> For room temperature saturation and anisotropy measurements, the magnet geometry permitted an applied field of 20 kOe. Calibration was accomplished using a 190 mg nickel sample. A spherical nickel sample was used to check the error induced by

purposely displacing the sample from the center of the epoxy mount. It was found that an error of 2% in the magnetization measurements and 5% in the anisotropy measurements could be introduced by a poorly centered sample. In the actual experimental work, great care was taken to insure that the sample was positioned as precisely as possible.

The samples were aligned in the sample holder by placing the sample and holder between the poles of an electromagnet. The sample rotated in its holder and aligned its easy direction of magnetization with the applied field. A plastic setscrew was used to fix the orientation of the sample. The sample rod is then placed in the magnetometer in the same configuration as when the sample was aligned, that is, so that the easy direction of magnetization was parallel to the magnetic field. The field was slowly increased to 20 kOe over a 10-minute period, and the easy axis plot of magnetization versus applied field was obtained on an x-y recorder. A digital printer provided a permanent record of the saturation magnetization with a higher resolution than the x-y recorder could provide.

After the field had been reduced to zero, the sample rod was rotated  $90^{\circ}$  so as to make the applied field in the direction of hardest magnetization. The field was again brought up to 20 kOe over a 25-minute period and the hard axis curve obtained. The extremely slow speed of this trace was necessitated by the small size and moderate noise level of the samples in general and by the fact that the hard axis curve is needed to determine the anisotropy constants.

Low temperature anisotropy measurements were obtained in much the same manner. The addition of a dewar to contain the liquid nitrogen (see Figure 4) necessitated increasing the magnet gap, which reduced the obtainable field to 14 kOe. The phenolic protection tube surrounding the sample rod was continuously flushed with helium cooled to liquid nitrogen temperature to prevent ice or frost from forming on the pickup coils or the rod itself. The sample temperature was monitored with a copper-constantan thermocouple placed in the sample rod about 1 cm from the sample.

The dewar was filled with a sufficient quantity of liquid nitrogen to cool the sample to the neighborhood of  $77^{\circ}\text{K}$  and maintain that temperature for about one hour during which time the anisotropy traces were obtained. After the liquid nitrogen in the dewar had fallen to a certain level the sample would begin to heat up to room temperature, a process which normally required at least 90 minutes. The applied field was held at 14 kOe during this period and a record of the variation of magnetization with temperature at fixed field was obtained.

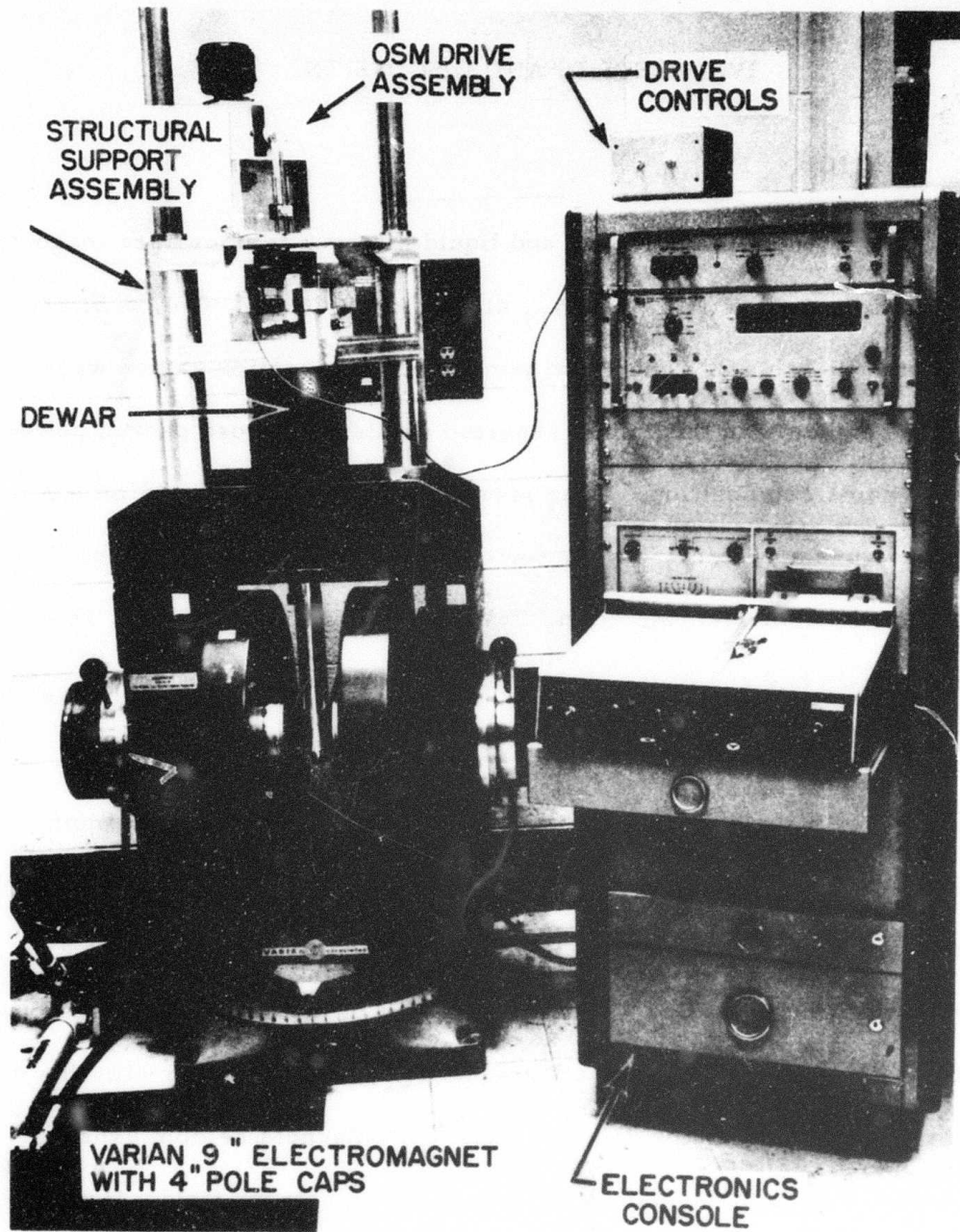


Figure 4. Magnetometer with Dewar Attached.

#### IV. RESULTS AND DISCUSSION

##### A. $Y_2(Co_{1-x}Fe_x)_{17}$

The room temperature and liquid nitrogen temperature magnetic properties of the  $Y_2(Co_{1-x}Fe_x)_{17}$  alloys ( $x = 0.1, 0.2, 0.4, 0.5$ ) are reported in Table 2. The room temperature saturation values were 1 to 8% higher than the values reported earlier for loose packed powders of the same composition.<sup>3</sup> The room temperature and liquid nitrogen temperature anisotropy curves for the  $Y_2(Co_{0.6}Fe_{0.4})_{17}$  composition, corrected for the demagnetizing field, are shown in Figure 5. This composition had one of the highest anisotropy fields of the  $Y_2(Co_{1-x}Fe_x)_{17}$  alloys studied.

For a material with a square hysteresis loop, the maximum energy product is  $4\pi^2 M_s^2$ . For  $Y_2(Co_{0.8}Fe_{0.2})_{17}$ , this maximum energy product would be 49 MGOe. However, this would require a coercive force of 7 kOe, which is about half of the observed anisotropy field. The fabrication of a bulk magnet of this composition with this energy product would be difficult since bulk magnets seldom exhibit coercive forces more than 10 or 15% of the anisotropy field. However, it may be possible to fabricate magnets with twice the coercive force and 10% higher saturation magnetization than the highest saturation alnicos.

TABLE 2  
SUMMARY OF  $Y_2(Co_{1-x}Fe_x)_{17}$  DATA

x	T [OK]	$\sigma^*$ [Emu/g]	$4\pi M_S^*$ [Gauss]	K1		K2		H <sub>A</sub> [Oe]
				[ x10 <sup>7</sup> Erg/cm <sup>3</sup> ]		[ x10 <sup>7</sup> Erg/cm <sup>3</sup> ]		
0.1	300	134.5 ± 1	13,330 ± 100	0.23 ± 0.01	0.02 ± 0.01	0.07 ± 0.01	4,700 ± 200	
	77	138.9 ± 1	13,770 ± 100	0.27 ± 0.01	0.07 ± 0.01	0.07 ± 0.01	6,200 ± 200	
0.2	300	143.0 ± 1	14,020 ± 100	0.75 ± 0.01	0.03 ± 0.01	0.03 ± 0.01	13,900 ± 200	
	77	146.9 ± 1	14,400 ± 100	0.80 ± 0.01	0.04 ± 0.01	0.04 ± 0.01	14,700 ± 200	
0.4	300	153.1 ± 1	14,650 ± 100	0.67 ± 0.01	0.02 ± 0.01	0.02 ± 0.01	11,900 ± 200	
	77	161.5 ± 1	15,430 ± 100	1.14 ± 0.03	0.02 ± 0.02	0.02 ± 0.02	18,800 ± 500	
0.5	300	162.7 ± 1	15,370 ± 100	0.40 ± 0.01	0.01 ± 0.01	0.01 ± 0.01	6,800 ± 200	
	77	172.9 ± 1	16,320 ± 100	0.76 ± 0.03	0.04 ± 0.02	0.04 ± 0.02	12,400 ± 500	

\*Measured in the c-axis direction.

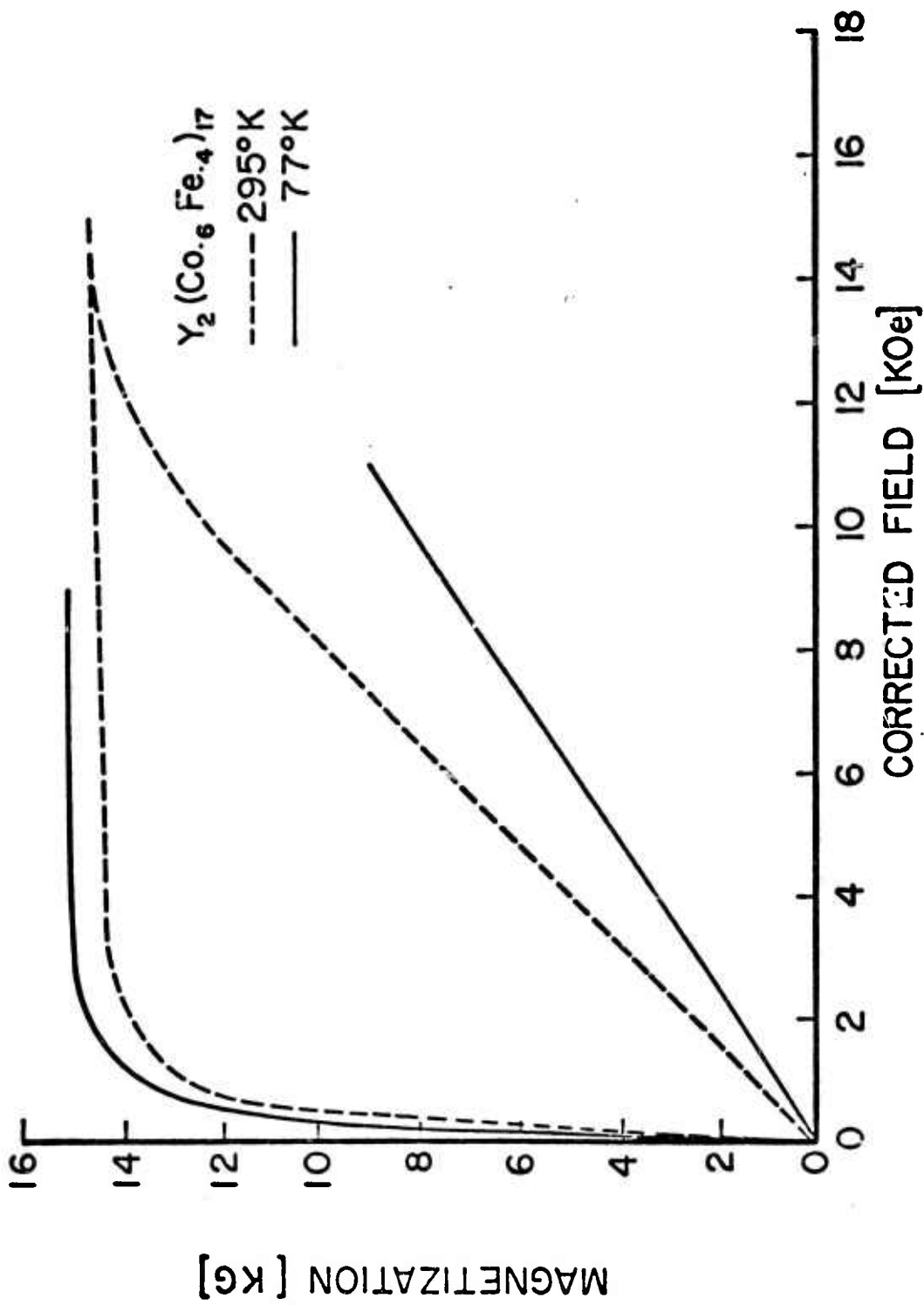


Figure 5. Magnetization Curves for Y<sub>2</sub>(Co<sub>0.6</sub>Fe<sub>0.4</sub>)<sub>17</sub>.

The variation of the saturation magnetization of the four  $Y_2(Co_{1-x}Fe_x)_{17}$  alloys is presented in Figure 6. The magnetization was observed to increase with increasing iron content due to the higher dipole moment of iron compared to that of cobalt. The saturation also increased for each composition as the temperature was decreased, due to the greater degree of ordering at low temperatures. Cooling to 77°K resulted in a 3 to 5% rise in magnetization.

B.  $Pr_2(Co_{1-x}Fe_x)_{17}$

In the alloy system  $Pr_2(Co_{1-x}Fe_x)_{17}$ , two crystals of each composition where  $x = 0.2, 0.3, 0.4$  were studied. The room temperature and liquid nitrogen temperature magnetic properties of these alloys are reported in Table 3. The room temperature saturation values were 2 to 8% higher than the previously reported values for loose packed powders.<sup>3</sup>

At room temperatures, the easy direction of magnetization for these alloys is the c-axis.  $Pr_2(Co_{0.7}Fe_{0.3})_{17}$  and  $Pr_2(Co_{0.6}Fe_{0.4})_{17}$  maintain this anisotropy at low temperatures, but  $Pr_2(Co_{0.8}Fe_{0.2})_{17}$  develops an easy basal plane on cooling. The anisotropy curves for this composition are shown in Figure 7.

One possible explanation of the behavior of  $Pr_2(Co_{0.8}Fe_{0.2})_{17}$  is that there is a set of cones of preferred directions of magnetization located about the c-axis direction, as shown in Figure 8. At low temperatures, the angle  $\theta$  from the c-axis is larger so that the

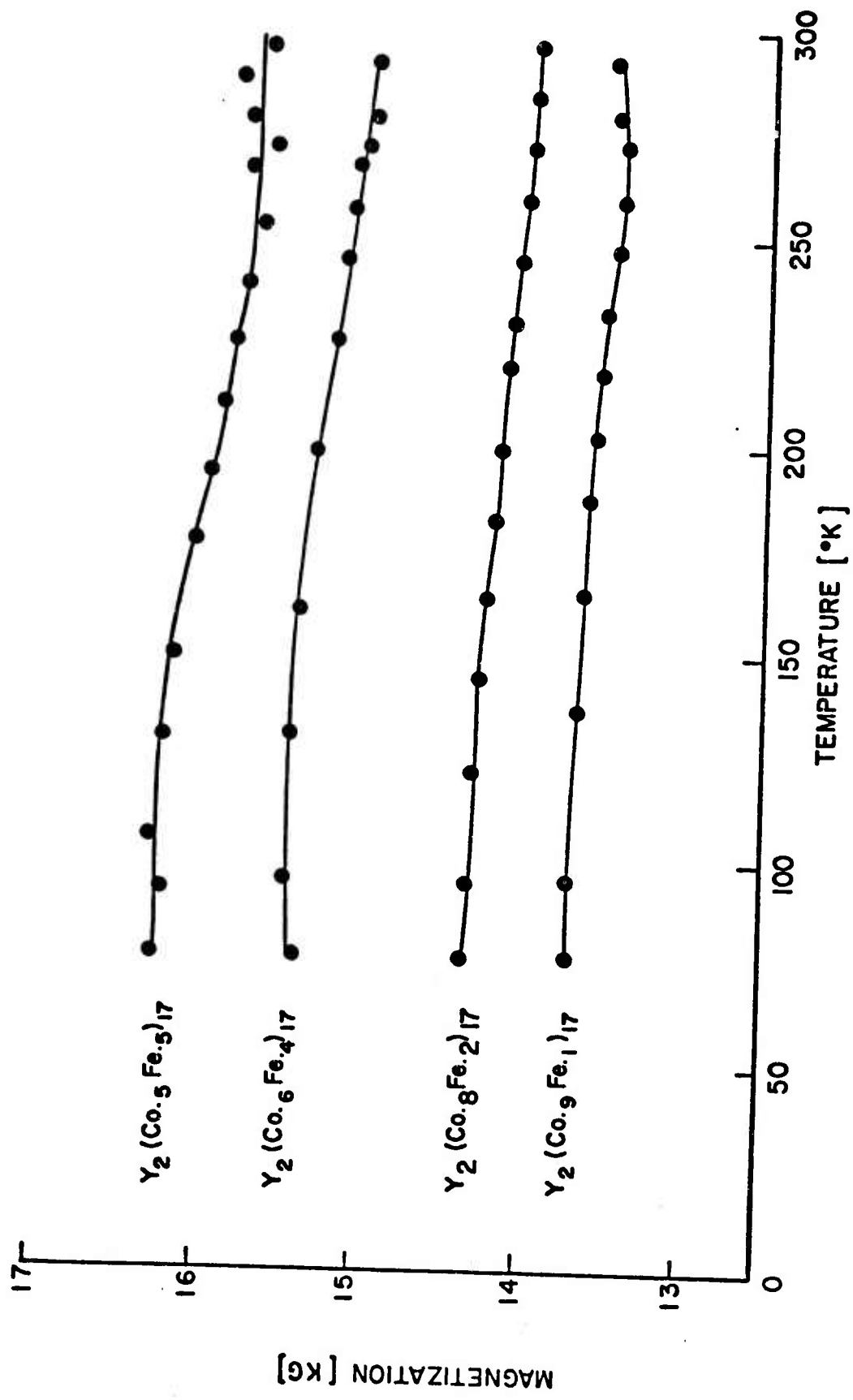


Figure 6. Temperature Dependence of Magnetization for Four Y<sub>2</sub>(Co,Fe)<sub>17</sub> Alloys.

TABLE 3  
SUMMARY OF Pr<sub>2</sub>(Co<sub>1-x</sub>Fe<sub>x</sub>)<sub>17</sub> DATA

x	T [°K]	$\sigma^*$ [Emu/g]	$4\pi M_S^*$ [Gauss]	$K_1$ [x10 <sup>7</sup> Erg/cm <sup>3</sup> ]	$K_2$	$H_A$ [Oe]
0.2	300	144.5 ± 1	15,030 ± 100	0.8 ± 0.2	-0.2 ± 0.05	5,000 ± 1,000
	77	140.9 ± 1	13,480 ± 300	----	----	----
0.3	300	158.7 ± 1	16,310 ± 100	1.8 ± 0.2	-0.3 ± 0.05	23,000 ± 3,000
	77	178.4 ± 1	18,350 ± 100	5.5 ± 0.5	-0.07 ± 0.05	37,200 ± 3,000
0.4	300	157.5 ± 1	16,050 ± 100	1.7 ± 0.2	-0.4 ± 0.2	20,500 ± 3,000
	77	177.5 ± 1	18,080 ± 100	4.5 ± 0.5	----	31,300 ± 3,000

\*Measured in the c-axis direction.

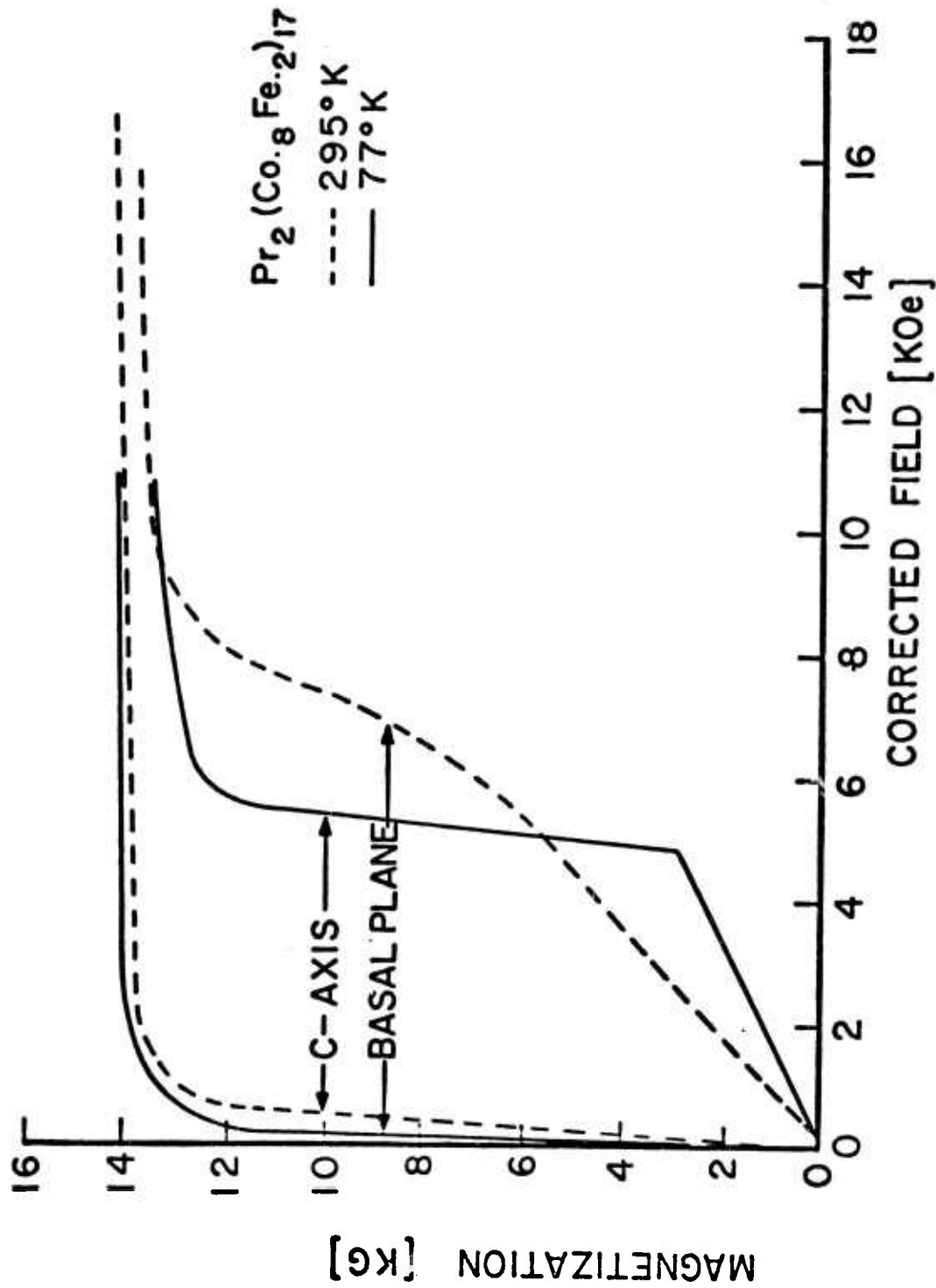


Figure 7. Magnetization Curves for  $\text{Pr}_2(\text{Co}_{0.8}\text{Fe}_{0.2})_{17}$ .

preferred direction of magnetization is in the basal plane rather than the c-axis. This situation would correspond to an angle of  $\theta > 45^\circ$ .

In the easy direction of magnetization, the basal plane, the magnetization process would proceed as illustrated in Figure 8. A small field in the basal plane direction would be sufficient to rotate the moments in the cone as in Figure 8B. The application of a larger field, as in 8C, would cause the moments to rotate out of the cones. Finally, as in 8D, the moments would all be aligned with the applied field and saturation would be achieved.

In the hard direction of magnetization, the magnetization process would proceed as illustrated in Figure 9. A field applied in the c-axis direction would slowly rotate the spins out of the cone, as in Figure 9B. When the moments are  $90^\circ$  to the c-axis, as in 9C, the slightest additional field would cause them to spontaneously fall into the upper cone. Additional applied field would then slowly rotate the moments into the c-axis, as illustrated in Figure 9D.

The relationship between temperature and magnetization for  $\text{Pr}_2(\text{Co}_{0.7}\text{Fe}_{0.3})_{17}$  and  $\text{Pr}_2(\text{Co}_{0.6}\text{Fe}_{0.4})_{17}$  is shown in Figure 10. Low temperature saturation values were found to be 12% higher than room temperature values, indicating that these alloys decrease in magnetization with increasing temperature much more quickly than the yttrium alloys. The fact that the saturation magnetization values of these crystals are so close to one another suggests that they may have

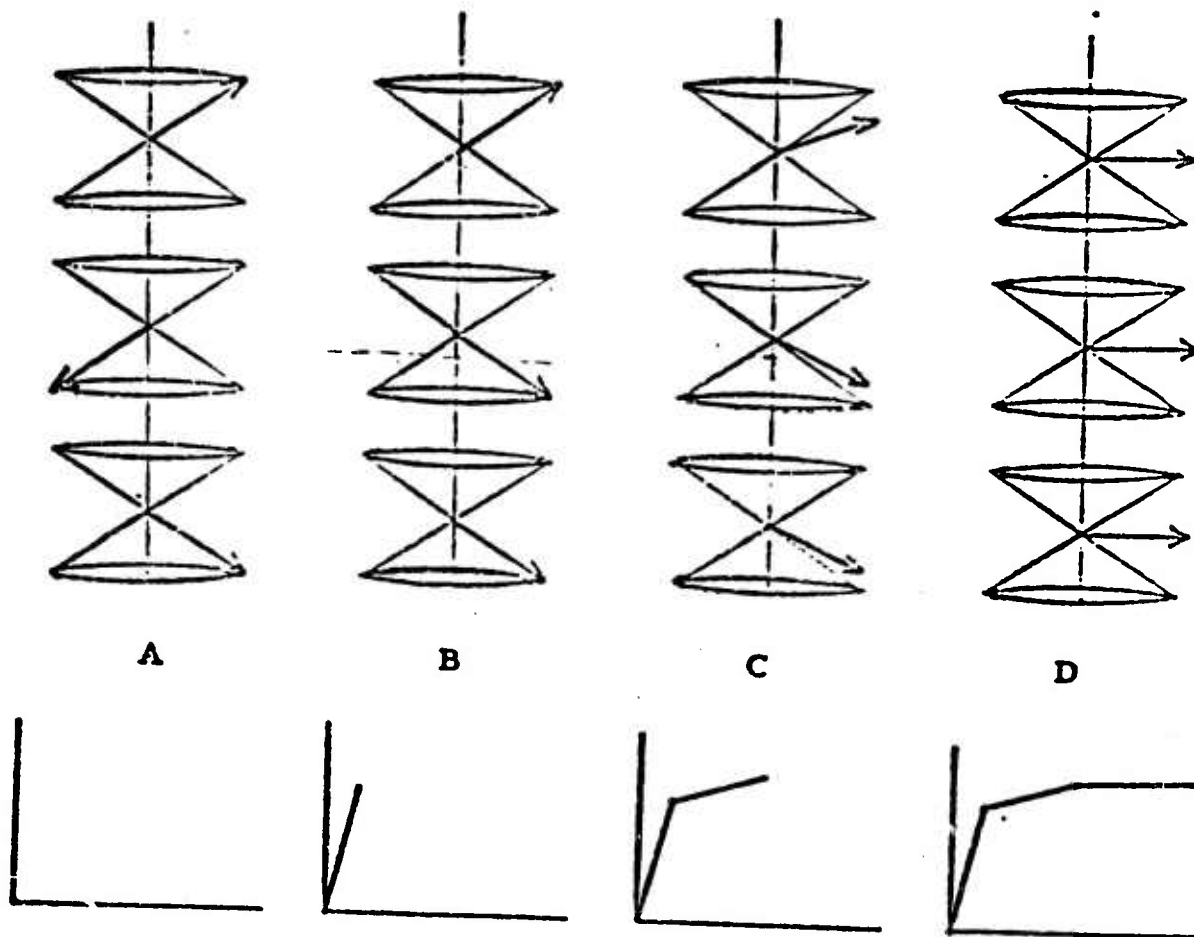


Figure 8. Magnetization in the Easy Basal Plane;  
Field Applied Left to Right.

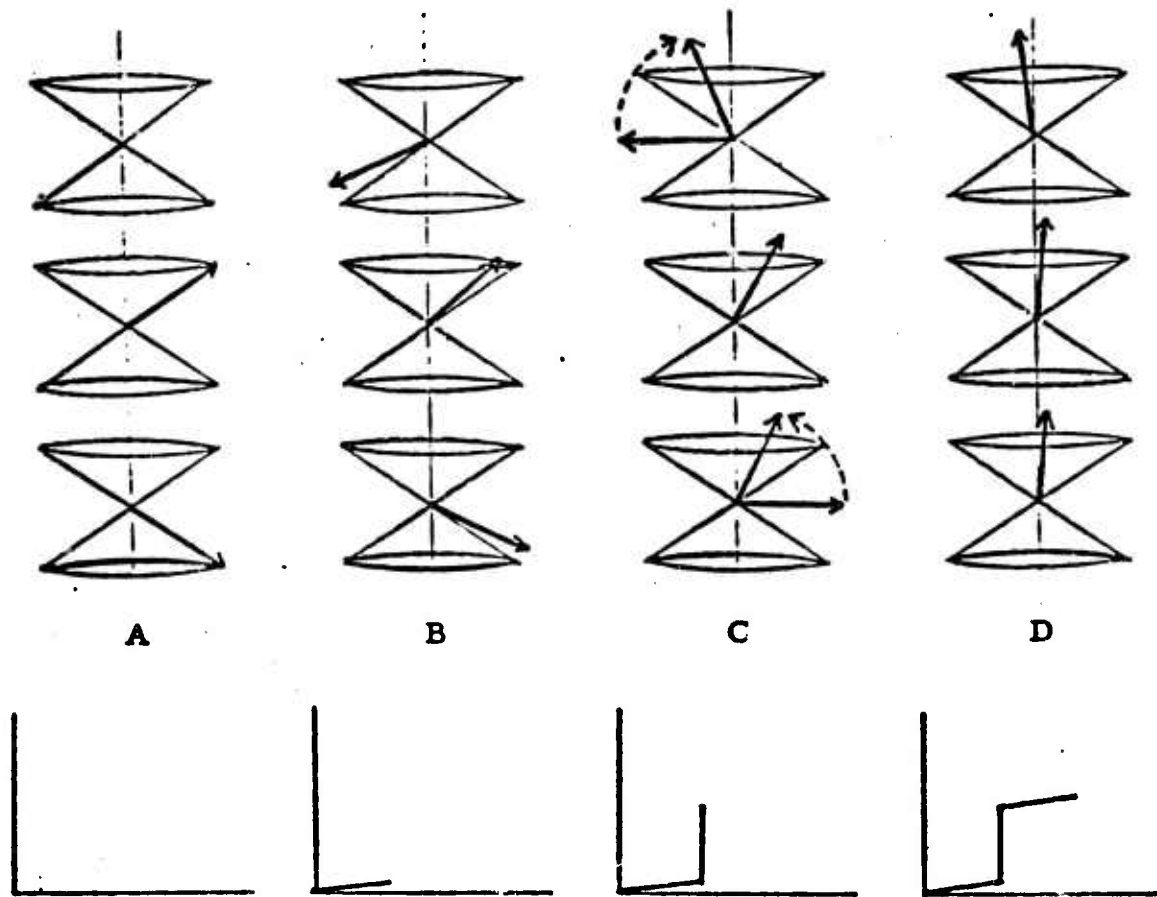


Figure 9. Magnetization in the Hard C-Axis; Field Applied from Bottom to Top.

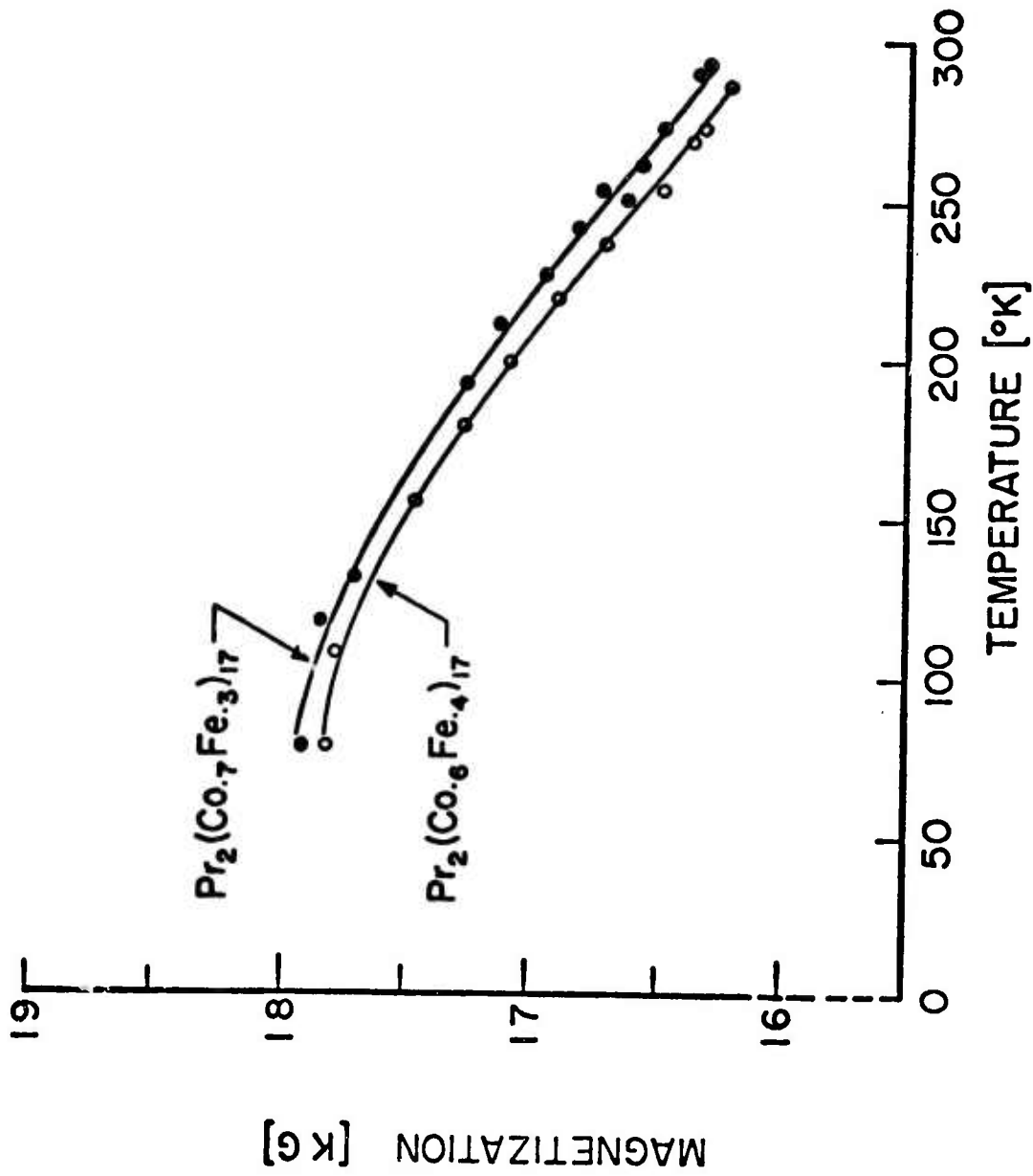


Figure 10. Temperature Dependence of Magnetization for Two  $\text{Pr}_2(\text{Co}_{1-x}\text{Fe}_x)_{17}$  Alloys.

nearly the same composition. Local inhomogeneities in the cobalt-iron ratios in the alloy buttons might shift the actual composition of a specific crystal to some extent. Microprobe analyses should eventually be made on all the crystals to insure that the nominal compositions are the same as the actual compositions.

The temperature variation of magnetization in a 14 kOe field in the c-axis direction is illustrated in Figure 11 for two  $\text{Pr}_2(\text{Co}_{0.8}\text{Fe}_{0.2})_{17}$  crystals. The samples have an easy basal plane at liquid nitrogen temperatures. As the temperature increases, the magnetization also increases until about  $140^\circ\text{K}$ , at which point the anisotropy has changed from an easy basal plane to an easy c-axis. As the temperature increases further, the magnetization decreases in the usual manner as the dipoles are disordered.

While this model qualitatively describes the results for  $\text{Pr}_2(\text{Co}_{0.8}\text{Fe}_{0.2})_{17}$  at low temperatures, it does not do so quantitatively. The actual magnetization process is probably more complex. Neutron diffraction will probably be required to completely solve the problem.

An interesting result was that although the room temperature saturation magnetization was the same for both crystals, the magnetization differs by 5.5% at  $77^\circ\text{K}$ . The difference decreases with increasing temperature until the sample develops an easy c-axis. Cobalt-to-iron ratios were determined using a scanning electron

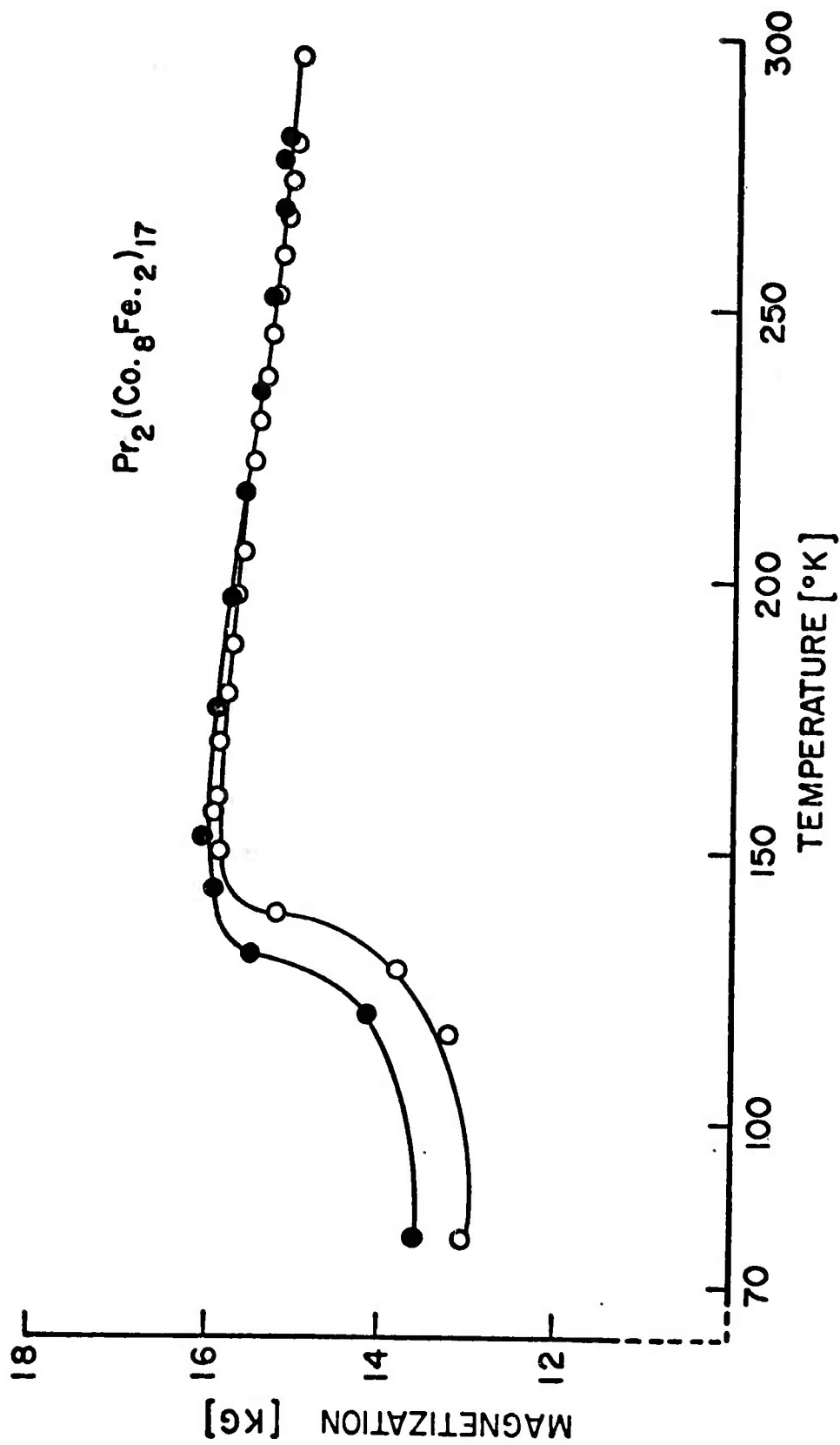


Figure 11. Temperature Dependence of Magnetization for Two  $\text{Pr}_2(\text{Co}_0.8\text{Fe}_0.2)_{17}$  Crystals.

microscope equipped with an energy dispersive X-ray analyzer. Results indicated a higher percentage of iron in the sample with the higher saturation at 77°K.

The most promising permanent magnet material of the praseodymium alloys studied was  $\text{Pr}_2(\text{Co}_{0.7}\text{Fe}_{0.3})_{17}$ . With a saturation magnetization at room temperature of 16300 Gauss, this material has a maximum theoretical energy product,  $4\pi^2 M_s^2$ , of 66.5 MGOe. In order to achieve this value, a coercive force of 8.2 kOe would be required, that is, 34% of the anisotropy field. Such a coercive force is probably in excess of what can be obtained in a bulk magnet, but it can be anticipated that magnets of  $\text{Pr}_2(\text{Co}_{0.7}\text{Fe}_{0.3})_{17}$  may replace alnicos in application where high field strength is required.

## V. SUMMARY

The saturation magnetization and anisotropy constants of the compositions  $\text{Pr}_2(\text{Co}_{1-x}\text{Fe}_x)_{17}$ ,  $x = 0.2, 0.3, 0.4$ , and  $\text{Y}_2(\text{Co}_{1-x}\text{Fe}_x)_{17}$ ,  $x = 0.1, 0.2, 0.4, 0.5$  have been obtained. All these compositions have the magnetically favorable c-axis magnetocrystalline anisotropy at room temperatures, but when cooled below  $140^\circ\text{K}$  in a 14 kOe field,  $\text{Pr}_2(\text{Co}_{0.8}\text{Fe}_{0.2})_{17}$  develops an easy basal plane. This transformation may be qualitatively explained by hypothesizing a cone of easy directions whose opening angle is a function of temperature and applied field.

For the other alloys studied, cooling to  $77^\circ\text{K}$  increases the saturation magnetization and anisotropy as the moments become more ordered. The change in saturation magnetization is more pronounced in the praseodymium alloys than in the yttrium alloys.

The composition which seems to have the most promise as a permanent magnet material is  $\text{Pr}_2(\text{Co}_{0.7}\text{Fe}_{0.3})_{17}$ . This alloy has a saturation magnetization of 16300 Gauss and an anisotropy field of about 24 kOe. A coercive force in a bulk magnet of this composition equal to 10% of the anisotropy field would yield a magnet with 25% greater saturation magnetization and three times the coercive force of the high saturation alnico magnets. If a coercive force equal to 34% of the anisotropy field could be achieved, it would make possible a magnet with an energy product of 66.6 MGOe.

## REFERENCES

1. W. Ostertag and K. J. Strnat, "Rare Earth-Cobalt Compounds with the  $A_2B_{17}$  Structure," *Acta Cryst.*, Vol. 21, pp. 560-565, 1966.
2. K. Strnat, G. Hoffer, W. Ostertag, and J. C. Olson, "Ferrimagnetism of the Rare Earth-Cobalt Intermetallic Compounds  $R_2Co_{17}$ ," *J. Appl. Physics*, Vol. 37, pp. 1252-1253, 1966.
3. H. Mildrum, J. Tront, M. Hartings, and K. Strnat, "Saturation Magnetization of Rare Earth-Transition Metal Phases of the Type  $R_2(Co,Fe)_{17}$ ," *Proceedings of 10th Rare Earth Research Conference, April 30-May 3, 1973, Carefree, Arizona.*
4. W. M. Hubbard, E. Adams, and J. V. Gilfrich, "Magnetic Moments of Alloys of Gadolinium with Some of the Transition Elements," *J. Appl. Phys.*, Vol. 31, p. 3685, 1960.
5. E. A. Nesbitt, H. J. Williams, J. H. Wernick, and R. C. Sherwood, "Magnetic Moment of Compounds of Cobalt with Rare Earth Elements Having a  $Cu_5Ca$  Structure," *J. Appl. Phys.*, Vol. 33, pp. 1674-1678, May 1962.
6. K. Nassau, L. V. Cherry, and W. E. Wallace, "Intermetallic Compounds Between Lanthanons and Transition Metals of the First Long Period--Part II, Ferrimagnetism of  $AB_5$  Cobalt Compounds," *J. Phys. Chem. Solids*, Vol. 16, pp. 131-137, 1960.
7. G. Hoffer and K. J. Strnat, "Magnetocrystalline Anisotropy of  $YCo_5$  and  $Y_2Co_{17}$ ," *IEEE Trans. Magnetics*, Vol. MAG-2, p. 487, 1966.
8. See, for example, A. E. Ray, "A Review of the Cobalt-Rare Earth Binary Alloy Systems," to be presented at the 10th INTERMAG Conference, Washington, D. C.; to be published in a forthcoming issue of *Cobalt*.
9. J. B. Tsui and K. J. Strnat, "Sintering of  $PrCo_5$  Permanent Magnets," *Appl. Phys. Letters*, Vol. 18, p. 107, 1971.
10. J. Schweizer, K. J. Strnat, and J. B. Tsui, "Coercivity of Heat Treated Pr-Co Powder Compacts," *IEEE Trans. Magnetics*, MAG-7, pp. 429-431, 1971.

11. K. H. J. Buschow, P. A. Naastepad, and F. F. Westendorp, "Preparation of  $\text{SmCo}_5$  Permanent Magnets," J. Appl. Phys., Vol. 40, p. 4029, 1969.
12. M. G. Benz and D. L. Martin, "Cobalt-Samarium Permanent Magnets Prepared by Liquid Phase Sintering," Appl. Phys. Letters, Vol. 17, p. 176, 1970.
13. For example, see the AFML Report Series, A. E. Ray and K. J. Strnat, "Research and Development of Rare Earth-Transition Metal Alloys as Permanent Magnet Materials," AFML-TR-71-53, March 1971; AFML-TR-71-210, October 1971; AFML-TR-72-99, April 1972; AFML-TR-72-202, August 1972, Air Force Materials Lab, Wright-Patterson Air Force Base, Dayton, Ohio.
14. J. D. Livingston, "Present Understanding and Coercivity in Cobalt-Rare Earths," Paper 6D-1, 18th Conference on Magnetism and Magnetic Materials, Nov. 28-Dec. 1, 1972, Denver, Colorado; to be published in AIP Conference Proceedings in 1973.
15. J. Schweizer, "Research on Rare Earth-Cobalt Alloys and Compounds," AFML-TR-72-82, Air Force Materials Laboratory, Wright-Patterson Air Force Base, Dayton, Ohio, May 1972.
16. K. Strnat, G. Hoffer, and A. E. Ray, "Magnetic Properties of Rare Earth-Iron Intermetallic Compounds," IEEE Trans. Magnetics, MAG-2, pp. 489-493, 1966.
17. A. E. Ray and K. J. Strnat, "Easy Directions of Magnetization in Ternary  $\text{R}_2(\text{Co,Fe})_{17}$  Phases," IEEE Trans. Magnetics, MAG-8, p. 516, September 1972.
18. A. E. Ray and K. J. Strnat, "Research and Development of Rare Earth-Transition Metal Alloys as Permanent Magnet Materials," AFML-TR-72-99, Air Force Materials Laboratory, Wright-Patterson Air Force Base, Dayton, Ohio, April 1972.
19. A. E. Ray and K. J. Strnat, "Metallurgical and Magnetic Properties of the Intermetallic Phases  $\text{R}_2(\text{Co,Fe})_{17}$ ," presented at the 7th Rare Earth Conference, 12-17 September 1972, Moscow, USSR.
20. H. Mildrum, "Design of Development of Two Oscillating Sample Magnetometer Systems," M. S. Thesis, E. E. Department, University of Dayton, Ohio, 1971.

## APPENDIX \*

The crystal anisotropy energy for a crystal of uniaxial symmetry can be expressed by:

$$E_C = K_1 \cos^2 \phi + K_2 \cos^4 \phi ,$$

where  $K_1$  and  $K_2$  are the anisotropy constants, and  $\phi$  is the angle between the direction of magnetization and the basal plane, as shown in Figure 12.

The energy of a dipole in an effective field  $H_i$  (that is, the applied field minus the demagnetization field) is:

$$E_H = -H_i M_s \cos \phi ,$$

where  $H_i$  is the effective field and  $M_s$  is the saturation magnetization.

The total energy of the system is:

$$E_{TOT} = E_C + E_H = K_1 \cos^2 \phi + K_2 \cos^4 \phi - H_i M_s \cos \phi .$$

An extremum of this function occurs at:

$$\frac{\partial E}{\partial \phi} = 2K_1 \cos \phi + 4K_2 \cos^3 \phi - H_i M_s \cos \phi \stackrel{\text{set}}{=} 0 .$$

---

\* Based largely on the analysis given by W. Sucksmith and J. E. Thompson, "The Magnetic Anisotropy of Cobalt," Proc. Royal Soc. (London) V. 225 (1954) p. 362; and discussed by H. Zilstra, Experimental Methods in Magnetism, " Vol. IX, p. 168, of "Selected Topics in Solid State Physics. "

From Figure 12, we see that  $\cos \phi = \frac{M}{M_s}$  so,

$$2K_1 \left[ \frac{M}{M_s} \right] + 4K_2 \left[ \frac{M^3}{M_s^3} \right] = HM_s.$$

Multiplying by  $I/M_s M$ , we have

$$\frac{2K_1}{M_s^2} + 4K_2 \left[ \frac{I^2}{M_s^4} \right] = \frac{H}{M},$$

which is of the form  $B + mx = y$ ; that is, a straight line of

slope  $\frac{4K_2}{M_s^4}$  and intercept  $\frac{2K_1}{M_s^2}$  so that if we plot  $H/M$  versus  $M^2$ ,

as in Figure 13, the anisotropy constants  $K_1$  and  $K_2$  may be easily determined.

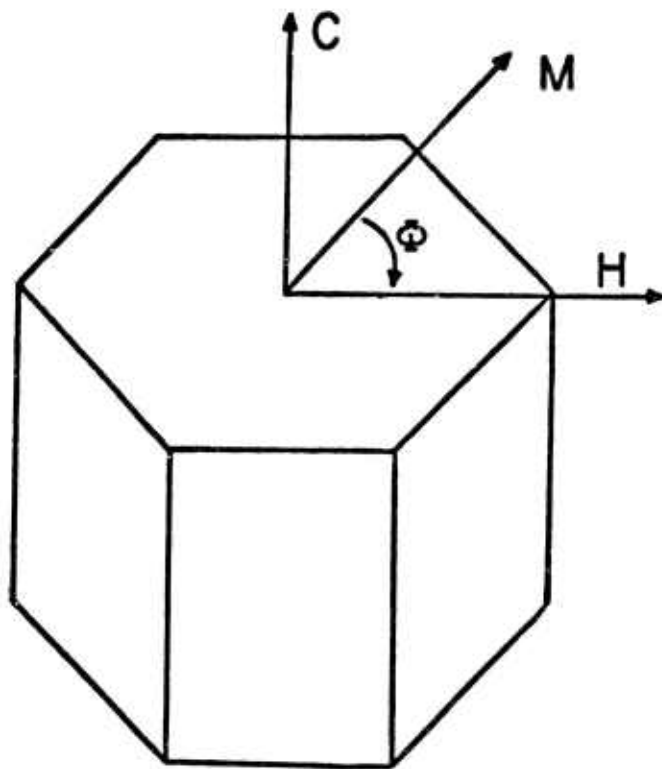


Figure 12. Determination of the Angle  $\phi$ .

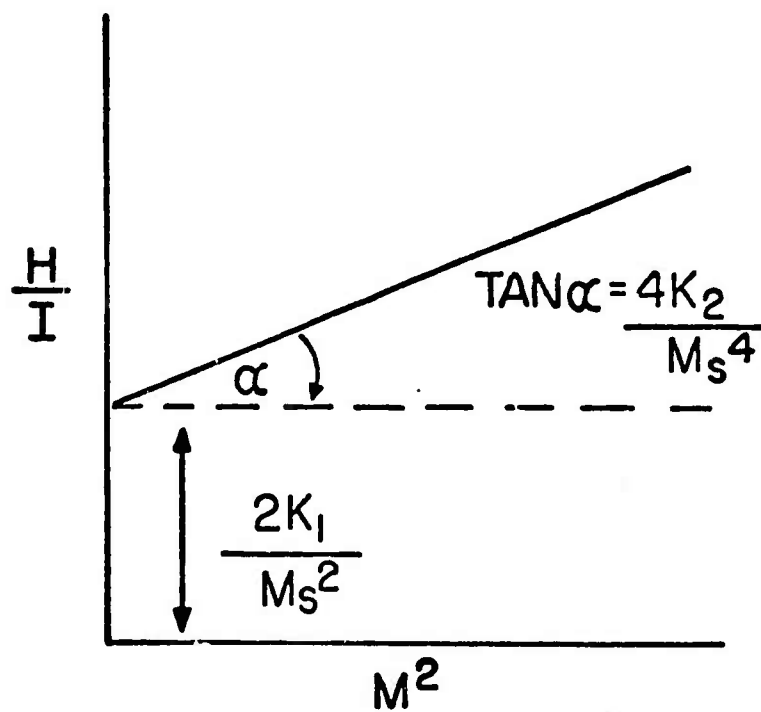


Figure 13. Determination of Anisotropy Constants.

## ADDENDUM

Since the completion of the preceding work, questions have been raised as to the propriety of the use of the expression  $2(K_1 + K_2)/M_s$  as the correct estimate of the anisotropy field,  $H_A$ . In the presentation of the work,  $2(K_1 + K_2)/M_s$  was intended to be an estimate of the maximum coercive force that could be obtained for a magnet of the composition being studied and not the single crystal anisotropy field. In this usage, we feel the expression is correct and agree with our critics that the single crystal anisotropy field,  $H_A$ , should be calculated using the expression,  $H_A = 2(K_1 + 2K_2)/M_s$ . In Section II-A of this report, the single crystal data is presented using this expression and the reader is referred there for the anisotropy field data.

APPENDIX II

REVISED PHASE DIAGRAMS FOR THE BINARY SYSTEMS  
CERIUM-COBALT, PRASEODYMIUM-COBALT,  
AND NEODYMIUM-COBALT

A. E. Ray, A. T. Biermann, R. S. Harmer, and J. E. Davison

REVISED PHASE DIAGRAMS FOR THE BINARY SYSTEMS  
CERIUM-COBALT, PRASEODYMIUM-COBALT,  
AND NEODYMIUM-COBALT\*

A. E. Ray, A. T. Biermann, R. S. Harmer, and J. E. Davison  
School of Engineering, University of Dayton  
Dayton, Ohio 45469

INTRODUCTION

Tentative but incomplete phase diagrams for the Ce-Co, Pr-Co, and Nd-Co were reported earlier by Ray and Hoffer.<sup>1</sup> More recent investigations at the University of Dayton<sup>2-4</sup> have revealed the existence of previously unrecognized phases in these alloy systems. It is felt that some of these phases, namely the  $R_5Co_{19}$ 's, may play significant roles in the achievement of high coercive forces in sintered rare earth-cobalt permanent magnets.<sup>5,6</sup> In view of the importance of reliable phase diagrams as guides for alloy preparation, heat treatment, and the understanding and control of the magnetic properties of these alloys, we have revised and completed these three binary systems.

EXPERIMENTAL

Chemical analyses and sources of the metals used for the preparation of the alloys are given in Table I. Alloys were prepared by arc melting in a purified argon-helium atmosphere. The alloys were melted, cooled, inverted, and remelted several times to enhance mixing. Weight losses on melting seldom exceeded 0.1%. Alloy compositions were assumed to be the nominal compositions, excluding the additions of 1.0 wt. % Pr and 2.0 wt. % Nd to each of the Pr-Co and Nd-Co alloys, respectively, to compensate for the impurity content, primarily oxygen, in these metals.

---

\* This research was supported by the Advanced Research Projects Agency of the Department of Defense and was monitored by the Air Force Materials Laboratory, AFSC, USAF under Contract No. F33615-70-C-1625.

The values of 1.0% Pr and 2.0% Nd were determined by the amount of excess rare earth required to prepare metallographically single phase alloys of the stoichiometric phases,  $\text{Pr}_3\text{Co}$  and  $\text{PrCo}_2$  and  $\text{Nd}_3\text{Co}$  and  $\text{NdCo}_2$ , respectively. No cerium additions were required to produce metallographically single phase alloys of  $\text{Ce}_2\text{Co}_{11}$  or  $\text{CeCo}_2$ , undoubtedly due to the low impurity level of the cerium metal supplied to us by the Ames Laboratory, USAEC, Iowa State University, through the cooperation of Dr. F. H. Spedding.

Metallography, X-ray diffraction, and differential thermal analyses were generally performed on rare earth-rich alloys in the arc melted condition. Alloys containing more than approximately 25 at. % Co were wrapped in tantalum foil and homogenized in vacuum for two to five days at temperatures  $25^\circ\text{C}$  to  $100^\circ\text{C}$  below the lowest melting phase known to be present in the particular alloy.

X-Ray diffraction patterns were obtained with a G. E. XRD-6 diffractometer and Type 700 detector system, using  $\text{CrK}\alpha$  radiation. Precision lattice constants were computed using the methods of Vogel and Kempter<sup>7</sup> with the aid of an RCA Spectra 70/40 computer. Nickel powder was used as an internal standard to correct for zero  $2\theta$  errors.

Quantitative analyses were performed on selected alloys to confirm their compositions. Raw data was refined using the computer program MAGIC III by J. W. Colby.\* Standards used in the analyses were:  $\text{Nd}_3\text{Co}$  and  $\text{NdCo}_2$  for Nd;  $\text{CeCo}_2$  for Ce;  $\text{PrCo}_2$  for Pr; and pure Co for Co.

The differential thermal analyses were performed on equipment described in detail elsewhere.<sup>8</sup> Tantalum crucibles and thermocouple sheaths were used for alloys containing  $\leq 25$  at. % Co, while high density alumina crucibles and sheaths were used for the alloys of higher cobalt content. The thermocouples employed were W/26 Re vs. W/3 Re obtained from Englehard Industries. High purity Ag (99.95) and AISI Fe (36 ppm total impurities) were used as checks on the thermocouple calibration.

## RESULTS

### Cerium-Cobalt

The phase diagram for the Ce-Co alloy system is given in Figure 1. The cerium-rich half of the system is in good agreement with the results of Ellinger et al.,<sup>9</sup> who studied the system

\* Bell Telephone Laboratories, Allentown, Pa.

between 0 and 50 at. % Co. Eutectics occur at 24.1 at. % Co and at 34.0 at. % Co. Between these,  $\text{Ce}_{24}\text{Co}_{11}$  is observed to melt congruently at  $446 \pm 2^\circ\text{C}$ . Six peritectically melting, cobalt-rich intermediate phases are observed:  $\text{CeCo}_2$ ,  $\text{CeCo}_3$ ,  $\text{Ce}_2\text{Co}_7$ ,  $\text{Ce}_5\text{Co}_{19}$ ,  $\text{CeCo}_5$ , and  $\text{Ce}_2\text{Co}_{17}$ . In the previous investigation,<sup>1</sup> the  $\text{Ce}_5\text{Co}_{19}$  peritectic was incorrectly assigned to  $\text{Ce}_2\text{Co}_7$  and the  $\text{Ce}_2\text{Co}_7$  peritectic was assumed to be due to a solid state transformation in  $\text{Ce}_2\text{Co}_7$ . In another investigation of the Ce-Co system, Buschow<sup>10</sup> did not detect  $\text{Ce}_5\text{Co}_{19}$ . The peritectic melting temperatures we observe are  $21^\circ\text{C}$  to  $27^\circ\text{C}$  lower than those reported by Buschow for  $\text{CeCo}_2$ ,  $\text{CeCo}_3$ ,  $\text{Ce}_2\text{Co}_7$ ,  $\text{CeCo}_5$ , and  $\text{Ce}_2\text{Co}_{17}$ . Although the  $\alpha$ - $\text{Ce}_2\text{Co}_{17}$  (rhombohedral) to  $\beta$ - $\text{Ce}_2\text{Co}_{17}$  (hexagonal) transformation of  $\text{Ce}_2\text{Co}_{17}$  was not detected by DTA, X-ray diffraction patterns of alloys homogenized at  $1100^\circ\text{C}$  showed only  $\beta$ - $\text{Ce}_2\text{Co}_{17}$ , and those homogenized at  $1000^\circ\text{C}$  showed only  $\alpha$ - $\text{Ce}_2\text{Co}_{17}$ .

Crystal structure data for the intermediate phases are given in Table II. Lattice constant measurements indicate the  $\beta$ - $\text{Ce}_2\text{Co}_{17}$  phase field may extend slightly toward the Co-rich side of  $\text{Ce}_2\text{Co}_{17}$  stoichiometry.

#### Praseodymium-Cobalt

The Pr-Co phase diagram is shown in Figure 2. The major change in the cobalt-rich portion of the system is the identification of the higher of the two closely-spaced thermal events as the  $\text{Pr}_5\text{Co}_{19}$  peritectic and the lower as the  $\text{Pr}_2\text{Co}_7$  peritectic. A total of nine intermediate phases are observed:  $\text{Pr}_3\text{Co}$ ,  $\text{Pr}_{\sim 7}\text{Co}_{\sim 3}$ ,  $\text{Pr}_2\text{Co}_{1.7}$ ,  $\text{PrCo}_2$ ,  $\text{PrCo}_3$ ,  $\text{Pr}_2\text{Co}_7$ ,  $\text{Pr}_5\text{Co}_{19}$ , and  $\text{Pr}_2\text{Co}_{17}$ . Crystal structure data for these phases are given in Table II. Only  $\text{Pr}_3\text{Co}$  melts congruently. Metallographic analysis indicates  $\text{Pr}_{\sim 7}\text{Co}_{\sim 3}$  contains slightly less than 29.5 at. % Co. Eutectics are observed at 19.5 and 34 at. % Co.

Thermal analyses of alloys containing 50, 55, and 61.5 at. % Co show an event at  $580 \pm 4^\circ\text{C}$ . The nature of this event is unknown. X-Ray diffraction patterns of these alloys, annealed at  $500^\circ\text{C}$ , show only  $\text{Pr}_2\text{Co}_{1.7}$  and  $\text{PrCo}_2$  to be present.

Lattice parameter measurements indicated narrow ranges of solubility for  $\text{Pr}_3\text{Co}$ ,  $\text{PrCo}_3$ ,  $\text{Pr}_2\text{Co}_7$ , and  $\text{Pr}_5\text{Co}_{19}$ . For  $\text{PrCo}_5$  we observe  $a = 5.032 \pm .002 \text{ \AA}$  and  $c = 3.992 \pm .002 \text{ \AA}$  in both the  $\text{Pr}_5\text{Co}_{19} + \text{PrCo}_5$  phase field and for the stoichiometric  $\text{PrCo}_5$  composition for alloys annealed at  $1100^\circ\text{C}$ . In the  $\text{PrCo}_5 + \text{Pr}_2\text{Co}_{17}$  phase field, however, we observe  $a = 5.021 \pm .005 \text{ \AA}$  and  $c = 4.028 \pm .007 \text{ \AA}$ . The relatively large increase in the c-axis accompanied by a smaller decrease in the a-axis suggests some of

the Pr atomic sites have been replaced by pairs of Co atoms aligned parallel to the c-axis.

Only the rhombohedral form of  $\text{Pr}_2\text{Co}_{17}$  is observed. X-Ray diffraction patterns of alloys annealed at  $1100^\circ\text{C}$  indicate a very narrow solid solubility range for  $\text{Pr}_2\text{Co}_{17}$ .

#### Neodymium-Cobalt

The Nd-Co phase diagram, Figure 3, contains ten intermediate phases:  $\text{Nd}_3\text{Co}$ ,  $\text{Nd}_{17}\text{Co}_{13}$ ,  $\text{Nd}_2\text{Co}_{1.7}$ ,  $\text{Nd}_2\text{Co}_3$ ,  $\text{NdCo}_2$ ,  $\text{NdCo}_3$ ,  $\text{Nd}_2\text{Co}_7$ ,  $\text{Nd}_5\text{Co}_{19}$ ,  $\text{NdCo}_5$ , and  $\text{Nd}_2\text{Co}_{17}$ . All but  $\text{Nd}_3\text{Co}$  form by peritectic reaction. Eutectics are observed at  $20 \pm 0.5$  and  $36 \pm 0.5$  at. % Co. Electron microprobe analysis shows  $\text{Nd}_{17}\text{Co}_{13}$  to contain  $28.96 \pm 0.22$  at. % Co (using  $\text{Nd}_3\text{Co}$  as a standard). The X-ray diffraction patterns of  $\text{Nd}_{17}\text{Co}_{13}$  and  $\text{Pr}_{17}\text{Co}_{13}$  are very similar and the two are probably isostructural.

The phases  $\text{Nd}_2\text{Co}_{1.7}$ ,  $\text{Nd}_2\text{Co}_3$ , and  $\text{Nd}_5\text{Co}_{19}$  were not reported in the previous study.<sup>1</sup>  $\text{Nd}_2\text{Co}_{1.7}$  forms by peritectic reaction at  $599 \pm 6^\circ\text{C}$ .  $\text{Nd}_2\text{Co}_3$  also forms by peritectic reaction but the exact temperature is uncertain. A dashed isotherm at  $640 \pm 9^\circ\text{C}$  indicates the statistical center of DTA events observed on heating homogenized alloys containing from 45 to 65 at. % Co. A cooling event which could be definitely associated with the formation of  $\text{Nd}_2\text{Co}_3$  was not observed. Apparently  $\text{Nd}_2\text{Co}_3$  is not readily nucleated from the liquid +  $\text{NdCo}_2$  phase field and forms simultaneously with  $\text{Nd}_2\text{Co}_{17}$  on cooling. Electron microprobe analysis shows  $\text{Nd}_2\text{Co}_3$  to contain  $60.8 \pm 0.3$  at. % Co. X-Ray diffraction results indicate  $\text{Nd}_2\text{Co}_3$  is isostructural with  $\text{La}_2\text{Co}_3$ .<sup>11</sup>

An unexplained thermal event is observed at  $583 \pm 3^\circ\text{C}$  for alloys containing 52.5 to 65 at. % Co. A similar event is observed in the same temperature-composition range in the Pr-Co system.

As in the Ce-Co and Pr-Co systems, the  $\text{Nd}_2\text{Co}_7$  and  $\text{Nd}_5\text{Co}_{19}$  peritectics are only a few degrees apart. In this case, the  $\text{Nd}_2\text{Co}_7$  peritectic is at  $1161 \pm 4^\circ\text{C}$  and the  $\text{Nd}_5\text{Co}_{19}$  is at  $1166 \pm 5^\circ\text{C}$ .

A very narrow solubility range is indicated for  $\text{NdCo}_5$  at  $1100^\circ\text{C}$ . At the stoichiometric composition, lattice constants of  $a = 5.028 \pm 1 \text{ \AA}$  and  $c = 3.977 \pm 2 \text{ \AA}$  were obtained while in the  $\text{NdCo}_5 + \text{Nd}_2\text{Co}_{17}$  phase field we found  $a = 5.027 \pm 1 \text{ \AA}$  and  $c = 3.981 \pm 2 \text{ \AA}$ .

## DISCUSSION

Schweizer<sup>3</sup> reports  $\text{Pr}_5\text{Co}_{19}$  to exist in both rhombohedral and hexagonal forms, with  $a_{\text{rh}} \approx a_{\text{hex}}$  and  $c_{\text{rh}} = 3/2 c_{\text{hex}}$ . The rhombohedral forms of  $\text{Ce}_5\text{Co}_{19}$ ,  $\text{Pr}_5\text{Co}_{19}$ , and  $\text{Nd}_5\text{Co}_{19}$  were strongly dominant in the heat treated alloys of this investigation and it is likely that if stable ranges for the hexagonal forms exist, they must be very close to the peritectic decomposition temperature of the phases. The possibility that  $\text{M}_5\text{X}_{19}$  phases might exist was suggested and their crystal structures correctly predicted by Cromer and Larson<sup>12</sup> in 1959.

Buschow<sup>13</sup> has recently indicated that all of the rare earth-cobalt phases with the  $\text{CaCu}_5$  structure become unstable when cooled, decomposing by eutectoid reaction into the adjacent  $\text{R}_2\text{Co}_7$  and  $\text{R}_2\text{Co}_{17}$  phases. He indicates  $\text{CeCo}_5$ ,  $\text{PrCo}_5$ , and  $\text{NdCo}_5$  are unstable below about  $600^\circ\text{C}$ . We do not detect any evidence of instability of alloys containing  $\text{CeCo}_5$ ,  $\text{PrCo}_5$ , or  $\text{NdCo}_5$  in our DTA traces. In addition, we have heated slightly rare earth-rich alloys of each of these phases for 420 hours at  $500^\circ\text{C}$  and examined them metallographically, by scanning electron microscopy, and by electron microprobe analysis and observed nothing to suggest instability of these  $\text{RCo}_5$  phases.

## REFERENCES

1. A. E. Ray and G. I. Hoffer, Proc. 8th Rare Earth Research Conf., Reno, Nevada, 1970, p. 524.
2. A. E. Ray and K. J. Strnat, Technical Report AFML-TR-71-210, Wright-Patterson AFB, Ohio, October 1971.
3. J. Schweizer, Technical Report ARML-TR-72-82, Wright-Patterson AFB, Ohio, May 1972.
4. A. E. Ray and K. J. Strnat, Technical Report AFML-TR-72-99, Wright-Patterson AFB, Ohio, April 1972.
5. J. B. Y. Tsui and K. J. Strnat, IEEE Trans. Magnetics, MAG-7 (1971) 427.
6. J. Schweizer, K. J. Strnat, and J. B. Y. Tsui, IEEE Trans. Magnetics, MAG-7 (1971) 429.
7. R. E. Vogel and C. P. Kempter, Acta Cryst., 14 (1961) 1130.
8. A. E. Ray and K. J. Strnat, Technical Report AFML-TR-71-53, Wright-Patterson AFB, Ohio, March, 1971.
9. F. H. Ellinger, C. C. Land, K. A. Johnson, and V. O. Struebing, Trans. Met. Soc., AIME, 236 (1966) 1577.
10. K. H. J. Buschow, Philips Res. Repts., 26 (1971) 49.
11. K. H. J. Buschow and W. A. J. J. Velge, J. Less-Common Metals, 13 (1967) 11.
12. D. T. Cromer and A. C. Larson, Acta Cryst. 12 (1959) 855.
13. K. H. J. Buschow, J. Less-Common Metals, 29 (1972) 283.

TABLE I

ANALYSIS OF METALS USED FOR ALLOY PREPARATION, IN ppm.

Sources: Ce- Ames Laboratory, USAEC, Iowa State University  
 Pr, Nd - Lunex Company, Pleasant Valley, Iowa  
 Co(1) - African Metals Corporation, New York, N. Y.  
 Co(2) - Materials Research Corporation, Orangeburg, N. Y.

Element	Ce	Pr	Nd	Co(1)	Co(2)	Element	Ce	Pr	Nd	Co(1)	Co(2)
H	1	*	*	*	*	Ni	3	<1	<1	430	120
N	97-101	12	27	*	*	Cu	1	<1	<1	20	10
O	36-61	515	540	*	*	Zn	--	<50	<50	30	3
C	13-17	*	*	70	40	Ge	<2	*	*	*	*
F	28	*	*	*	*	Zr	<2	--	<20	*	*
B	--	<50	<50	*	*	Mo	<2	*	*	*	*
Na	--	<5	<5	*	*	Ta	20	<10	<10	*	*
Mg	--	<5	--	--	2	Pb	--	--	<10	4	<1
Al	3	--	--	--	3	Y	3	*	*	*	*
Si	--	<50	--	20	<10	La	7	<10	*	*	*
S	<4	*	*	30	<8	Pr	≤50	*	<50	*	*
Cl	20	*	*	*	*	Nd	≤3	<50	*	*	*
K	1	--	<1	--	--	Sm	--	<5	<5	*	*
Ca	4	<200	<200	--	<10	Gd	≤2	--	<1	*	*
Ti	1	--	--	*	*	Tb	≤1	<50	<50	*	*
Cr	1	<1	<1	--	--	Dy	--	<5	<5	*	*
Mn	--	--	<1	5	3	Ho	≤1	<50	<50	*	*
Fe	6	--	<1	30	400	Er	2	<100	<100	*	*
Co	--	<1	<1	*	*	Other R.E.	<1	<5	<5	*	*

\* Not reported; -- Not detected.

TABLE II  
CRYSTALLOGRAPHIC PARAMETERS FOR THE INTERMETALLIC COMPOUNDS  
OF THE BINARY SYSTEMS Ce-Co, Pr-Co, AND Nd-Co

Intermetallic Compound	Crystal Class	Structure Type	Space Group	Lattice Constants
$\beta$ -Ce <sub>2</sub> Co <sub>17</sub>	Hexagonal	Th <sub>2</sub> Ni <sub>17</sub>	P6 <sub>3</sub> /mmc	a = 8.382±1, c = 8.130±2
$\alpha$ -Ce <sub>2</sub> Co <sub>17</sub>	Rhombohedral	Th <sub>2</sub> Zn <sub>17</sub>	R $\bar{3}$ m	a = 8.381±1, c = 12.207±1
Pr <sub>2</sub> Co <sub>17</sub>	Rhombohedral	Th <sub>2</sub> Zn <sub>17</sub>	R $\bar{3}$ m	a = 8.436±2, c = 12.276±2
Nd <sub>2</sub> Co <sub>17</sub>	Rhombohedral	Th <sub>2</sub> Zn <sub>17</sub>	R $\bar{3}$ m	a = 8.426±2, c = 12.425±2
CeCo <sub>5</sub>	Hexagonal	CaZn <sub>5</sub>	P6/mmm	a = 4.928±8, c = 4.0151±9
PrCo <sub>5</sub>	Hexagonal	CaZn <sub>5</sub>	P6/mmm	a = 5.032±2, c = 3.992±2
NdCo <sub>5</sub>	Hexagonal	CaZn <sub>5</sub>	P6/mmm	a = 5.028±1, c = 3.977±2
Ce <sub>5</sub> Co <sub>19</sub>	Rhombohedral	Pr <sub>5</sub> Co <sub>19</sub>	R $\bar{3}$ m	a = 4.939±1, c = 48.71±4
Pr <sub>5</sub> Co <sub>19</sub>	Rhombohedral	Pr <sub>5</sub> Co <sub>19</sub>	R $\bar{3}$ m	a = 5.053±2, c = 48.71±3
Nd <sub>5</sub> Co <sub>19</sub>	Rhombohedral	Pr <sub>5</sub> Co <sub>19</sub>	R $\bar{3}$ m	a = 5.054±2, c = 48.66±3
Ce <sub>2</sub> Co <sub>7</sub>	Hexagonal	Ce <sub>2</sub> Ni <sub>7</sub>	P6 <sub>3</sub> /mmc	a = 4.949±2, c = 24.47±1
Pr <sub>2</sub> Co <sub>7</sub>	Hexagonal	Ce <sub>2</sub> Ni <sub>7</sub>	P6 <sub>3</sub> /mmc	a = 5.072±3, c = 24.51±1
Nd <sub>2</sub> Co <sub>7</sub>	Hexagonal	Ce <sub>2</sub> Ni <sub>7</sub>	P6 <sub>3</sub> /mmc	a = 5.063±2, c = 24.45±1
CeCo <sub>3</sub>	Rhombohedral	PuNi <sub>3</sub>	R $\bar{3}$ m	a = 4.957±5, c = 24.784±7
PrCo <sub>3</sub>	Rhombohedral	PuNi <sub>3</sub>	R $\bar{3}$ m	a = 5.066±1, c = 24.77±1
NdCo <sub>3</sub>	Rhombohedral	PuNi <sub>3</sub>	R $\bar{3}$ m	a = 5.070±1, c = 24.75±1
CeCo <sub>2</sub>	Cubic	MgCu <sub>2</sub>	Fd $\bar{3}$ m	a = 7.1602±7
PrCo <sub>2</sub>	Cubic	MgCu <sub>2</sub>	Fd $\bar{3}$ m	a = 7.306±1
NdCo <sub>2</sub>	Cubic	MgCu <sub>2</sub>	Fd $\bar{3}$ m	a = 7.297±2
Nd <sub>2</sub> Co <sub>3</sub>	Orthorhombic	La <sub>2</sub> Co <sub>3</sub>	--	a = 10.006±2; b = 4.963±2; c = 7.569±4
Pr <sub>2</sub> Co <sub>17</sub>	Hexagonal	Pr <sub>2</sub> Co <sub>17</sub>	--	a = 4.81±1, c = 4.09±2
Nd <sub>2</sub> Co <sub>17</sub>	Hexagonal	Pr <sub>2</sub> Co <sub>17</sub>	--	a = 4.795±2, c = 4.08±2
Ce <sub>2</sub> Co <sub>11</sub>	Hexagonal	--	P6 <sub>3</sub> mc	a = 9.61±1, c = 21.85±2
Pr <sub>7</sub> Co <sub>3</sub>	--	--	--	(29.09±0.31 At.% Co by microprobe)
Nd <sub>7</sub> Co <sub>3</sub>	--	--	--	(28.96±0.22 At.% Co by microprobe)
Pr <sub>3</sub> Co	Orthorhombic	Fe <sub>3</sub> C	Pnma	a = 7.13±1; b = 9.82±2; c = 6.42±1
Nd <sub>3</sub> Co	Orthorhombic	Fe <sub>3</sub> C	Pnma	a = 7.125±2; b = 9.764±3; c = 6.408±3

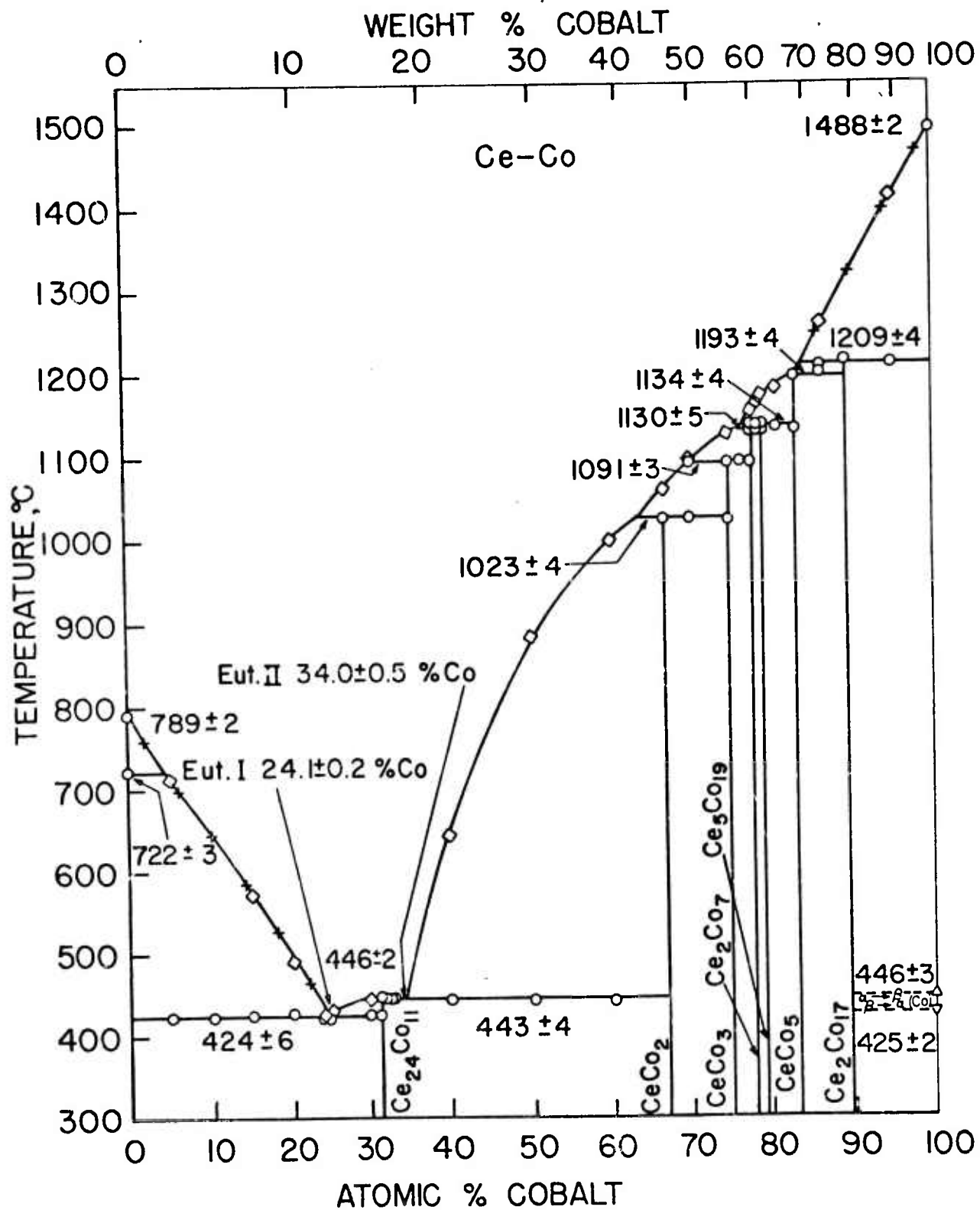


Figure 1. Phase Diagram for the Cerium-Cobalt System.

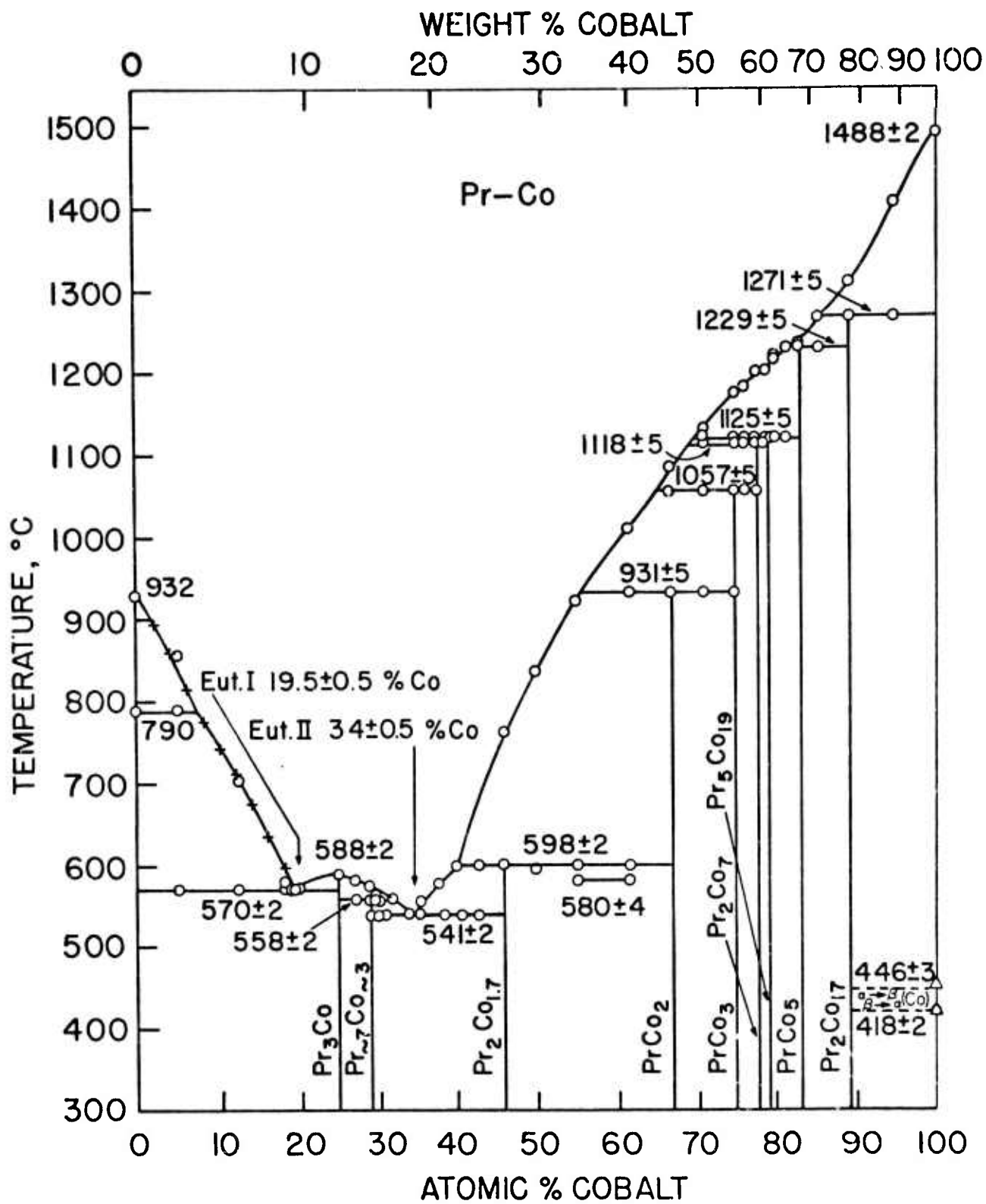


Figure 2. Phase Diagram for the Praseodymium-Cobalt.

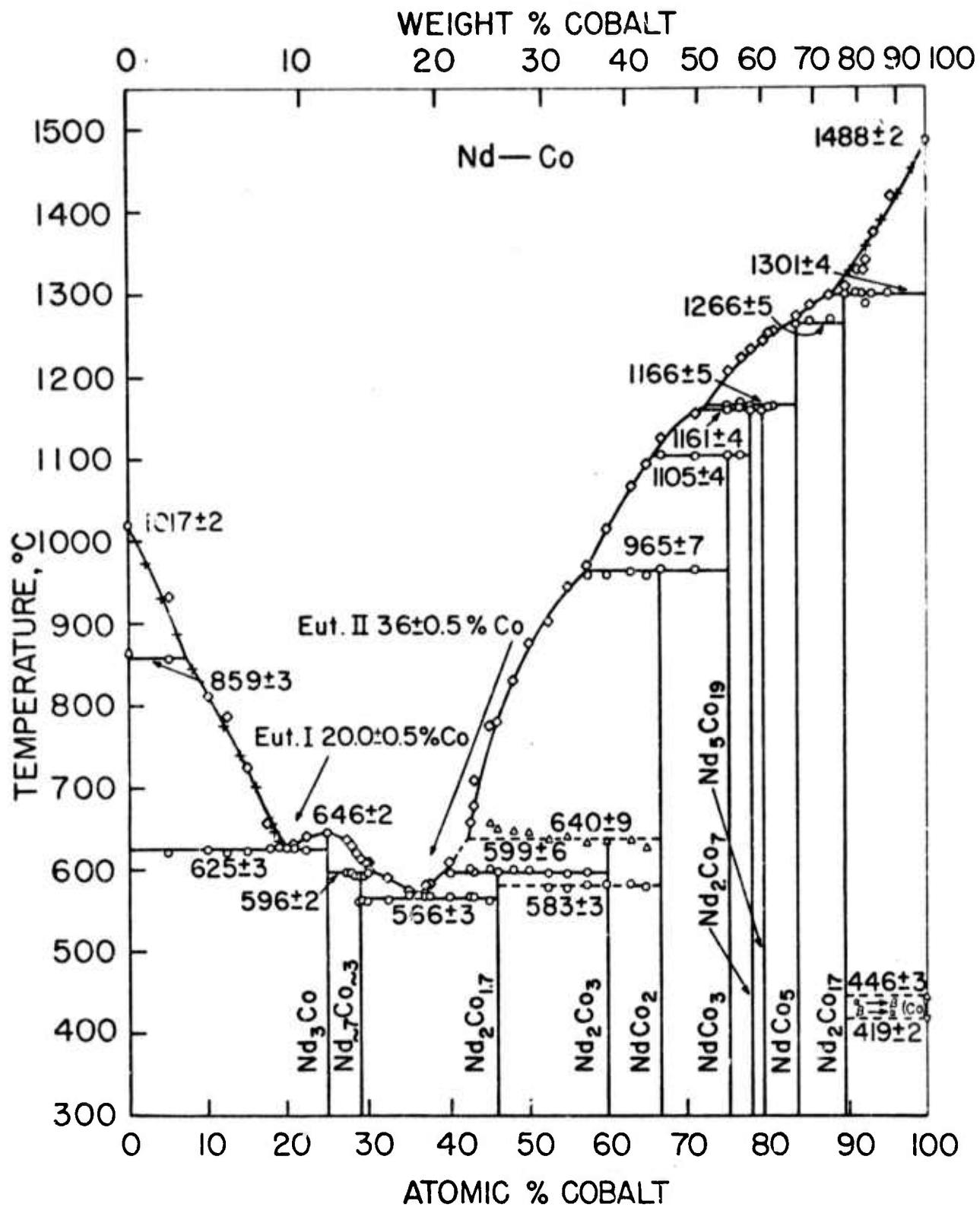


Figure 3. Phase Diagram for the Neodymium-Cobalt.

APPENDIX III

A REVIEW OF  
THE BINARY RARE EARTH-COBALT ALLOY SYSTEMS

A. E. Ray

# A REVIEW OF THE BINARY RARE EARTH-COBALT ALLOY SYSTEMS\*

A. E. Ray  
School of Engineering, University of Dayton  
Dayton, Ohio 45469

## INTRODUCTION

The binary phase diagrams of cobalt with all the technologically important rare earths have now been investigated.<sup>1-16</sup> Lemaire<sup>17</sup> has given an excellent review of the published data concerning the metallurgical and magnetic properties of rare earth-cobalt alloys and intermetallic phases up to 1966. Examination of Table I, which lists papers describing phase diagram investigations chronologically, shows that most of the phase diagram work has been published after 1966, when Strnat and others<sup>18-20</sup> demonstrated the potential of some  $\text{RCO}_5$  as permanent magnet materials. This recent and unusually large body of information, coupled with the chemical similarity of the lanthanides, permits reasonably safe assumptions to be made concerning the metallurgical behavior of rare earth-cobalt alloys in general, and the properties to be expected of mixed rare earth-cobalt alloys in particular. Care should be taken, however, in attempting to apply information obtained under carefully controlled, quasi-equilibrium conditions to production processes, or in ascribing greater accuracy to the published information than is warranted or intended.

This paper reviews the present understanding of the binary rare earth-cobalt phase diagrams and attempts to relate this information to the processes and resultant properties likely to be observed in the production of permanent magnets from these alloys. The discussion is limited to Y and the light rare earth metals, La through Sm, since these

\* This research was supported by the Advanced Research Projects Agency of the Department of Defense and was monitored by the Air Force Materials Laboratory, AFSC, USAF under Contract F33615-70-C-1625.

TABLE I  
 CHRONOLOGICAL LISTING OF RARE EARTH-COBALT  
 PHASE DIAGRAM INVESTIGATIONS

Year	System	Authors	Ref. No.
1947	Ce-Co	Vogel	1
1961	Gd-Co	Novy, Vickery, and Kleber	2
1962	Gd-Co	Savitsky, Terekhova, and Burov	3
1964	Dy-Co	Wood and Conard	4
1965	Y-Co	Pelleg and Carlson	5
	Y-Co	Strnat, Ostertag, Adams, and Olson	6
1966	Ce-Co	Ellinger, Land, Johnson, and Struebing	7
	Er-Co	Buschow	8
1967	La-Co	Buschow and Velge	9
1968	Sm-Co	Buschow and Van der Goot	10
1969	Sm-Co	Lihl, Ehold, Krichmayr, and Wolf	11
	Gd-Co	Lihl, Ehold, Krichmayr, and Wolf	11
	Gd-Co	Buschow and Van der Goot	12
	Ho-Co	Buschow and Van der Goot	13
1970	Ce-Co	Ray and Hoffer	14
	Pr-Co	Ray and Hoffer	14
	Nd-Co	Ray and Hoffer	14
1971	Ce-Co	Buschow	15
	Dy-Co	Buschow	15
	Y-Co	Buschow	15
1973	Ce-Co	Ray, Harmer, and Biermann	16
	Pr-Co	Ray, Harmer, and Biermann	16
	Nd-Co	Ray, Harmer, and Biermann	16
	La-Co	Ray and Biermann, unpublished	--
19??	Pm-Co, Eu-Co, Tb-Co, Tm-Co, Yb-Co, Lu-Co		

would seem to hold the most promise for permanent magnet applications in the immediate future.

### Y-Co

A slightly modified version of the Y-Co phase diagram proposed by Strnat and his co-workers<sup>6</sup> in 1965 is shown in Figure 1. Buschow<sup>15</sup> has also recently studied this system. His version is similar except for some minor differences in melting temperatures. The Y-Co diagram proposed by Pelleg and Carlson<sup>5</sup> differs rather significantly from these in the composition range between 75 and 95 at. % Co. The latter authors did not observe  $Y_2Co_7$  but rather a congruently melting phase with the approximate composition  $YCo_4$ , and they indicate  $Y_2Co_{17}$  to melt by peritectic reaction. Strnat, et al. outline a wide homogeneity range for  $Y_2Co_{17}$ . Although Buschow does not show the homogeneity regions in his diagram, he reports having observed wide homogeneity ranges for both  $Y_2Co_{17}$  and  $YCo_5$  in the text of his paper. The unpublished results of H. Garrett<sup>\*</sup> suggest that the Y-Co diagram between  $YCo_5$  and  $Y_2Co_{17}$  is much more complex than indicated by either of these diagrams. This writer believes that the published "Y-Co" phase diagrams actually represent cuts through the Y-Co-O ternary system.

A number of years ago, when we prepared most of the yttrium-cobalt alloys for the Air Force Materials Laboratory, which Strnat and his group used in their phase diagram study, we found it virtually impossible to eliminate the cast structure of the alloys without annealing them within a few degrees of their melting temperatures. It appeared that oxide particles trapped in the grain boundaries inhibited homogenization and grain growth at lower temperatures. Commercially produced yttrium contains from 1000 to 5000 ppm oxygen, and, unlike most of the rare earth metals, very little oxygen is removed from yttrium alloys

---

\* H. Garrett, unpublished results, Air Force Materials Laboratory, Wright-Patterson Air Force Base, Ohio, 1970.

during melting by the formation of an oxide slag which segregates to the top of the melt. An example of the complex microstructures which we have observed in annealed yttrium-cobalt alloys is shown in Figure 2.

It was the discovery of the large magnetocrystalline anisotropy of  $\text{YCo}_5$  that initiated the interest in the  $\text{RCo}_5$  phases as permanent magnet materials.<sup>18</sup> Moreover, Becker<sup>21</sup> has achieved an energy product of nearly 28 MGOe in a single particle of  $\text{YCo}_5$ . However, no one has reported achieving a usefully high coercive force in an  $\text{RCo}_5$ -based permanent magnet incorporating a substantial amount of yttrium. It is possible that oxide particles in Y-Co alloys provide nucleation sites for reverse domains. If this is the case, then techniques for preparing commercial quantities of low oxygen yttrium-cobalt alloys, and magnet production processes for maintaining the oxygen at low levels will have to be developed before  $\text{YCo}_5$ -based permanent magnets become of commercial interest.

#### La-Co

The lanthanum-cobalt system was first described by Buschow and Velge,<sup>9</sup> who identified six intermediate phases.  $\text{La}_3\text{Co}$  was observed to melt congruently at  $545^\circ\text{C}$ , while  $\text{La}_x\text{Co}$  (~ 46 at. % Co),  $\text{La}_2\text{Co}_3$ ,  $\text{La}_2\text{Co}_7$ ,  $\text{LaCo}_5$ , and  $\text{LaCo}_{13}$  were observed to melt by peritectic reaction at  $570^\circ\text{C}$ ,  $695^\circ\text{C}$ ,  $800^\circ\text{C}$ ,  $1090^\circ\text{C}$ , and  $1185^\circ\text{C}$ , respectively. The authors indicate that the phase diagram they propose is tentative and that they have relied heavily on metallographic evidence in the vicinity of 25 at. % Co. The compositions of the eutectics are not stated and the authors do not indicate how the points of intersection of the peritectic isotherms with the liquidus lines were determined. The latter would appear to be based primarily on extrapolations from observed liquidus points.

We have studied a few alloys on the cobalt-rich side of this system. Our results verify that  $\text{La}_2\text{Co}_{1.7}$ ,  $\text{La}_2\text{Co}_3$ ,  $\text{La}_2\text{Co}_7$ ,  $\text{LaCo}_5$ , and  $\text{LaCo}_{13}$  form peritectically, but we observed these reactions to occur at significantly higher temperatures:  $\text{La}_2\text{Co}_{1.7}$  at  $596^\circ\text{C}$ ,  $\text{La}_2\text{Co}_3$  at  $727^\circ\text{C}$ ,  $\text{La}_2\text{Co}_7$  at  $843^\circ\text{C}$ ,  $\text{LaCo}_5$  at  $1124^\circ\text{C}$ , and  $\text{LaCo}_{13}$  at  $1275^\circ\text{C}$ . In addition, we observe a strong thermal event at  $868^\circ\text{C}$  indicating that a peritectic phase exists between  $\text{La}_2\text{Co}_7$  and  $\text{LaCo}_5$ . Preliminary X-ray diffraction data suggest this new phase corresponds to the composition  $\text{La}_5\text{Co}_{19}$  with  $a = 5.127 \text{ \AA}$  and  $c = 48.74 \text{ \AA}$ . Schweizer, Strnat, and Tsui<sup>22</sup> have shown that the phase reported as  $\text{La}_x\text{Co}$  is, in fact,  $\text{La}_2\text{Co}_{1.7}$ , has a hexagonal structure with  $a = 4.89 \text{ \AA}$ ,  $c = 4.31 \text{ \AA}$ , and is isostructural with  $\text{Pr}_2\text{Co}_{1.7}$  and  $\text{Nd}_2\text{Co}_{1.7}$ .<sup>23</sup> On the basis of these new data, this writer proposes a revised La-Co diagram shown in Figure 3. It should be emphasized that this revision must also be viewed as tentative. Many potentially important features remain to be clarified when, and if, more accurate details are required.

The relative abundance of lanthanum, coupled with the magnetic properties which have been reported for  $\text{LaCo}_5$ ,<sup>24</sup> would appear to make this phase very attractive for some permanent magnet applications. Indeed, some excellent permanent magnets, especially in terms of intrinsic coercive force, have been prepared with  $\text{La}_{0.5}\text{Sm}_{0.5}\text{Co}_5$  as the basic magnetic component.<sup>25, 26</sup> To prepare  $\text{LaCo}_5$  by standard melting practices, an annealing step is required. Buschow and Velge also observed this. The  $\text{LaCo}_{13}$  peritectic isotherm, which evidently extends well beyond the stoichiometric  $\text{LaCo}_5$  composition (83.3 at. % Co),

interferes with the formation of  $\text{LaCo}_5$ . Unless the cooling rate is carefully controlled, very little  $\text{LaCo}_5$  will be observed in the cast alloy. The problem is illustrated by the microstructure of an arc melted, nominally 16.7 at. % La - 83.3 at. % Co alloy button, shown in Figure 4a. X-Ray analysis showed this alloy to contain Co,  $\text{LaCo}_{13}$ , and several more La-rich phases but only a trace of  $\text{LaCo}_5$ . Annealing the alloy for 96 hours at  $1025^\circ\text{C}$  produced the nearly single phase microstructure shown in Figure 4b. X-Ray analysis of the annealed alloy showed only the  $\text{LaCo}_5$  diffraction pattern, with  $a = 5.120 \pm 1 \text{ \AA}$  and  $c = 3.972 \pm 1 \text{ \AA}$ . In larger castings, the segregation is likely to be more severe, and higher annealing temperatures and/or longer annealing times may be required to produce single phase alloys of  $\text{LaCo}_5$ .

#### Ce-Co

The Ce-Co system was first studied by Vogel<sup>1</sup> in 1947. The most recent version of the Ce-Co phase diagram, proposed by Ray, Harmer, and Biermann,<sup>16</sup> is shown in Figure 5. The Ce-rich half of the system is in good agreement with the results of Ellinger, et al.<sup>7</sup> who studied the system between 0 and 50 at. % Co. Eutectics are observed at 24.1 and 34.0 at. % Co, and between these,  $\text{Ce}_{24}\text{Co}_{11}$  is observed to melt congruently at  $446 \pm 2^\circ\text{C}$ . Six peritectically melting Co-rich intermediate phases are observed:  $\text{CeCo}_2$ ,  $\text{CeCo}_3$ ,  $\text{Ce}_2\text{Co}_7$ ,  $\text{Ce}_5\text{Co}_{19}$ ,  $\text{CeCo}_5$ , and  $\text{Ce}_2\text{Co}_{17}$ . In an earlier study of the Co-rich portion of the system, Ray and Hoffer<sup>14</sup> incorrectly assigned the  $\text{Ce}_5\text{Co}_{19}$  peritectic to  $\text{Ce}_2\text{Co}_7$ , and the  $\text{Ce}_2\text{Co}_7$  peritectic was assumed to be a solid state transformation. In another investigation, Buschow<sup>15</sup> did not detect  $\text{Ce}_5\text{Co}_{19}$ , and reports peritectic reaction temperatures which are 21 to  $27^\circ\text{C}$  higher than those given in Figure 5.

Cerium is by far the most abundant and potentially the least expensive of the individual rare earth elements. Procedures for the preparation of large quantities of  $\text{CeCo}_5$  were described by Ray and Millott.<sup>27</sup>

However, because Ce-rich mischmetal (MM) is presently less expensive than cerium metal, and  $\text{MMCo}_5$  possesses some permanent magnet properties which are superior to those of  $\text{CeCo}_5$ ,<sup>25, 28-30</sup> very little effort has been made to develop permanent magnets with  $\text{CeCo}_5$ , as such, as the basic magnetic phase. Most of the development efforts with cerium metal have been made with the precipitation hardenable Ce-Co-Cu alloys.<sup>31-34</sup>

### Pr-Co

The phase diagram for the Pr-Co system<sup>16</sup> is shown in Figure 6. A total of nine intermediate phases are observed:  $\text{Pr}_3\text{Co}$ ,  $\text{Pr}_{-7}\text{Co}_{-3}$ ,  $\text{Pr}_2\text{Co}_{1.7}$ ,  $\text{PrCo}_2$ ,  $\text{PrCo}_3$ ,  $\text{Pr}_2\text{Co}_7$ ,  $\text{Pr}_5\text{Co}_{19}$ ,  $\text{PrCo}_5$ , and  $\text{Pr}_2\text{Co}_{17}$ . Only  $\text{Pr}_3\text{Co}$  melts congruently. Thermal analysis of alloys containing 50, 55, and 61.5 at. % Co indicates an event at  $580 \pm 4^\circ\text{C}$ . The nature of this event is unknown. X-Ray diffraction patterns of these alloys annealed at  $500^\circ\text{C}$ , show only  $\text{Pr}_2\text{Co}_{1.7}$  and  $\text{PrCo}_2$  to be present. In an earlier investigation,<sup>14</sup> although we detected both the  $\text{Pr}_2\text{Co}_7$  and  $\text{Pr}_5\text{Co}_{19}$  peritectic reactions, we incorrectly assigned the higher event to  $\text{Pr}_2\text{Co}_7$  and the lower to a solid state reaction in this phase. Schweizer<sup>22</sup> first identified the existence of  $\text{Pr}_5\text{Co}_{19}$  and determined its crystal structure. Lattice parameter measurements indicate only very narrow ranges of solubility for  $\text{PrCo}_3$ ,  $\text{Pr}_2\text{Co}_7$ , and  $\text{Pr}_5\text{Co}_{19}$  at  $1000^\circ\text{C}$  and for  $\text{Pr}_2\text{Co}_{17}$  at  $1100^\circ\text{C}$ . We detected a significant extension of the  $\text{PrCo}_5$  phase field toward higher cobalt at  $1100^\circ\text{C}$ , however. In the  $\text{Pr}_5\text{Co}_{19} + \text{PrCo}_5$  phase field and for stoichiometric  $\text{PrCo}_5$ , we found  $a = 5.032 \pm 2 \text{ \AA}$  and  $c = 3.997 \pm 2 \text{ \AA}$ , while in the  $\text{PrCo}_5 + \text{Pr}_2\text{Co}_{17}$  phase field we obtained  $a = 5.021 \pm 5 \text{ \AA}$  and  $c = 4.028 \pm 7 \text{ \AA}$ . The relatively large increase in the c-axis accompanied by a smaller decrease in the a-axis suggests that some of the Pr-sites in  $\text{PrCo}_5$  have been replaced by pairs of Co atoms aligned parallel to the c-axis.

Among the binary  $\text{RCo}_5$  phases,  $\text{PrCo}_5$  has the highest potential energy product, 36 MGOe.<sup>28</sup> Moreover, praseodymium is more than eight times as plentiful as samarium in bastnasite, the major source of rare earth metals in the United States.<sup>35</sup> Procedures have been developed for the preparation of large quantities of  $\text{PrCo}_5$ ,<sup>27</sup> the magnetic properties of  $\text{PrCo}_5$  powders determined,<sup>36</sup> and some very encouraging preliminary results with  $\text{PrCo}_5$  as the basic magnetic phase have been reported.<sup>37-39</sup> In spite of its potential, the development of  $\text{PrCo}_5$ -based permanent magnets have been neglected in favor of those based on  $\text{SmCo}_5$  and on  $\text{Sm}_{1-x}\text{Pr}_x\text{Co}_5$ .<sup>25, 40</sup> Indeed, the highest energy product yet reported in a sintered permanent magnet,  $(\text{BH})_{\text{max}} = 26 \text{ MGOe}$ , has been achieved with  $\text{Sm}_{0.24}\text{Pr}_{0.76}\text{Co}_5$  as the base metal powder.<sup>41</sup>

In their experiments with  $\text{PrCo}_5$  and Pr-rich, Pr-Co alloys as sintering additives, Schweizer, Strnat, and Tsui<sup>39</sup> found an extremely sensitive dependence of the intrinsic coercive force with sintering temperature. Their results are shown in Figure 7. They noted that the steep rise in  $M^H_c$  corresponded exactly to the temperature range of the closely spaced thermal events between  $1118^\circ\text{C}$  and  $1125^\circ\text{C}$  in the Pr-Co phase diagram. As pointed out previously, the event at  $1118^\circ\text{C}$  was originally thought to be a phase transition in  $\text{Pr}_2\text{Co}_7$  and the event at  $1125^\circ\text{C}$ , the  $\text{Pr}_2\text{Co}_7$  peritectic. It was postulated that the steep rise in  $M^H_c$  could be due to an epitaxial shell of  $\text{Pr}_2\text{Co}_7$  surrounding the  $\text{PrCo}_5$  grains, on cooling through the phase transition at  $1118^\circ\text{C}$ , this shell would develop a large number of stacking faults which could act as pinning sites for domain walls. It is now known that the thermal event at  $1118^\circ\text{C}$  is, in fact, the  $\text{Pr}_2\text{Co}_7$  peritectic, and that the sintering window lies in the temperature range corresponding to the liquid plus  $\text{Pr}_5\text{Co}_{19}$  phase field. This new evidence does not invalidate the epitaxial shell concept. In fact, it may lend additional support to the basic theory. Now, however, in addition to stacking faults, several other factors which could possibly influence  $M^H_c$  can be postulated.

## Nd-Co

The recently revised and completed version of the Nd-Co phase diagram<sup>16</sup> is shown in Figure 8. The system contains ten intermediate phases:  $\text{Nd}_3\text{Co}$ ,  $\text{Nd}_{1.7}\text{Co}_{1.3}$ ,  $\text{Nd}_2\text{Co}_{1.7}$ ,  $\text{Nd}_2\text{Co}_3$ ,  $\text{NdCo}_2$ ,  $\text{NdCo}_3$ ,  $\text{Nd}_2\text{Co}_7$ ,  $\text{Nd}_5\text{Co}_{19}$ ,  $\text{NdCo}_5$ , and  $\text{Nd}_2\text{Co}_{17}$ . All but  $\text{Nd}_3\text{Co}$  melt peritectically. A tentative phase diagram for the Nd-Co system was proposed earlier,<sup>14</sup> although the portion of the system between 40 and 60 at. % Co was left incomplete. The phases  $\text{Nd}_2\text{Co}_{1.7}$ ,  $\text{Nd}_2\text{Co}_3$ , and  $\text{Nd}_5\text{Co}_{19}$  were not reported in the previous study.  $\text{Nd}_2\text{Co}_3$  forms by peritectic reaction, but the exact temperature is uncertain. The dashed isotherm at  $640 \pm 9^\circ\text{C}$  indicates the statistical center of DTA events observed on heating alloys containing from 45 to 65 at. % Co and homogenized at  $500^\circ\text{C}$ . A cooling event which could be definitely associated with  $\text{Nd}_2\text{Co}_3$  was not observed. An unexplained thermal event is observed at  $583 \pm 3^\circ\text{C}$  in alloys containing 52.5 to 65 at. % Co. A similar event is observed in the same temperature-composition range in the Pr-Co system. As in the Ce-Co and Pr-Co systems, the  $\text{Nd}_2\text{Co}_7$  and  $\text{Nd}_5\text{Co}_{19}$  peritectics are only a few degrees apart. In this case, the  $\text{Nd}_2\text{Co}_7$  peritectic is at  $1161 \pm 4^\circ\text{C}$  and the  $\text{Nd}_5\text{Co}_{19}$  at  $1166 \pm 5^\circ\text{C}$ .

A very narrow solubility range is indicated for  $\text{NdCo}_5$  by alloys annealed at  $1100^\circ\text{C}$ . At the stoichiometric composition, lattice constants of  $a = 5.028 \pm 1 \text{ \AA}$  and  $c = 3.977 \pm 2 \text{ \AA}$  were obtained while in the  $\text{NdCo}_5 + \text{Nd}_2\text{Co}_{17}$  phase field we found  $a = 5.027 \pm 1 \text{ \AA}$  and  $c = 3.981 \pm 2 \text{ \AA}$ .

The relative abundance of neodymium,<sup>35</sup> coupled with the high saturation and Curie temperature of  $\text{NdCo}_5$ <sup>17</sup> would appear to make it attractive for some magnetic applications. The relatively small anisotropy constant of  $\text{NdCo}_5$  and the fact that it changes sign just below room temperature<sup>42, 43</sup> have apparently discouraged development efforts with this material. Tsui, Strnat, and Schweizer,<sup>44</sup> however, have reported dramatic increases in the intrinsic coercive forces of  $\text{NdCo}_5$  and  $\text{DyCo}_5$

(Di = didymium, a commercial alloy composed principally of Nd and Pr in about a 3:1 ratio) by sintering these powders with Pr-rich and Sm-rich cobalt alloy sintering additives. The properties of the sintered magnets were observed to be very sensitive to composition and especially to sintering temperature.

### Sm-Co

Tentative phase diagrams for the system Sm-Co have been proposed for the entire system by Buschow and Van der Goot,<sup>10</sup> Figure 9, and by Lihl, et al.,<sup>11</sup> for the system between 60 and 100 at. % Co. There is general agreement between these investigations as to the Co-rich phases that exist and whether the phases melt congruently or by peritectic reaction. The major differences are the melting temperature of  $\text{Sm}_2\text{Co}_{17}$ ,  $1335^\circ\text{C}$  and  $1375^\circ\text{C}$ , and the peritectic temperature of  $\text{SmCo}_2$ ,  $1075^\circ\text{C}$  and  $1050^\circ\text{C}$ , respectively. Both indicate relatively wide high temperature solubility ranges for  $\text{SmCo}_5$  extending toward  $\text{Sm}_2\text{Co}_{17}$  and for  $\text{Sm}_2\text{Co}_{17}$  toward  $\text{SmCo}_5$ . Reference 10 indicates the  $\text{SmCo}_5$  phase field extends from approximately 83.0 to 85.5 at. % Co just below the peritectic at  $1320^\circ\text{C}$ , but becomes quite narrow below  $800^\circ\text{C}$ . The lattice parameter data of Martin, Benz, and Rockwood<sup>45</sup> indicate the  $\text{SmCo}_5$  phase field to extend from 83.15 to 83.65 at. % Co in alloys sintered for 1 hour at  $1120^\circ\text{C}$ , slowly cooled to  $900^\circ\text{C}$ , then rapidly cooled. Their density measurements suggest a slightly narrower range from 83.30 to 83.65 at. % Co.

We have studied a number of Sm-Co alloys by metallographic, X-ray diffraction, and differential thermal analysis. Some of our observations are not in accord with the published diagrams and suggest significant changes. We have concluded that  $\text{Sm}_2\text{Co}_{17}$  forms by peritectic reaction at  $1310 \pm 5^\circ\text{C}$ . The primary basis for this conclusion is shown in Figure 10. On heating a metallographically single phase  $\text{Sm}_2\text{Co}_{17}$  alloy, we observe an intense thermal event at  $1310^\circ\text{C}$ , and on cooling, what we interpret to be a liquidus above this reaction at  $1355^\circ\text{C}$ .

To account for this observation from either of the proposed phase diagrams would require that a very substantial portion of the samarium initially present in our alloy was lost during a single heating cycle to 1450°C. Both previous investigations concluded that a eutectic occurs between  $\text{Sm}_2\text{Co}_{17}$  and Co near 90 at. % Co. If it is assumed that  $\text{Sm}_2\text{Co}_{17}$  melts congruently, and the fact that a nearly single phase microstructure can be obtained directly from the melt, Figure 11a, would tend to support this assumption, then a eutectic between  $\text{Sm}_2\text{Co}_{17}$  and Co must occur; and again, there is metallographic evidence to suggest that a eutectic may exist in this composition range. We have noted that alloys slightly Co-rich of  $\text{Sm}_2\text{Co}_{17}$  stoichiometry have a eutectic-like microconstituent, Figure 11b. This writer believes that these are non-equilibrium microstructures resulting from the strong propensity of alloys in this composition range to supercool well below the equilibrium solidification temperature of  $\text{Sm}_2\text{Co}_{17}$ . The observed microstructures result from the peculiarities of the mode of solidification of the supercooled alloys. The strong supercooling coupled with the very consistent temperature at which solidification initiates suggests that  $\text{Sm}_2\text{Co}_{17}$  is nucleated by a phase richer in samarium. The formation of the nucleating phase (perhaps  $\text{SmCo}_5$ ) would result in a liquid strongly supersaturated with respect to cobalt, and a massive nucleation of excess cobalt could account for the observed eutectic-like microstructure. Our results indicate that the  $\text{Sm}_2\text{Co}_{17}$  peritectic isotherm extends to 78-79 at. % Co. This interpretation would explain the previous investigators' observations of thermal events occurring at nearly the same temperature on either side of the stoichiometric  $\text{Sm}_2\text{Co}_{17}$  composition, and also for the large (40°C) discrepancy of the suggested melting point of  $\text{Sm}_2\text{Co}_{17}$ . A discrepancy of this magnitude can be reconciled with a steeply rising liquidus and small changes in composition. It is noted that our liquidus point at 1355°C is midway between the previous investigators' measurements. As shown in Figure 12, no liquidus is observed in alloys containing nominally

79 to 80 at. % Co, (corrected for Sm weight loss during arc melting). When such alloys, homogenized 48 hours at 1125°C, are initially heated in this range, thermal events are observed at 1234 ± 3°C and 1296 ± 3°C. On cooling from approximately 1400°C, there is strong supercooling to 1280 ± 8°C, whereupon the samples reheat to 1310 ± 2°C. In subsequent heating cycles, the 1234°C event is not detected, but the 1296°C and an additional event at 1310°C, which was not observed on the initial cycle, are noted. Only the 1310°C event, accompanied by the strong supercooling, is observed for second and third cooling cycles. The standard deviations given for these observations reflect the precision of the apparatus rather than the accuracy of our measurements. The probable accuracy of these data (not including the rather consistent point to which the alloys supercool) is ± 5°C. One is tempted to associate the vent at 1296°C with the peritectic melting temperature of SmCo<sub>5</sub>, but this and further interpretation without supporting measurements would only be speculative.

From our preliminary studies, we have concluded that many important features of the Sm-Co phase diagram remain to be established. In order to understand the metallurgical and magnetic behavior of Sm-Co alloys during sintering, post-sintering heat treatments, and the aging characteristics of finished "SmCo<sub>5</sub>" permanent magnets, these important features must be accurately determined.

#### Comments on the Stability of the RCo<sub>5</sub> Phases

It has recently been reported that SmCo<sub>5</sub> and GdCo<sub>5</sub>,<sup>46</sup> and indeed all of the RCo<sub>5</sub> phases,<sup>47, 48</sup> become unstable on cooling, decomposing by the eutectoid reaction  $RCo_5 \rightarrow R_2Co_7 + R_2Co_{17}$ . The eutectoid reactions are reported to occur near 600°C for R = La, Ce, Pr, and Nd and between 700°C and 750°C for Sm, Gd, and Y. It is suggested that the reaction is connected with a coercivity loss in RCo<sub>5</sub> powder compacts heated in this range. The practical implications of these conclusions to the utilization of permanent magnets based on the RCo<sub>5</sub> phases are significant and should be carefully tested.

The conclusions that the  $\text{RCo}_5$  phases of Y and the light rare earths La through Gd are unstable are based primarily on metallographic evidence. Initially single phase alloys, after annealing for long periods at low temperatures, are shown to have a lighter phase located along the grain boundaries and striations within the original  $\text{RCo}_5$  grains. The lighter phase is identified as the  $\text{R}_2\text{Co}_{17}$  phase and its presence in the annealed alloys is confirmed by X-ray diffraction analysis. The striations are interpreted to be the  $\text{R}_2\text{Co}_7$  phase but this phase is not observed in the X-ray diffraction patterns and no other tests to confirm its presence are reported. Thus, only one of the products of the proposed eutectoid decomposition is positively identified and the presence of the  $\text{R}_2\text{Co}_7$  phase, which should exceed the amount of  $\text{R}_2\text{Co}_{17}$  formed,\* is only surmised.

This writer feels that an equally plausible explanation of the observed microstructures is that the initially single phase alloys are hyperstoichiometric with respect to cobalt and that the excess cobalt is precipitated as  $\text{R}_2\text{Co}_{17}$  when annealed at low temperatures. We have annealed an Y-Co alloy containing nominally 86.5 at. % Co for long periods at various temperatures and obtained microstructures very similar to those shown to illustrate eutectoid decomposition. After 120 hours at  $1275^\circ\text{C}$  we obtained a nearly single phase microstructure, but 42 days at  $900^\circ\text{C}$  and 120 days at  $535^\circ\text{C}$  produced the microstructures shown in Figure 13a and 13b, respectively. The excess cobalt in the hyperstoichiometric "YCo<sub>5</sub>" has precipitated as  $\text{Y}_2\text{Co}_{17}$ , both at the grain boundaries and within the grains of the original microstructure. X-Ray diffraction analysis confirms the presence of only YCo<sub>5</sub> and  $\text{Y}_2\text{Co}_{17}$  in the annealed alloys.

---

\* Assuming that the composition of the  $\text{RCo}_5$  phase undergoing the eutectoid reaction is stoichiometric (83.3 at. % Co), the fractional amounts of  $\text{R}_2\text{Co}_7$  (77.8 at. % Co) and  $\text{R}_2\text{Co}_{17}$  (89.5 at. % Co) formed are given by the lever rule:

$$\text{R}_2\text{Co}_7 = \frac{89.5-83.3}{89.5-77.8} \times 100 = 53\%$$

$$\text{R}_2\text{Co}_{17} = \frac{83.3-77.8}{89.5-77.8} \times 100 = 47\%.$$

We have shown that in the Ce-Co, Pr-Co, and Nd-Co alloy systems, the rare earth-rich phase adjacent to  $\text{RCo}_5$  has the stoichiometry  $\text{R}_5\text{Co}_{19}$ .<sup>16</sup> If  $\text{CeCo}_5$ ,  $\text{PrCo}_5$ , or  $\text{NdCo}_5$  were to undergo a eutectoid reaction, one would expect the reaction products to be  $\text{R}_5\text{Co}_{19}$  (60%) and  $\text{R}_2\text{Co}_{17}$  (40%). We felt that this amount of  $\text{R}_5\text{Co}_{19}$  should be easily detectable by several means. In a recent study,<sup>49</sup> we initially homogenized alloys of  $\text{CeCo}_5$ ,  $\text{PrCo}_5$ , and  $\text{NdCo}_5$  at  $1100^\circ\text{C}$  for 30 hours to obtain single phase microstructures, and then annealed them at  $500^\circ\text{C}$  for 420 hours to allow the reported eutectoid reactions to occur. We examined the alloys metallographically, by X-ray diffraction, and electron microprobe analysis and did not detect any evidence of decomposition of the  $\text{RCo}_5$  phases. Differential thermal analysis showed only the Curie temperatures of the  $\text{RCo}_5$  phases on heating and cooling through the  $300^\circ\text{C}$ - $700^\circ\text{C}$  range. Finally, we examined the annealed  $\text{CeCo}_5$  alloy by thermal magnetic analysis. Nothing was found in the TMA spectrum on cooling from room temperature to  $-180^\circ\text{C}$ . If more than a few percent of  $\text{Ce}_5\text{Co}_{19}$  ( $T_c \sim 0^\circ\text{C}$ ) or  $\text{Ce}_2\text{Co}_7$  ( $T_c = -122^\circ\text{C}$ ) were present, one would expect permeability peaks corresponding to one or the other of these magnetic transitions.

In conclusion, our findings show that  $\text{CeCo}_5$  does not undergo a eutectoid decomposition and we observe no evidence of instability on the part of  $\text{PrCo}_5$  or  $\text{NdCo}_5$ . We observed  $\text{YCo}_5$  to be present and apparently stable after annealing for 120 days at  $535^\circ\text{C}$ . Whether or not  $\text{SmCo}_5$  undergoes a eutectoid decomposition remains to be determined but the existence of one of the decomposition products, namely a phase rare earth-rich with respect to  $\text{SmCo}_5$ , and coexisting with  $\text{Sm}_2\text{Co}_{17}$  has not been established.

#### ACKNOWLEDGMENT

The author wishes to express his appreciation to his colleagues K. J. Strnat and R. S. Harmer for their assistance and encouragement, and for the experimental assistance of A. T. Biermann, A. R. Kraus, R. E. Leasure, and M. G. Hartings.

## REFERENCES

1. R. Vogel (W. Füllung), *Z. Metallk.* 38 (1947) 97.
2. V. F. Novy, R. C. Vickery, and E. V. Kleber, *Trans. AIME*, 221 (1961) 588.
3. E. M. Savitsky, V. F. Terekhova, and I. V. Burov, *Alloys of the Rare Earth Metals*, Publishing House, Academy of Sciences, USSR, Moscow, 1962.
4. J. Pelleg and O. N. Carlson, *J. Less-Common Metals*, 9 (1965) 281.
5. K. Strnat, W. Ostertag, N. J. Adams, and J. C. Olson, *Proc. 5th Rare Earth Research Conference, Iowa State University, Ames, Iowa, 1965. Book 5, p. 67.*
6. F. H. Ellinger, C. C. Land, K. A. Johnson, and V. O. Struebing, *Trans. AIME*, 236 (1966) 1577.
7. K. H. J. Buschow, *Z. Metallk.*, 57 (1966) 728.
8. K. H. J. Buschow and W. A. J. J. Velge, *J. Less-Common Metals*, 13 (1967) 11-17.
9. K. H. J. Buschow and A. S. Van der Goot, *J. Less-Common Metals*, 14 (1968) 323.
10. F. Lihl, J. R. Ehold, H. R. Kirchmayr, and H. D. Wolf, *Acta Physica Austriaca*, 30 (1969) 164.
11. K. H. J. Buschow and A. S. Van der Goot, *J. Less-Common Metals*, 17 (1969) 249.
12. J. D. Wood and G. P. Conard II, *Rare Earth Research II*, Gordon and Breach, New York, 1964, p. 209.
13. K. H. J. Buschow and A. S. Van der Goot, *J. Less-Common Metals*, 19 (1969) 153.
14. A. E. Ray and G. I. Hoffer, *Proc. 8th Rare Earth Research Conference, Reno, Nevada, 1970, Vol. II, p. 524.*

15. K. H. J. Buschow, Philips Res. Repts., 26 (1971) 49.
16. A. E. Ray, R. S. Harmer, and A. T. Biermann, Proc. 10th Rare Earth Research Conference, Carefree, Arizona, 1973, Vol. II, p. 711. (Submitted to Cobalt)
17. R. Lemaire, Cobalt, No. 32, September (1966) 132 and No. 33, December (1966) 201.
18. K. Strnat and G. Hoffer, "YCo<sub>5</sub>-A Promising New Permanent Magnet Material," AFML-TR-65-446, Wright-Patterson Air Force Base, Ohio, May 1966.
19. G. Hoffer and K. Strnat, IEEE Trans. Magnetics, MAG-2 (1966) 487.
20. K. Strnat, G. Hoffer, J. C. Olson, W. Ostertag, and J. J. Becker, J. Appl. Physics, 38 (1967) 1001.
21. J. J. Becker, J. Appl. Physics, 42 (1971) 1537.
22. J. Schweizer, K. J. Strnat, and J. B. Y. Tsui in J. Schweizer, "Research on Rare Earth-Cobalt Alloys and Compounds," AFML-TR-72-82, Wright-Patterson Air Force Base, Ohio, May 1972.
23. J. Schweizer, K. J. Strnat, and J. B. Y. Tsui, 9th Rare Earth Research Conference, Blacksburg, Virginia, 1971, Vol. I, p. 96.
24. K. H. J. Buschow and W. A. J. J. Velge, Z. angewandte Physik, 26 (1969) 157.
25. D. L. Martin and M. G. Benz, Cobalt, No. 50, March (1971) 11.
26. D. L. Martin, U. S. Patent No. 3,682,715, August 8, 1972.
27. A. E. Ray and H. Millott, IEEE Trans. Magnetics, MAG-7, (1971) 423.
28. K. J. Strnat, IEEE Trans. Magnetics, MAG-6, (1970) 182.
29. D. L. Martin and M. G. Benz, U. S. Patent No. 3,682,716, August 8, 1972.
30. C. J. Fellows and R. E. Johnson, Cobalt, No. 56, Sept. (1972) 141.
31. E. A. Nesbitt, R. H. Willens, R. C. Sherwood, E. Buehler, and J. H. Wernick, Appl. Phys. Letters, 12(1968) 361.

32. Y. Tawara and H. Senno, Japan J. Appl. Phys. 7 (1968) 966.
33. E. A. Nesbitt, J. Appl. Phys., 40 (1969) 1259.
34. H. Senno and Y. Tawara, Japan J. Appl. Phys., 8 (1968) 118.
35. See, for example, "Overview," Bulletin No. 36, published by Molybdenum Corporation of America, New York, 1972.
36. K. Strnat and J. B. Y. Tsui, Proc. 8th Rare Earth Research Conference, Reno, Nevada, 1970, Vol. I, p. 3.
37. J. Tsui and K. Strnat, Appl. Phys. Letters, 18 (1971) 107.
38. J. B. Y. Tsui and K. J. Strnat, IEEE Trans. Magnetics, MAG-7, (1971) 427.
39. J. Schweizer, K. J. Strnat, and J. B. Y. Tsui, *ibid.*, p. 429.
40. D. L. Martin, U. S. Patent No. 3,682,714, August 8, 1972.
41. R. J. Charles, D. L. Martin, L. Valentine, and R. E. Cech, AIP Conf. Proc. No. 5, Magnetism and Magnetic Materials - 1971, p. 1072.
42. E. Tatsumoto, T. Okamoto, H. Fujii, and C. Inoue, J. Phys. (Paris) 32 (1971), C1-550.
43. H. Bartholin, B. van Laar, R. Lemaire, and J. Schweizer, J. Phys. Chem. Solids, 27(1966) 1287.
44. J. B. Y. Tsui, K. J. Strnat, and J. Schweizer, Appl. Phys. Letters, 21(1972) 446.
45. D. L. Martin, M. G. Benz, and A. C. Rockwood, AIP Conf. Proc., No. 10, Magnetism and Magnetic Materials - 1972, p. 583.
46. F. J. A. den Broeder and K. H. J. Buschow, J. Less-Common Metals, 29 (1972) 65.
47. K. H. J. Buschow, J. Less-Common Metals, 29 (1972) 283.
48. K. H. J. Buschow, J. Less-Common Metals, 31 (1973) 359.
49. A. E. Ray and K. J. Strnat, "Research and Development of Rare Earth-Transition Metal Alloys as Permanent Magnet Materials," Technical Report AFML-TR-73-112, Wright-Patterson Air Force Base, Ohio, May 1973.

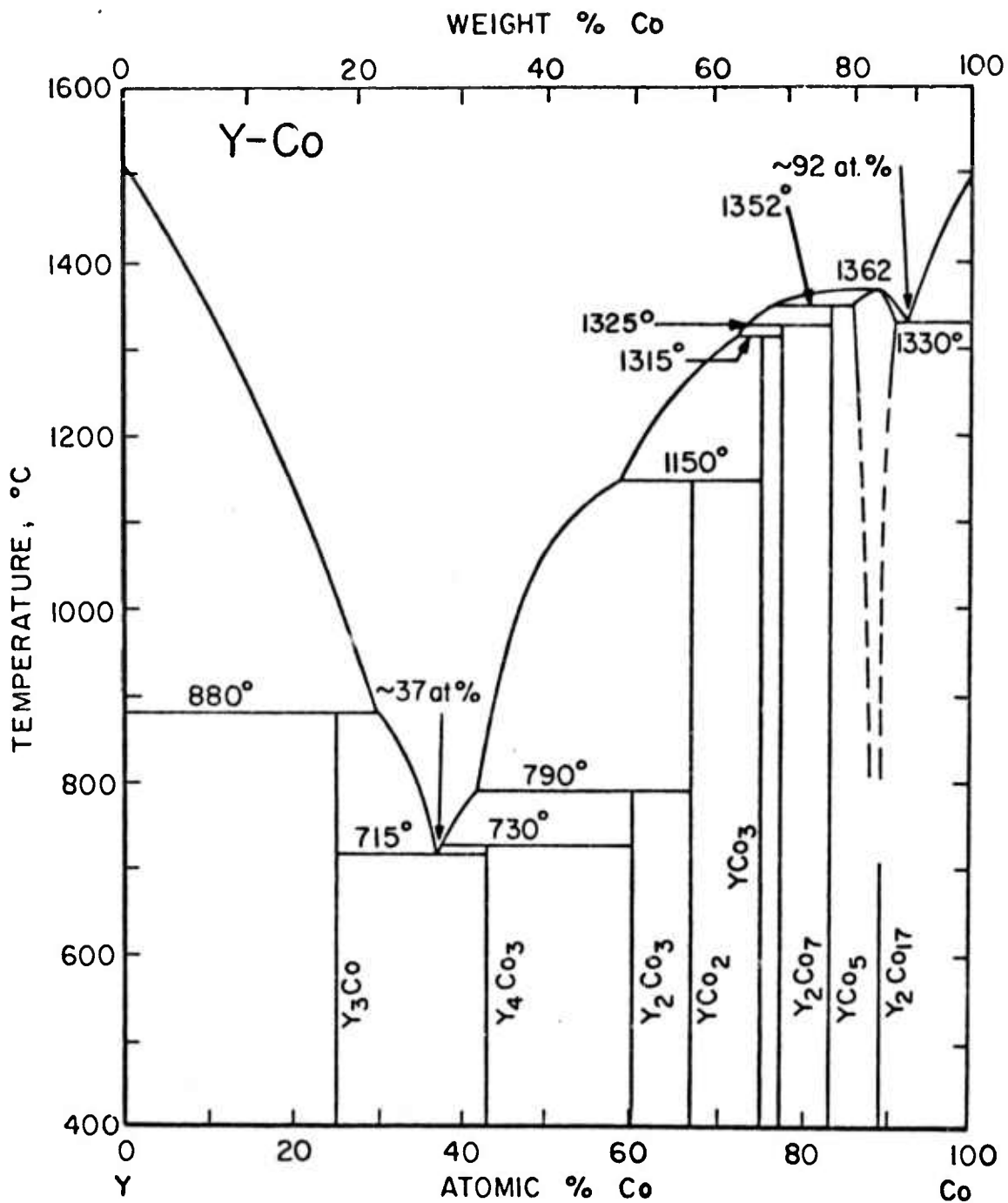


Figure 1. Phase Diagram for the Y-Co System Proposed by Strnat, Ostertag, Adams, and Olson.<sup>6</sup>

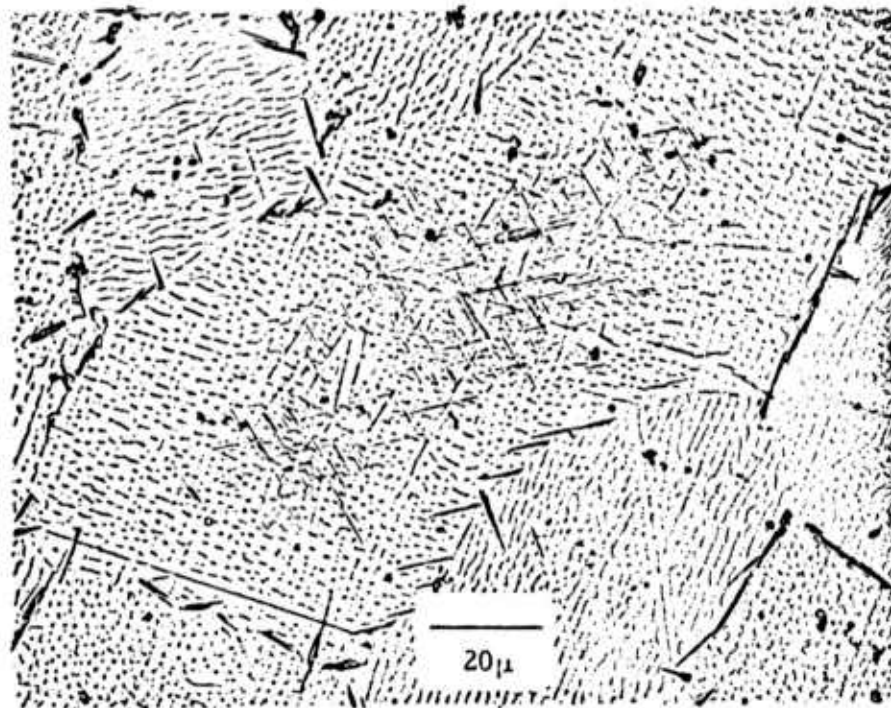


Figure 2. Complex microstructure developed in an Y-Co alloy, nominally  $YCo_2$ , on annealing for 270 hours at  $1100^{\circ}C$ . The persistence of the as-cast microstructure can be observed. The alloy was prepared from yttrium containing approximately 2000 ppm oxygen. The acicular phase in the grain boundaries and the Widmanstätten precipitate may be related to the high oxygen content.

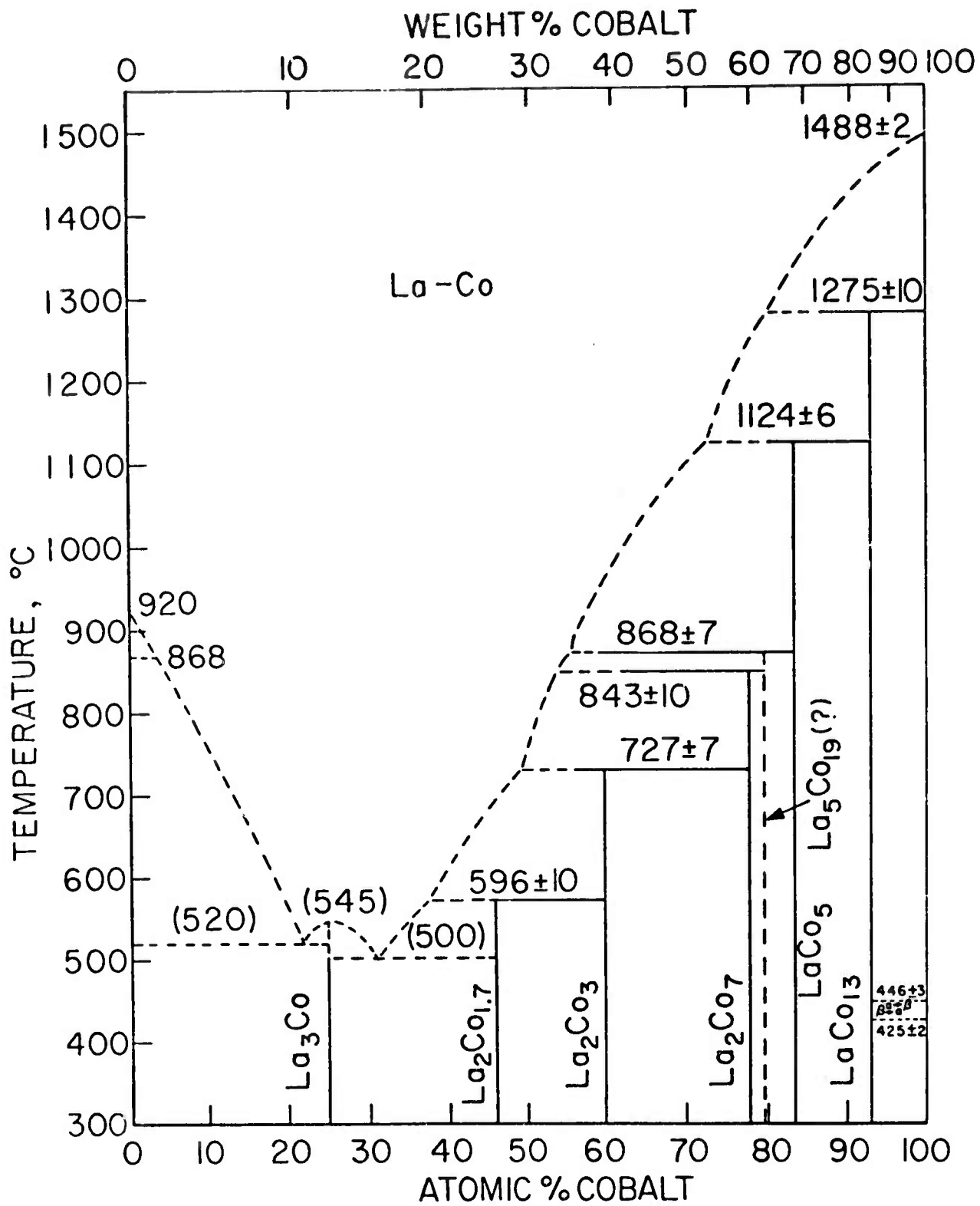


Figure 3. Revised Phase Diagram for the La-Co Alloy System. The original version was described by Buschow and Velge.



(a)



(b)

Figure 4. Microstructures of a La-Co Alloy, Nominally  $\text{LaCo}_5$ , (a) As-Cast, and (b) After Annealing 96 Hours at  $1025^\circ\text{C}$ .

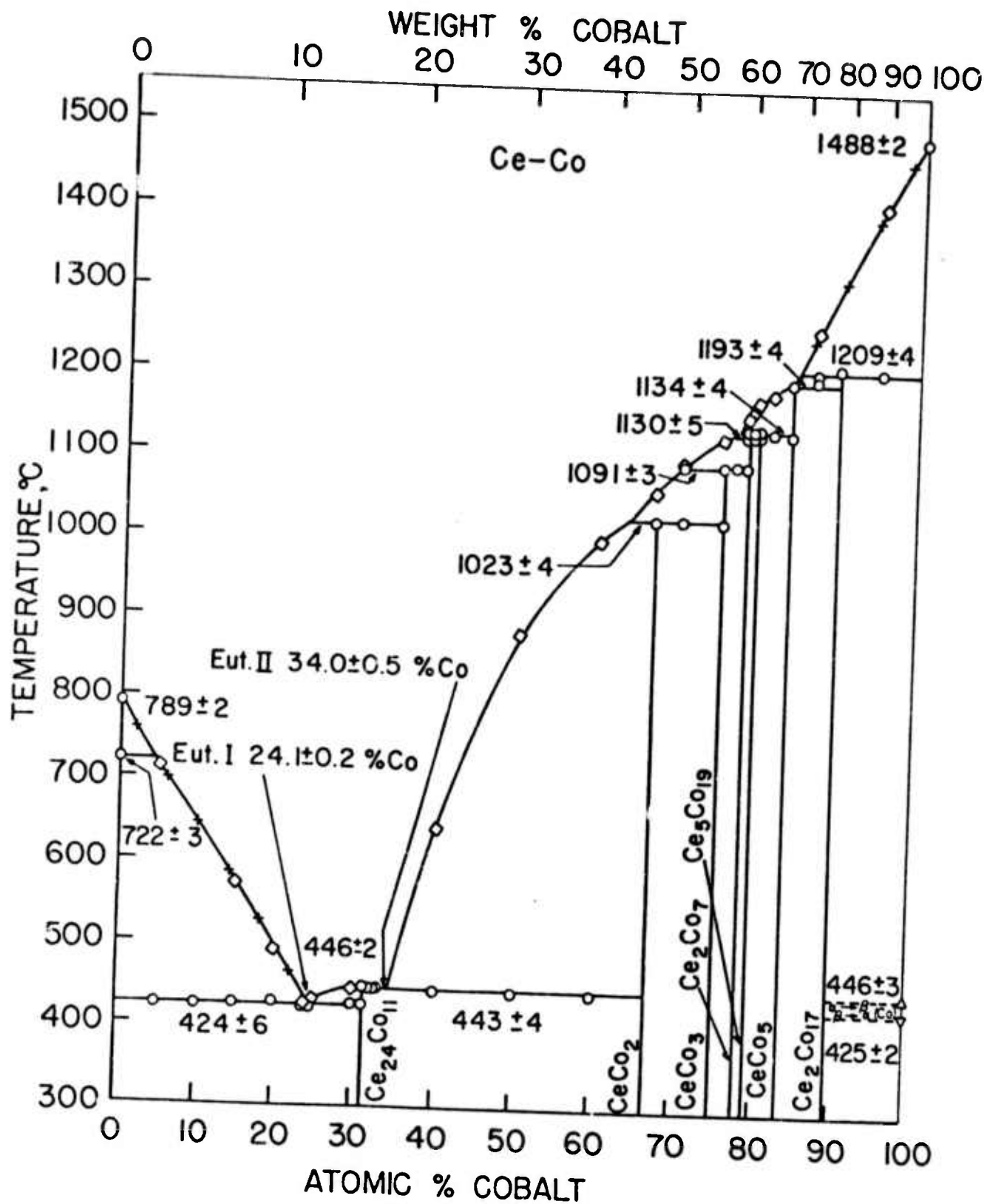


Figure 5. Phase Diagram for the System Ce-Co. <sup>16</sup>

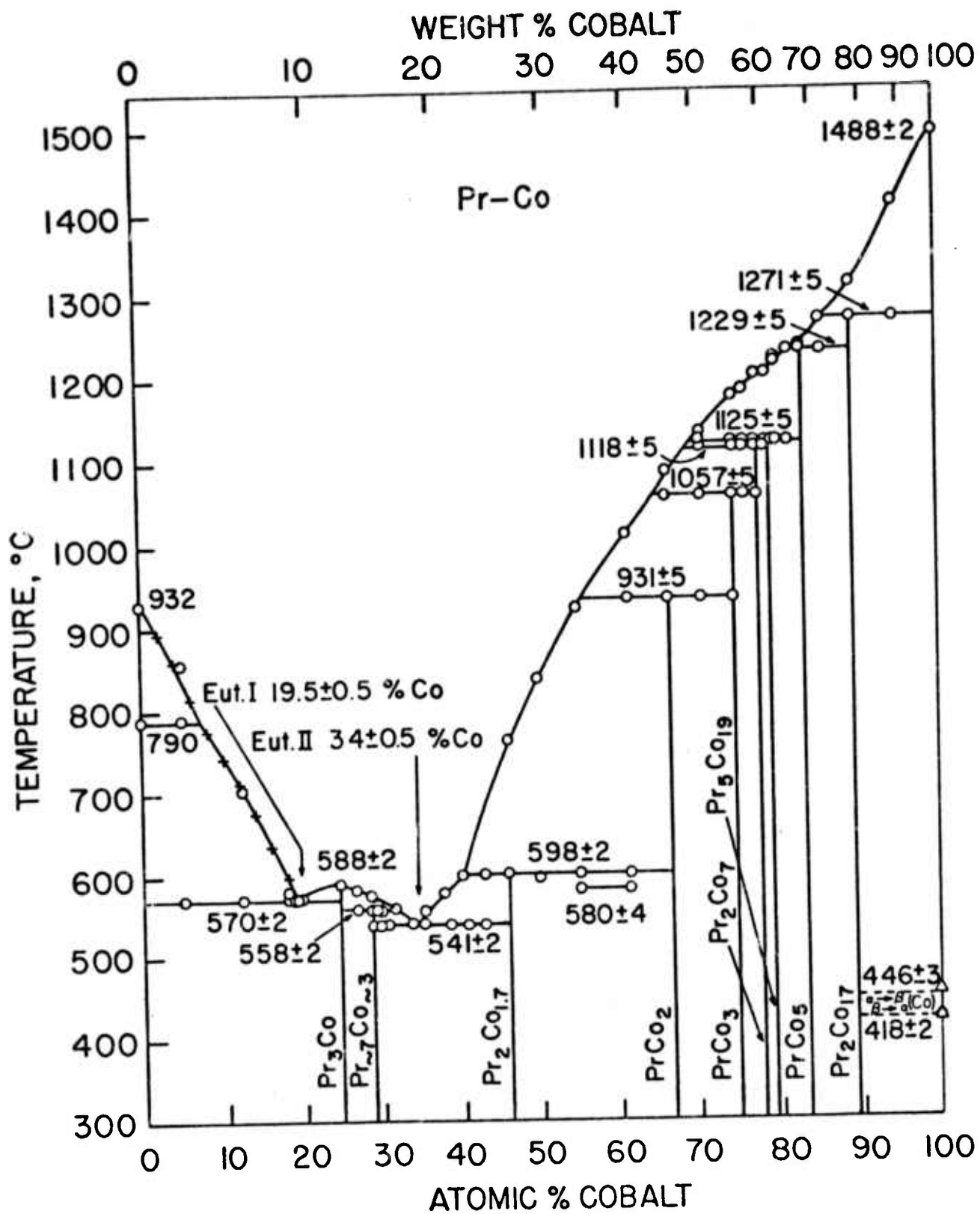


Figure 6. Phase Diagram for the System Pr-Co. <sup>16</sup>

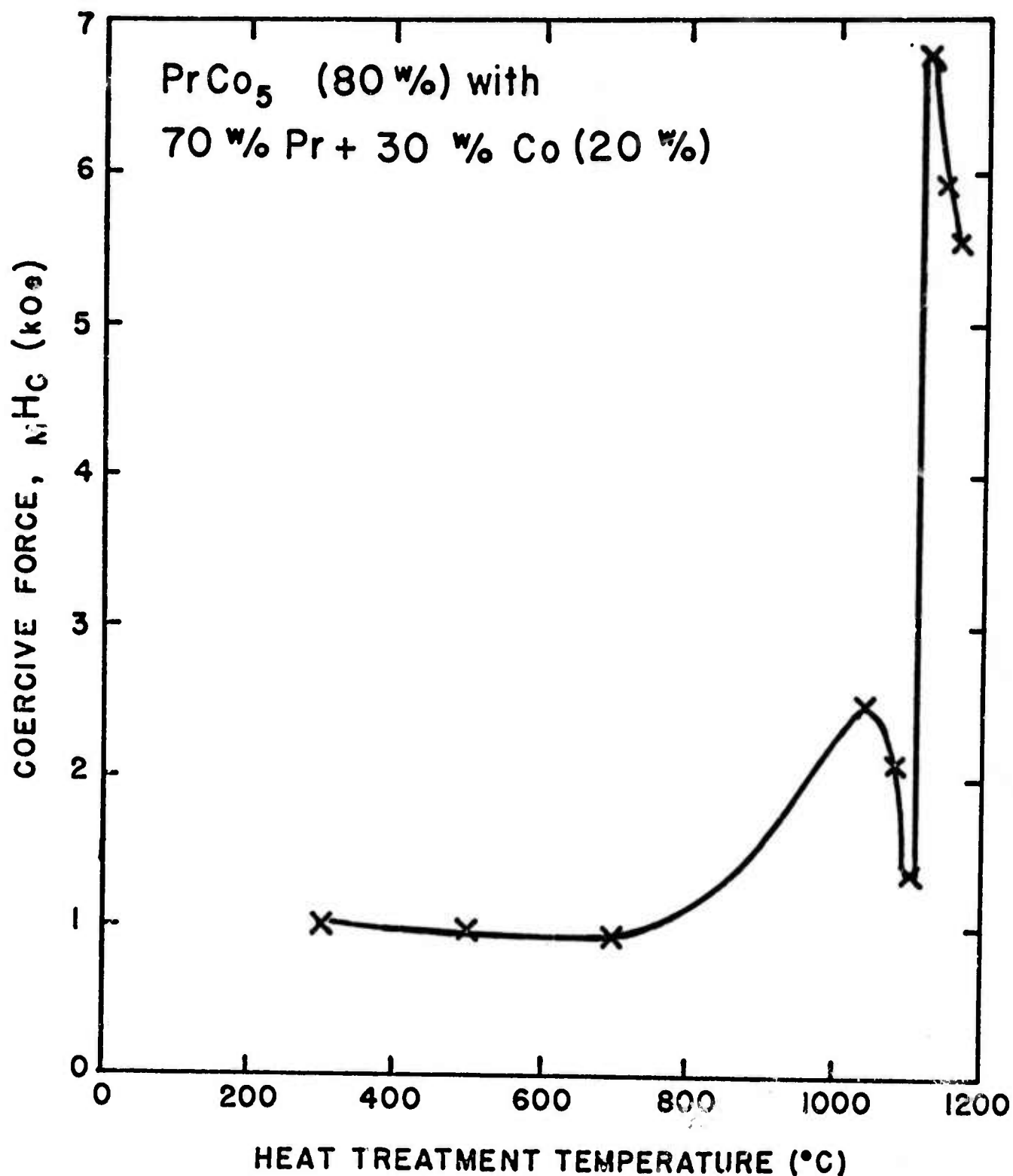


Figure 7. Intrinsic Coercive Force,  $M_c H_c$ , as a Function of Sintering Temperature for PrCo<sub>5</sub> plus a Pr-Co Sintering Additive.<sup>39</sup> The peak in  $M_c H_c$  corresponds to the temperature range between the Pr<sub>2</sub>Co<sub>7</sub> and Pr<sub>5</sub>Co<sub>19</sub> peritectic temperatures.

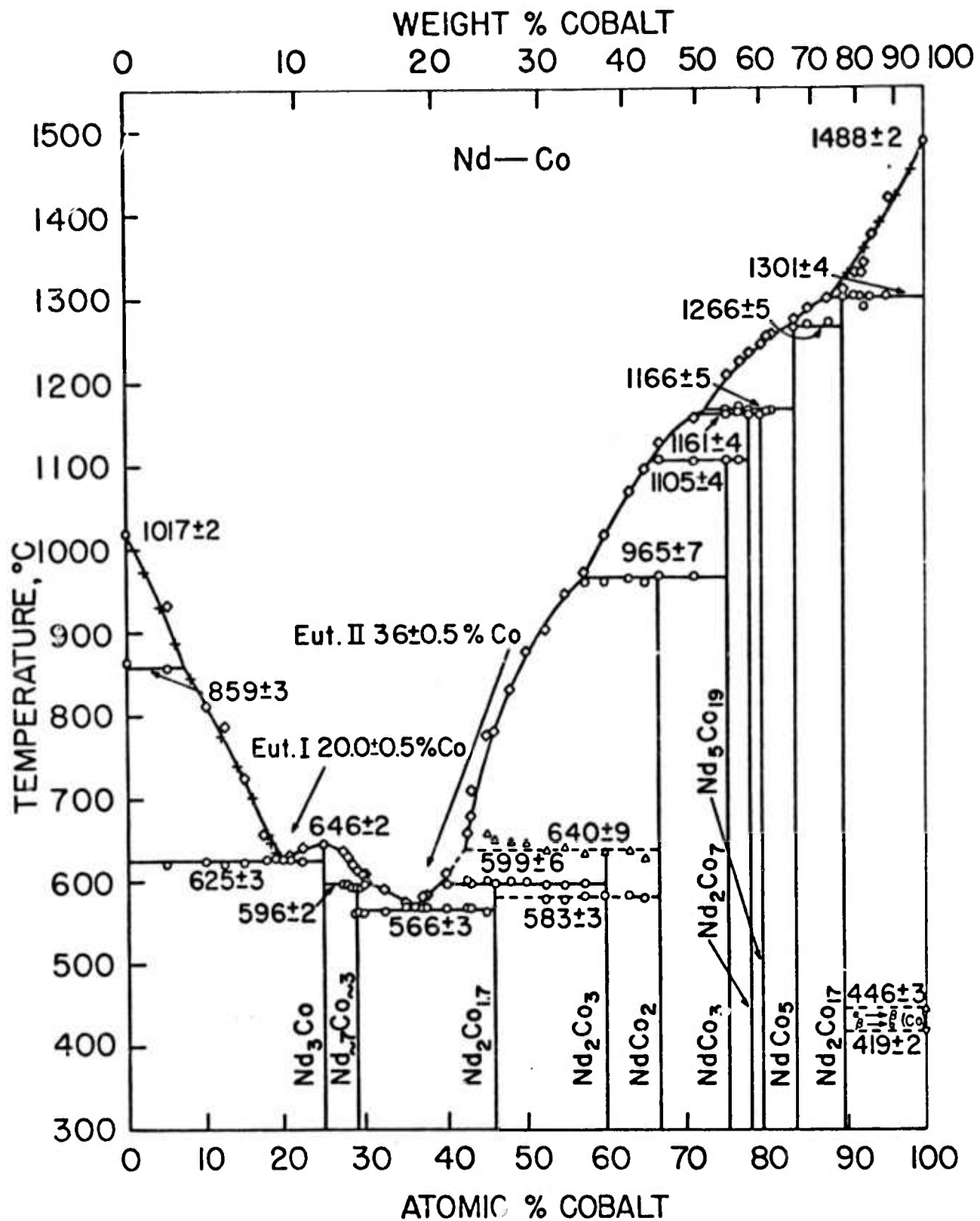


Figure 8. Phase Diagram for the System Nd-Co. <sup>16</sup>

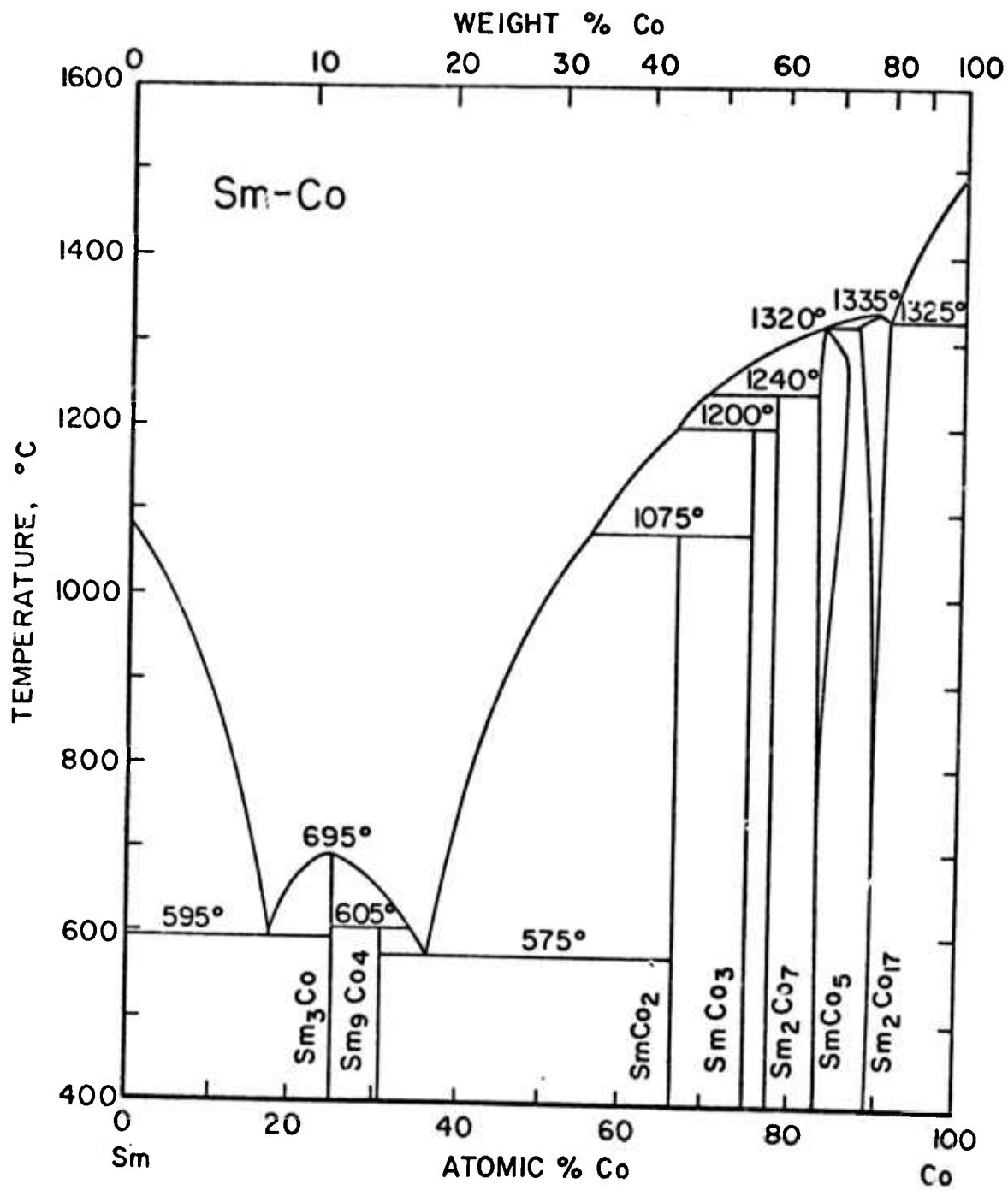
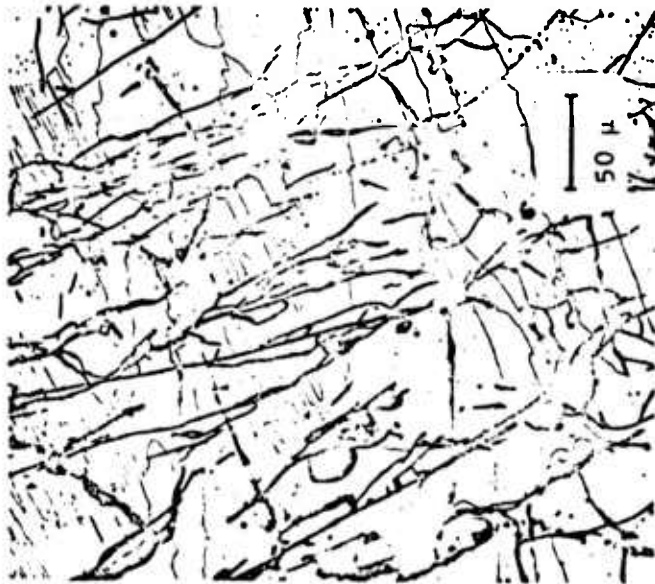
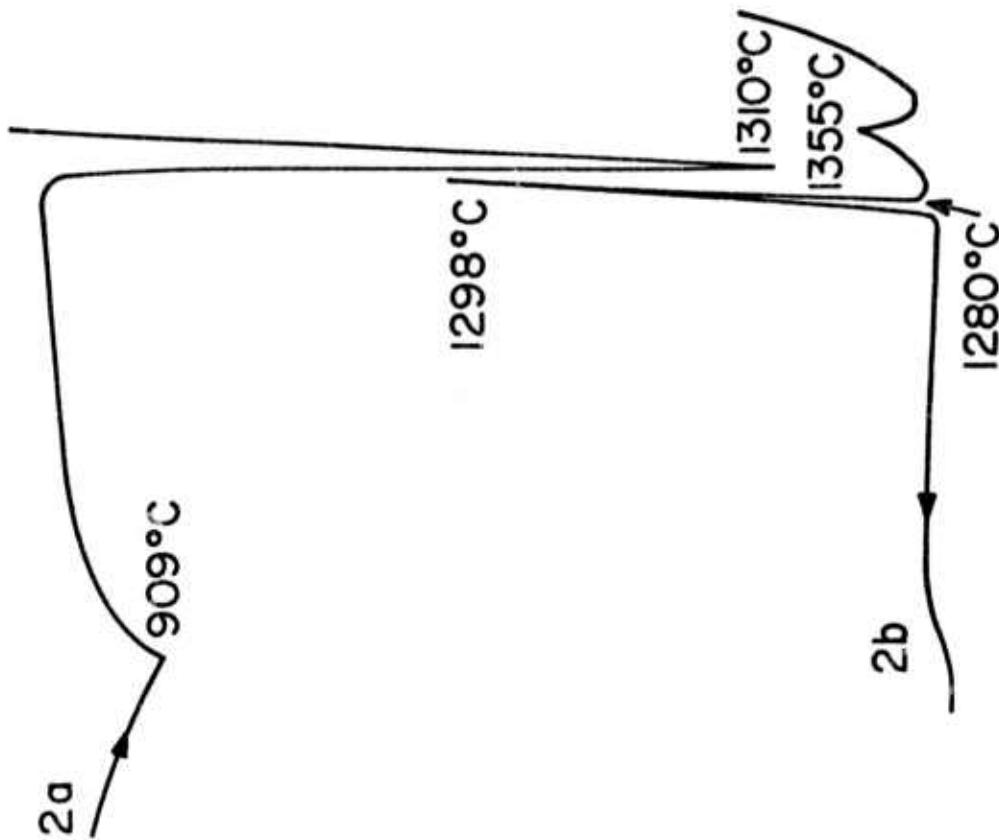


Figure 9. Phase Diagram for the System Sm-Co Proposed by Buschow and Van der Goot.<sup>10</sup>

# DTA, AR-779

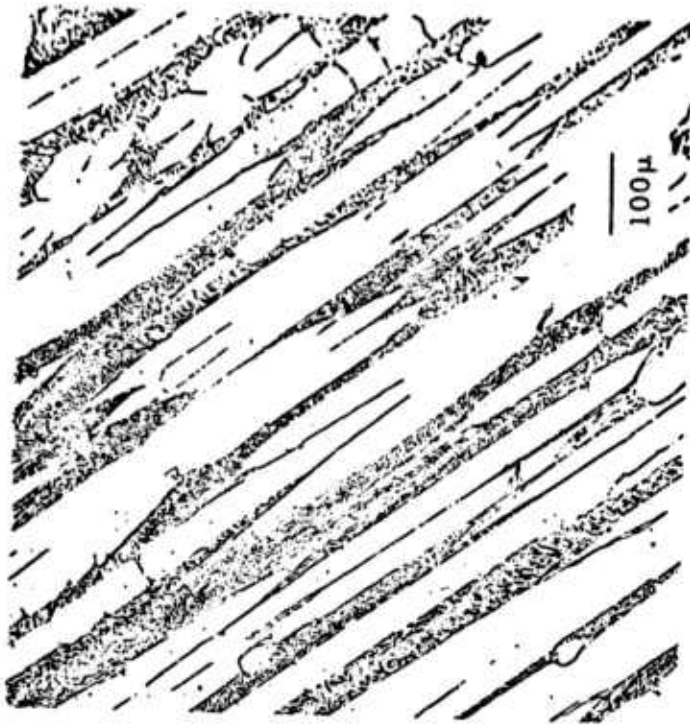


Sm - Co  
89.5 at. % Co  
6 hr. at 1200°C

Figure 10. Microstructure and differential thermal analysis trace of a Sm-Co alloy, nominally  $\text{Sm}_2\text{Co}_{17}$  (89.5 at. % Co). The heating curve, 2a, shows the  $\text{Sm}_2\text{Co}_{17}$  Curie point (909°C) and peritectic temperature (1310°C). The cooling curve, 2b, shows a liquidus (1355°C), supercooling (to 1280°C) then reheating toward the  $\text{Sm}_2\text{Co}_{17}$  peritectic.



(a)



(b)

Figure 11. Microstructures of As-Cast Sm-Co Alloys: (a) The Sm-89.5 at. % Co ( $\text{Sm}_2\text{Co}_{17}$ ) Alloy Appears Single Phase while (b) The Sm-90.5 at. % Co Alloy Appears to have a Eutectic Microconstituent.

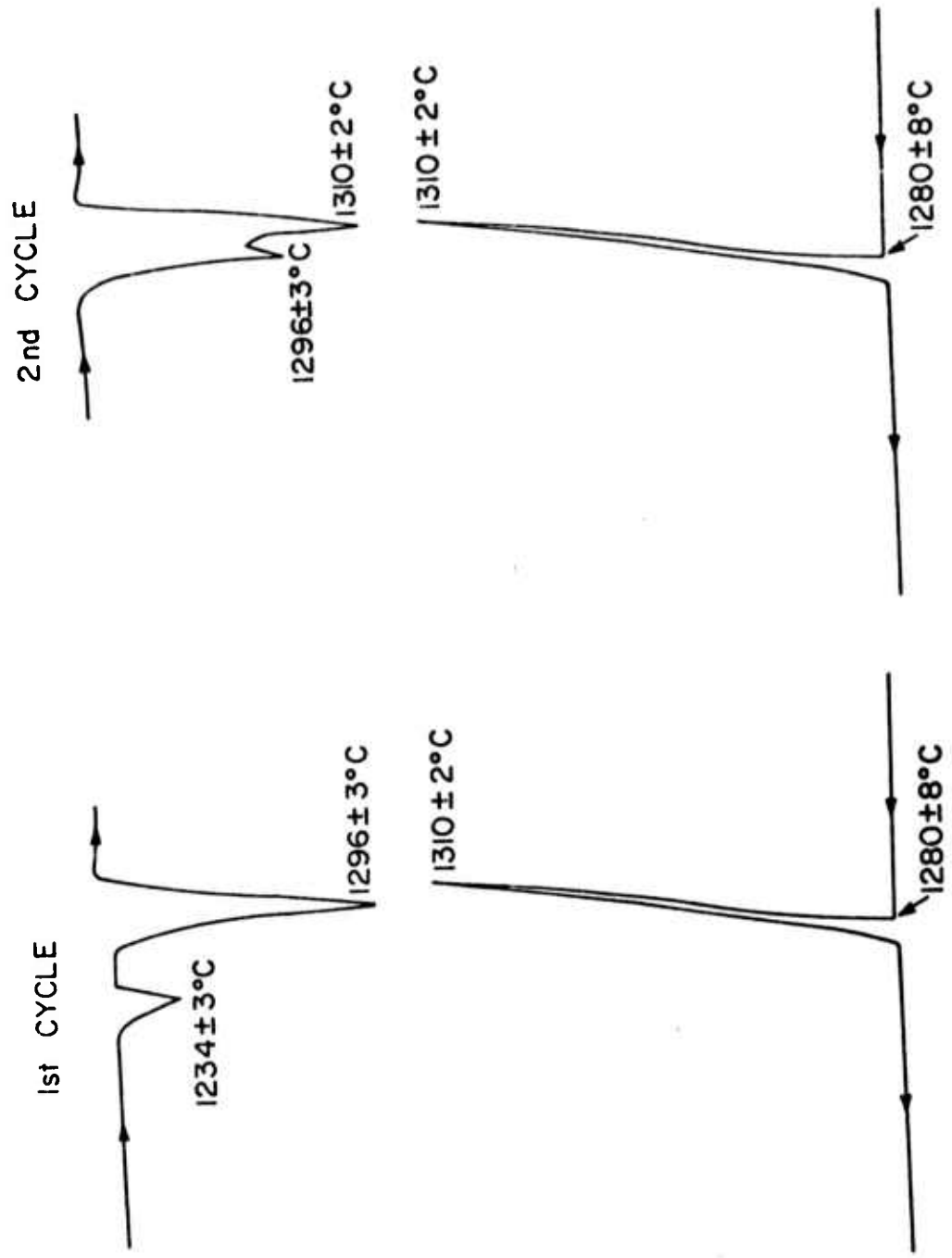
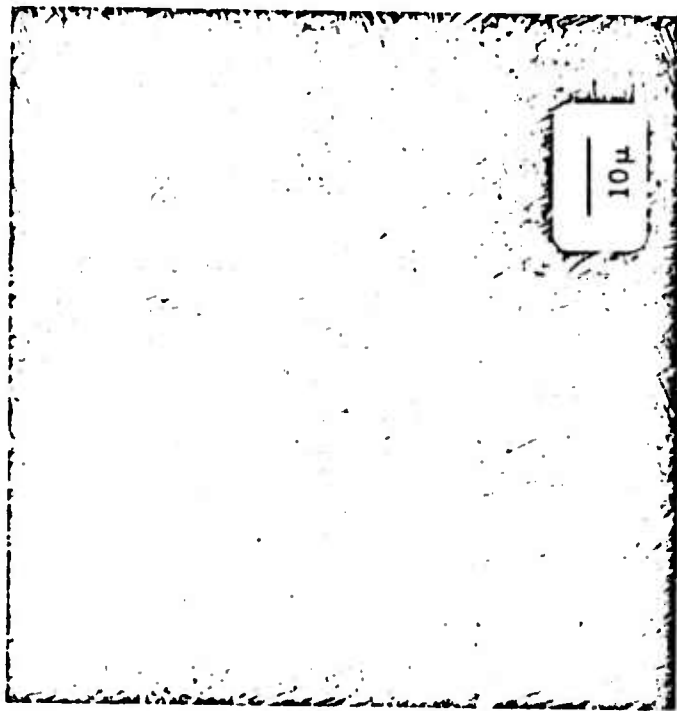
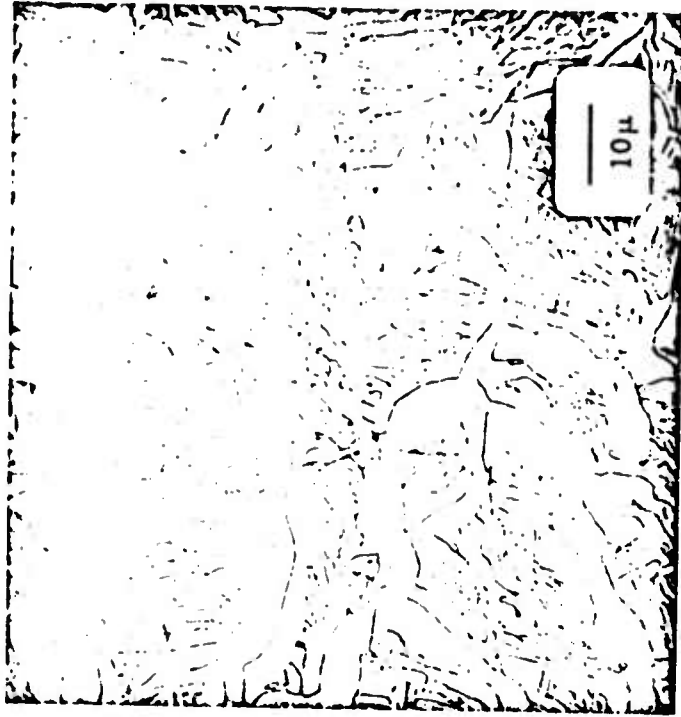


Figure 12. Differential thermal analysis curves for a Sm-Co alloy containing nominally 80.0 at. % Co and annealed 48 hours at 1125°C. Identical curves were obtained for an alloy containing 79.0 at. % Co.



(a)



(b)

Figure 13. Microstructures of an Y-Co Alloy, Nominally 86.5 at. % Co. (a) Annealed 42 days at 900°C. (b) Annealed 120 days at 535°C. X-Ray analysis shows only two phases present in each case,  $YCo_5$  and  $Y_2Co_{17}$ .